MODELLING SUBSURFACE WATER FLOW IN THE UNSATURATED ZONE

Tshanduko Mutandanyi

Submitted in fulfilment of the requirements for the degree

Magister Scientiae in Geohydrology

in the

Faculty of Natural and Agricultural Sciences

(Institute for Groundwater Studies)

at the

University of the Free State

Supervisor: Prof. Abdon Atangana

January 2019

DECLARATION

I, Tshanduko MUTANDANYI, hereby declare that the dissertation hereby submitted by me to the Institute for Groundwater Studies in the Faculty of Natural and Agricultural Sciences at the University of the Free State, in fulfilment of the degree of Magister Scientiae, is my own independent work. It has not previously been submitted by me to any other institution of higher education. In addition, I declare that all sources cited have been acknowledged by means of a list of references.

I furthermore cede copyright of the dissertation and its contents in favour of the University of the Free State.

In addition, the following article was submitted to one of the top tier journals.

Mutandanyi. T., Atangana. A., 2019. Modelling soil water flow: New proposed models

Tshanduko MUTANDANYI

January 2019

ACKNOWLEDGEMENTS

I would like to express my deepest gratitude to God who granted me the opportunity and wisdom to do my MSc degree in 2018.

I would also like to send deep appreciation to my supervisor, Prof. Abdon Atangana, for his constant encouragements, patient guidance and his valuable suggestions during the course of this research project. I would not have produced work of this quality if it was not because of him.

Not forgetting the University of the Free State for considering my application and granting me the opportunity to do my MSc degree in one of their institutions. I send my thanks to the Institute for Groundwater Studies for allowing me to expand my career with them.

All thanks to my family for the love and support that they showed me. To my mother Ndishavhelafhi Grace Mahada, my aunt Ntsieni Elisa Mahada, and my siblings Phathutshedzo Blessing Mutandanyi, Livhuwani Victor Mutandanyi, and Mbavhalelo Melba Mutandanyi if it wasn’t for you, I wouldn’t have achieved this.

To my dear friend, Murendeni Budeli, thank you for your advice and for giving me joy all the times. If it wasn’t for you 2018 would have been long for me.

Lastly, I would like to send my sincere gratitude to the National Research Foundation for funding my studies.

ABSTRACT

Modelling flow in the unsaturated zone has caught interest recently in many fields of science such as geohydrology; agriculture; and soil physics. Unsaturated zone flow has a significant effect on the quality and quantity of groundwater resources; thus, it is essential to understand it. This thesis aimed to model water flow in the unsaturated zone. There are many studies in literature that aimed at understanding flow in this zone by means of mathematical models. Richards' equation is commonly used in such studies and its performance has shown great success in reproducing the unsaturated flow system. However, complexities in the unsaturated zone and soil hydraulic properties make Richards' equation to be highly non-linear which makes it impossible to solve analytically. As a result, it is mostly solved numerically using computer codes to obtain numerical solutions. However, linearized Richards' equation can be solved analytically and reliable results can be obtained. The methodological approach of this thesis entails application of Brooks & Corey and Mualem non-linear hydraulic conductivity models to Richards' equation. The resultant models were solved numerically and numerical solutions were obtained. Following that a linearized Richards' equation was proposed and solved to obtain an exact solution. An exact solution was obtained using Laplace and inverse Laplace transform and Green's function. For numerical analysis, both models were discretized using Crank-Nicolson and the Laplace Adam-Bashforth numerical approximation methods. The stability analysis was provided for the linear model for both methods. From the stability analysis, it was found that both numerical approximation methods yield stable solutions provided the required conditions are met. For the considered unsaturated flow system, it is concluded that the proposed linear model showed good performance in expressing water flow. Models proposed by Brooks & Corey and Mualem seemed to overestimate hydraulic conductivity resulting in an overestimation of soil moisture. These models were revised and the resultant models were able to yield results that correspond to results obtained using the proposed linear model.

Key words: Unsaturated zone, unsaturated flow system, unsaturated hydraulic conductivity, non-linear model, linear model, Richards' equation, exact solution, numerical simulations

USED GREEK NOTATIONS

α	Alpha
β	Beta
δ	Delta
ε	Epsilon
η	Eta
γ	Gamma
λ	Lambda
$\mathcal{L}$	Laplace Transform Operator
μ	Mu
ω	Omega
∂	Partial Differential Operator
φ	Phi
ϕ	Phi Variant
ψ	Psi
ρ	Rho

σ	Sigma
τ	Tau
θ	Theta
ξ	Xi

USED ABBREVIATIONS

q	Darcy's flux
K	Hydraulic conductivity
h	Matric pressure head
D	Pore-water diffusivity
t	Time elapsed
z	Vertical distance

TABLE OF CONTENTS

LIST OF FIGURES

CHAPTER 1: INTRODUCTION

1.1 Background

Water on earth is always in motion which sometimes involves phase change. This motion and phase change are clearly described in the hydrological cycle (Zhang, 1991). When precipitation occurs in the form of rain some water becomes surface runoff (Neitsch et al., 2011) and drains to the closest drainage basin. Depending on the vegetation cover; soil and rock type; nature of precipitation and other controlling factors, instead of flowing on the surface water can seep into the subsurface. Water that seeps into the subsurface continues to move as unsaturated or saturated flow. The unsaturated flow is a multi-phase flow that occurs when pore spaces between soil particles are occupied by both water and air (Boulding and Ginn, 2013). The zone at which this type of flow occurs is called the unsaturated zone, vadose zone or aeration zone (Nimmo, 2005). The term unsaturated zone will be used in this study when referring to this zone. The unsaturated zone is the subsurface water zone between the earth's surface and the water table. The focus of this study is on the flow of water in this zone. To add, the unsaturated zone includes the capillary fringe where water is pulled up from groundwater resources by the capillary forces (Nimmo, 2005). Water in the unsaturated zone is mostly referred to as soil moisture. During extremely wet conditions surface water seepage can be very high in such a way that this zone becomes saturated with water for a short period until the normal conditions are retrieved. To expand, during or after a storm infiltration may be high enough to fill all available pores between soil particles with water leaving the soil being fully saturated. The saturation state is temporal and once drainage starts some water is replaced by air and unsaturated conditions retrieve. During extremely high temperatures this zone can become dry (Zhu et al., 2016).

The unsaturated zone plays a significant role in the hydrological cycle. It controls the partitioning of precipitation and irrigation water into runoff, infiltration or evaporation. It also controls the quantity of groundwater recharge through water fluxes such as evapotranspiration, interflow and vertical water drainage (Twarakavi et al., 2008). Furthermore, the unsaturated zone stores and transfers water to the saturated zone, it also aids in solute dilution and transportation. Most importantly, it filters and absorbs contaminants in soil water before water joins the groundwater resources. To expand, the unsaturated zone plays a significant role in the quality of groundwater. This is mainly controlled by the soil type and its organic content as well as the chemistry of mineral constituents in soil (Nimmo, 2005). Moreover, This zone connects the surface water resources and groundwater resources (Nimmo, 2005; Wong et al., 2017).

Soil moisture can be lost through plants evapotranspiration, and or evaporation (Wong et al., 2017). Since the Earth's gravitational force tends to pull all masses toward its centre (Nimmo, 2005), the remaining soil moisture is pulled down towards the saturated zone. As water flows in the vertical direction, some water is retained due to capillary forces acting against the pull of gravity. Water that escapes flow resistance due to capillary forces percolates to the water table as groundwater recharge (Nimmo, 2005; Zhang, 1991). At this point, soil moisture joins groundwater resources and continue to flow as part of the saturated flow. The zone at which groundwater occurs is called the saturated zone. It is found underneath the unsaturated zone. This is where all the pore spaces are filled with water. Groundwater flows through permeable geological formations called aquifers following the interconnected pore spaces towards the discharge areas.

Subsurface water flow is mainly gravity controlled especially in the unsaturated zone. Soil moisture flow is highly governed by the soil type and available soil moisture content. Groundwater flows down the hydraulic gradient through porous matrix towards the discharge areas or points of low hydraulic pressure (Eddebbarh et al., 2003). Sometimes flow can be through preferential pathways such as fractures in igneous rocks and bedding plane fractures in sedimentary rocks (Nimmo, 2005). In unconfined aquifers, groundwater tends to follow the surface topography and flow from a higher topographic elevation to a lower elevation (Zhang, 1991). On the other hand, in confined aquifers water does not necessarily follow the topography instead it flows from a region of high hydraulic head towards a region of a lower head. In general, the rate at which subsurface water flow can be a few feet per hour, day, or a week depending on the permeability of the media. For example, in primary porous media the flow is matrix flow which is mainly by diffusion, therefore the flow is considered slow. In contrast, in fractured systems conduction dominates and the water flows faster (Zhang, 1991).

The subsurface water flow is controlled by various factors in various media. Therefore, each subsurface water system is associated with a unique level of complexities. Understanding groundwater flow seems to be less complicated since aquifers' hydraulic properties do not vary randomly in space. This is not the case for soil moisture, soil hydraulic properties are not fixed throughout the soil. Regardless of complexities associated with the unsaturated zone, there are mathematical formulations that were developed to describe flow in this zone. The unsaturated flow in porous media was mathematically formulated by Henry Darcy in 1856 (Whitaker, 1986; Zhang, 1991). Darcy explained subsurface flow in a porous media by means of a law, Darcy's law (Soulaine, 2015). Darcy's law expresses the relationship between specific discharge, water discharge per unit area, and the hydraulic gradient with Darcy's permeability as the proportionality constant. This law assumes a steady state flow in porous media (Gordon, 1989). Therefore, it does not cater for transient flows. There is another equation developed to model water flow in the unsaturated zone, the well-known Richards' equation (Ojha et al., 2017; Zhang, 1991). Richards' equation has been a better mathematical way of expressing the unsaturated flow processes in the unsaturated zone. However, the effectiveness of Richards' equation seems to decrease with an increase in complexities and heterogeneities of the system. Spatial heterogeneities of water content in soils result in non-linear parametric functions to Richards' equation which makes it impossible to solve analytically. This led to the development of a Finite water-content method (Zhu et al., 2016) to accommodate complex problems that Richards' equation cannot solve. Despite the weaknesses associated with Richards' equation, it remains the governing equation to express soil water flow processes occurring in the unsaturated zone. Generally speaking, modelling flow in the unsaturated zone is complicated and requires knowledge of parameters that are most of the times impossible to obtain in the field. As a result, researchers proposed ways of reproducing the unsaturated system theoretically (e.g. Assouline et al., 1998; Burdine, 1953; Childs and Collis-George, 1950; van Genuchten, 1980) by utilizing soil hydraulic parameters that are easy to obtain. These parametric models are highly non-linear, therefore they can only be solved numerically. This study attempts to solve Richards' equation both numerically and analytically to obtain an exact solution and numerical solutions expressing the unsaturated zone flow system.

1.2 Problem statement

Groundwater resources have become a primary freshwater resource. The unsaturated zone system has a huge impact on subsurface water resources. Unsaturated zone flow processes control the quantity and quality of water entering the groundwater system. Depending on processes acting on soil water, the amount and chemistry of infiltration water may change as water migrates downwards. This poses a need to understand the movement of water through porous soil towards the water table. For years the unsaturated zone flow modelling has been a complicated issue due to the spatial evolution of soil hydraulic parameters. Regardless of complexities associated with this zone, researchers utilize Richards' equation to model flow in this zone. Richards' equation is associated with many problems because it is highly non-linear. Therefore, I see a need to develop a linear parametric model that will result in a linearized Richards' equation. I believe that the resultant equation will be free of problems associated with Richards' equation. Exact solutions can be obtained which allows the unsaturated zone flow problems to be solved without a computer code.

1.3 Aim and objectives

The main purpose of this study is to model the flow of water in the unsaturated zone. The following study objectives will assist in achieving this purpose:

1.3.1 To review existing models for estimating unsaturated hydraulic conductivity;

1.3.2 To perform numerical analysis of Richards' equation;

1.3.3 To develop a theoretical linear expression for estimating unsaturated hydraulic conductivity;

1.3.4 To develop a linear model for unsaturated flow in porous soils;

1.3.5 To obtain an exact solution of linearized Richards' equation;

1.3.6 To evaluate the stability of the proposed linear model using two different numerical approximation methods and

1.3.7 To produce numerical simulations for both non-linear and linear models representing subsurface water flow in the unsaturated zone.

1.4 Research framework

The framework of this thesis is presented in Figure 1.1 below.

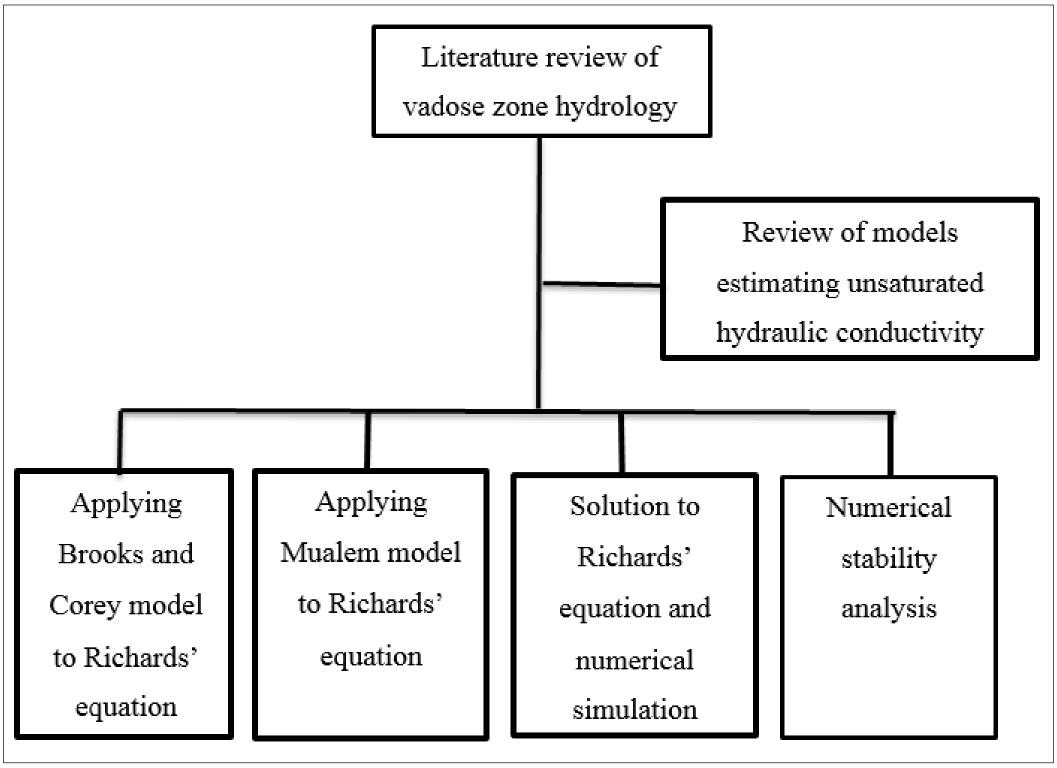

Figure 1: Framework of the study

1.5 Research outline

This thesis is divided into 7 chapters and they are outlined as follows: Chapter 1 introduces the unsaturated flow system and the governing flow equation as well as the associated problem that will be addressed in this study. Chapter 2 gives a literature review of unsaturated zone hydrology. Chapter 3 provides a review of the literature on characteristic functions required for parameterizing the governing flow equation. Chapter 3 also addresses objective 1.3.1. Chapter 4 provides the application of pre-existing mathematical models to the governing flow equation and numerical analysis using two distinct numerical approximating methods. The work on chapter 4 covers some part of objective 1.3.2. Chapter 5 covers developing a linear model for expressing water flow in the unsaturated zone followed by obtaining its exact solution. Towards the end of the chapter, a numerical analysis of the proposed model is covered. Part of objective 1.3.2 is addressed in this chapter as well. Objectives 1.3.3-1.3.6 are also addressed in chapter 5. Chapter 6 addresses the last objective of this thesis. It presents results for both non-linear and linear models for the unsaturated flow system and discussion of the results; new non-linear models are also proposed in this chapter. Chapter 7 provides a conclusion for the thesis.

1.6 Richards' equation

Modelling flow in the unsaturated zone is essential for understanding the subsurface water system. As a result of the complex nature of the subsurface water system, the modelling procedure is more sophisticated. Unlike unsaturated flows, modelling saturated flows is less sophisticated since the hydraulic conductivity is assumed to be constant throughout the media. For unsaturated flow, the story is different and more complex (Nimmo, 2005; Ojha et al., 2017) because unsaturated hydraulic conductivity varies randomly in space. There are mathematical formulations found in the literature that were suggested to describe unsaturated flow systems. There has been a great success achieved by these formulations in describing the unsaturated flow processes. The most common formulation of the unsaturated system that researchers have been using for decades to describe flow in unsaturated zone is Richards equation (Barari et al., 2009; Vereecken et al., 2008) which was introduced by Richards (1931) after conducting his studies in capillary tubes to mimic water movement in unsaturated porous media. To describe moisture flow in soils Richards (1931) adopted the concept of water conductivity in porous media which was suggested by Buckingham (1907) who also suggested that in unsaturated flows conductivity is highly affected by moisture content (Barari et al., 2009).

Richards' equation is a generalised equation for describing flow in unsaturated porous media; it assumes a general non-steady one-dimensional flow in the unsaturated zone. It is expected that water content varies throughout the medium. As a result, the hydraulic conductivity, as well as forces governing the water flux, are also not fixed throughout the medium. This is the cause of the highly non-linear nature of Richards' equation. The spatial variation in conductivity also leads to complexities in the field of modelling of unsaturated flow since it is quite difficult to measure non-uniform hydraulic conductivities throughout the medium. Richards (1931) formulated a non-linear Partial differential equation to describe one-dimension vertical flow in unsaturated non-swelling porous soils by combining mass conservation equation

$$\frac{\partial \theta}{\partial t} = -\frac{\partial q}{\partial z} \tag{1.1}$$

with Darcy's law

$$q = -K(\theta)\frac{\partial h}{\partial z} \tag{1.2}$$

to obtain

$$\frac{\partial\theta}{\partial t} = \frac{\partial}{\partial z}\left(K(\theta)\frac{\partial H}{\partial z}\right) \tag{1.3}$$

Where $H = h + z$. By substituting H into equation (1.3) the following is obtained

$$\frac{\partial\theta}{\partial t} = \frac{\partial}{\partial z}\left[K(\theta)\left(\frac{\partial h}{\partial z} + \frac{\partial z}{\partial z}\right)\right] \tag{1.4}$$

which is simplified into

$$\frac{\partial\theta}{\partial t} = \frac{\partial}{\partial z}\left[K(\theta)\left(\frac{\partial h}{\partial z} + 1\right)\right] \tag{1.5}$$

Where q is the water flux; θ is the dimensionless volumetric water content or moisture content; t is the time; z is the vertical distance; h is the pore water pressure head, also referred to as capillary pressure; and $K(\theta)$ is the unsaturated hydraulic conductivity.

Equation (1.5) above is the well-known mixed-form Richards' equation used in modelling unsaturated flows; it is commonly used to describe flows in unsaturated soils. Given its mixed form state, it is more expensive and time-consuming to obtain all the required data for this equation because it has two independent variables, namely soil volumetric moisture content θ and soil pore water pressure head h. Moreover, the mixed-form Richards equation does not cater for all circumstances in unsaturated flow such as conditions with wetting fronts and where the flow is not stable. This is due to the non-linear nature of Richards' equation which is caused by the strong dependence of the unsaturated hydraulic conductivity on capillary pressure head h and volumetric water content θ. Alternatively, there are two formulations of Richards' equation that consist of only one independent variable each. These formulations are soil moisture content based form, θ-based form; and pore water pressure head based form, h-based form. To obtain a head base form θ needs to be eliminated from equation (1.5) above to yield an equation that has only capillary pressure as an independent variable. θ is eliminated by introducing the derivative of the soil water retention curve, the specific water capacity concept, into equation (1.5) which yields

$$C(h)\frac{\partial h}{\partial t} = \frac{\partial}{\partial z}\left(K(\theta)\frac{\partial h}{\partial z}\right) + \frac{\partial K(\theta)}{\partial z} \tag{1.6}$$

Where

$$C(h) = \frac{d\theta}{dh} \tag{1.7}$$

is the rate of change of water content or saturation in relation to the matric pressure head.

A θ-based form Richards' equation is formulated by incorporating soil pore water diffusivity D term into the mixed-form Richards' equation to produce a transient unsaturated flow equation with only one independent variable θ. This is achieved by assuming that the flow is governed by water content only and neglecting the effect of soil matrix potential h. By incorporating pore-water diffusivity term

$$D = \frac{K(\theta)}{C(h)} = K(\theta)\frac{dh}{d\theta} \tag{1.8}$$

into equation (1.5), the following is obtained

$$\frac{\partial\theta}{\partial t} = \frac{\partial}{\partial z}\left(D\frac{\partial\theta}{\partial z}\right) + \frac{\partial K(\theta)}{\partial z} \tag{1.9}$$

Equation (1.9) above is a θ-based form of Richards' equation. Both forms are effective in mimicking flows in unsaturated systems and a choice on which one to use depends on the available data.

Both D and $K(\theta)$ highly depend on θ, but during data collection D is much easier to measure compared to $K(\theta)$ and h. In equation (1.9) a decrease in $K(\theta)$ due to a decrease in θ is compensated for by a typical increase of $\frac{dh}{d\theta}$ with a decline in θ. Therefore, D varies less than $K(\theta)$ in the field. It seems to be much easier to conduct θ measurements compared to h measurements in the field. Moreover, θ measurements are more reliable than h measurements because they cover the water content of the entire range whereas h measurements do not cover the entire media but only that part of the water retention curve that is wet. In this study, only a θ-based form of Richard's equation will be analyzed.

Despite the success of Richards' equation, its application is problematic since it requires knowledge of many soil hydraulic parameters (Ojha et al., 2017) that are sometimes impossible to obtain. Unlike groundwater flow, unsaturated zone flow is characterised by parameters that require spatial and temporal characterisation since they differ randomly in space as a result of system heterogeneity. To add, parameterizing functions required to solve Richards' equation are highly non-linear. This is because the soil hydraulic parameters extremely depend on volumetric water content which evolves randomly throughout a soil volume. As a result, Richards' equation is highly non-linear and difficult to solve. Obtaining analytical solutions requires oversimplification of the natural unsaturated system which may lead to underestimation or overestimation of flow parameters. For example, unsaturated hydraulic conductivity is commonly miss-predicted in models where the effect of capillarity is over-emphasized. Numerical solutions, on the other hand, are the most reliable ones. However, they are sometimes associated with convergence problems because of the highly non-linear nature of this equation. Moreover, computational procedures are complicated, time-consuming and expensive.

CHAPTER 2: LITERATURE REVIEW OF UNSATURATED ZONE HYDROLOGY

2.1 Introduction

The unsaturated zone flow processes control water transfer processes between the land surface and the groundwater table. Understanding processes occurring in the unsaturated zone is the key to understanding the geohydrological processes occurring in a groundwater system (Twarakavi et al., 2008). Basic unsaturated zone hydrology helps to understand hydraulic parameters influencing processes that water in the unsaturated zone undergoes starting from input to output processes. This chapter provides a review of the unsaturated zone hydrology including water flow processes.

2.2 Basic unsaturated zone hydrology

Soil hydrology can be simple and straight forward or complicated. Knowledge of hydrological characteristics of the unsaturated zone is the base of understanding soil moisture flow. The soil hydraulic parameters play a significant role in parameterizing the governing equation for modelling soil moisture movement. Some important parameters are covered in this section.

2.2.1 Soil hydraulic characterization

Soil hydraulic parameters are introductory components to unsaturated flow studies. Some important parameters are; porosity and effective porosity; volumetric water content and degree of saturation; density; soil water retention curve which will be covered in section 2.3.4; and one of the most important ones, unsaturated hydraulic conductivity. This section will cover a few hydraulic parameters and soil hydraulic characteristics namely: soil water potentials; soil moisture conditions; and types of soil water.

2.2.1.1Porosity

Porosity n describes a fraction of a medium that is occupied by pore spaces. In terms of soil, porosity is that fraction of soil volume that is occupied by empty spaces that can be filled with water or air (Tarboton, 2003). It is mathematically expressed as

$$n = \frac{volume\ of\ voids}{total\ volume\ of\ soil} \tag{2.1}$$

Its values range from 0 to 1. For soil, it usually ranges from 0.3 to 0.7 (Nimmo, 2004) and is controlled by many factors. Porosity is an important parameter in hydrology, to be specific effective porosity which is referred to as the fraction of a soil volume that is occupied by pores that are actually connected to allow conduction of flow. The size of these pores plays a significant role in understanding fluid conductivity through them which brings interest to the concept of pore size distribution. Pore size distribution describes the spread of pore sizes across the soil volume. For decades this concept has caught the interests of many researchers who aimed to study unsaturated hydraulic conductivity (Brooks and Corey, 1964; Burdine, 1953; Mualem, 1976; van Genuchten, 1980).

2.2.1.2 Unsaturated hydraulic conductivity

Unsaturated hydraulic conductivity describes an ease at which water can move through soils when both water and air occupy the pore spaces (Tarboton, 2003). It is known to be highly dependent on the water content and the pressure head. A decline in unsaturated hydraulic conductivity is the result of a decline in volumetric water content during redistribution or internal drainage. This leads to a decline in flow cross-sectional area leading to a more tortuous path and an increase in drag forces. Different soils conduct water differently and for this reason change in unsaturated hydraulic conductivity is different for different soils since it depends on individual soil properties (Childs and Collis-George, 1950). Figure 2, for example, presents how clay and sand conduct water flow. Sand tends to permit flow more compared to clay; this means that water moves fast in sands than in clays (Boulding and Ginn, 2013). Figure 2 also presents the strong dependence of hydraulic conductivity K on water content θ and matric pressure h_m, K tends to decrease with θ and h_m in both soil types.

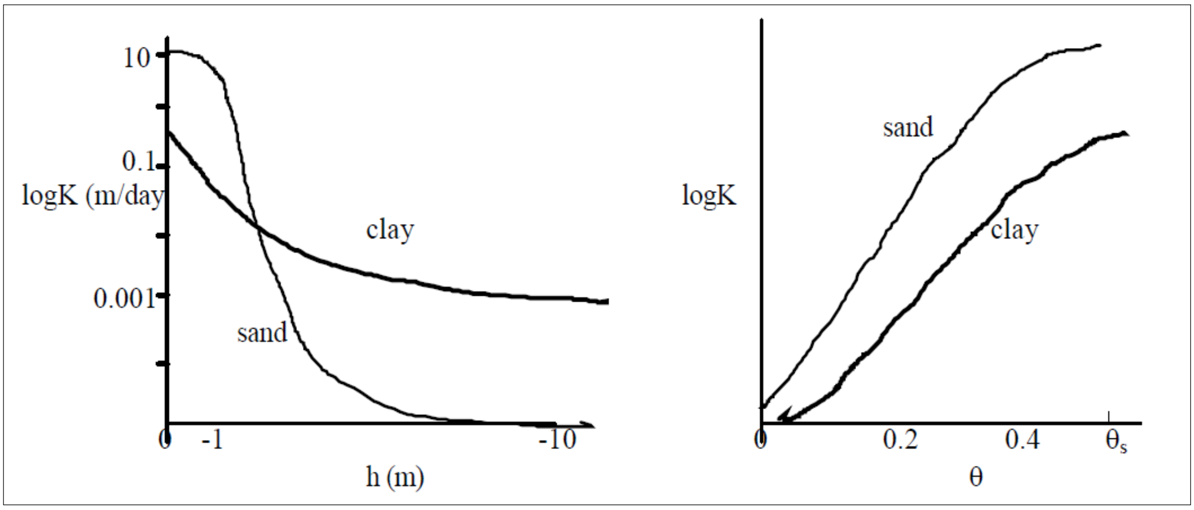

Figure 2: A schematic illustration of hydraulic conductivity for sand and clay in relation to soil matric head and volumetric water content ("Chapter 4 - Water flow in unsaturated soils," 2000)

Moreover, the relationship is highly nonlinear hence K varies randomly throughout the flow media. When modelling flow in the unsaturated zone unsaturated hydraulic conductivity is an important hydraulic parameter, it must be determined before carrying on with the modelling procedure. It can be determined using direct measurements or by utilizing theoretical models that are found in the literature. Direct measurements of unsaturated hydraulic conductivity can be conducted in the field or in the laboratory (McCartney et al., 2007). Field measurements require lots of manpower and relevant equipment to perform direct measurements. To add, sometimes it is highly impossible to conduct a field experiment given the complicated nature of the unsaturated zone.

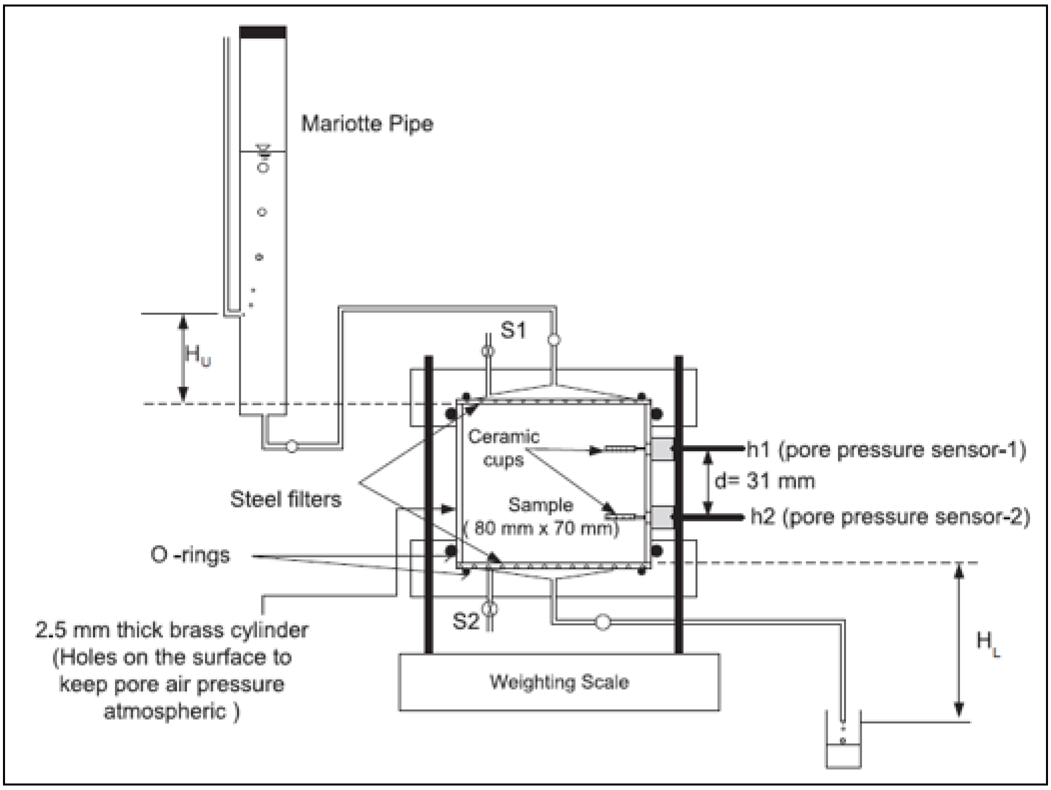

Figure 3: Schematic example of permeameter used in the laboratory to measure unsaturated hydraulic conductivity (Gallage et al., 2013).

In the laboratory a permeameter is used, see Figure 3, to measure unsaturated hydraulic conductivity; the results are correct and reliable. The disadvantage of using a permeameter in the laboratory is that it requires highly trained personnel (Gallage et al., 2013) to operate it and it takes time to conduct the whole experiment. Moreover, laboratory measurements are expensive. Because of the disadvantages associated with direct measurements, researchers have shown a great interest in predicting unsaturated hydraulic conductivity using theoretical models. A review of theoretical models for predicting unsaturated hydraulic conductivity is given in the next chapter of this thesis.

2.2.1.3 Soil water potentials

Gravitational potential (+ value)

Gravitational potential is energy due to the pull of force of gravity towards the centre of the Earth. It is associated with the depth of soil water from a reference point. It influences water flow in soils; water drains down to deeper parts of the unsaturated zone under the influence of gravity (Boulding and Ginn, 2013).

Matric potential (- value)

Matric potential is referred to as the relationship between the air in pore spaces and the pressure head (Mawer et al., 2015). It is associated with water attraction strength to the soil particles, thus it is commonly referred to as potential due to soil particles. It plays a major role in water flow in unsaturated soils. Water tends to flow from regions with relatively high moisture content to regions with relatively low moisture content (Hillel, 2004). This is from a less negative matric potential to a more negative matric potential.

Solute/Osmotic potential (-value)

This is a water potential that is determined by the concentration of solutes in the soil water. It is higher for high solute concentrations and lowers for low concentrations. In terms of soil water movement, water tends to move from regions with relatively high concentration to regions with relatively low concentration.

Pressure potential (+ or – value)

It is associated with the amount of pressure that soil water is exposed to. In most cases, it is equal to 0 for unsaturated soils.

The total potential energy in soils is given by the sum of all potentials acting on soil water. The direction at which water moves in the soil is determined by how the total potential energy is distributed across the soil. The direction can be vertical, downwards if the potential is greater at the top or upwards in cases such as that of capillary rise, or horizontal, left when right experiences high potential and right if higher potentials are at left.

2.2.1.4 Soil moisture conditions

Soil moisture content/volumetric water content

This is the amount of water that is present in the soil. In unsaturated flows, the water content is known to vary randomly across time and space. It is a function of physical and hydraulic soil properties and the rate of change is unique for different soils (Tarboton, 2003).

Saturation

The soil is fully saturated when all pore spaces are filled with liquid water, see Figure 4(a). It is common for the soil to be fully saturated from the top to a certain depth depending on hydraulic properties of the soil. This is only for a limited period of time after rain or irrigation; coarse sands will be saturated for a few hours because they drain quickly and fine sands can be saturated for a few hours to a few days due to their low permeability (Boulding and Ginn, 2013). At this stage, the air is totally absent and all pores are filled with water. This stage lasts until water is drained down by gravity reducing the moisture content. Large pores drain first (Gallage et al., 2013; Swartzendruber, 1954) and air fills the emptied pores. Therefore, both water and air will be present in the system and the unsaturated state will be retrieved.

Field capacity or storage

This is a condition that occurs after drainage; here larger pores are empty or contain both air and water, smaller pores are still filled with water, see Figure 4 (b). This is the unsaturated zone water storage, it describes all the water that is retained during drainage (Chanasyk and Verschuren, 1983). This water is available for roots uptake and sustains shallow subsurface life.

Permanent wilting point

The quantity of water that is put to storage decreases continuously due to evaporative processes and uptake by plants and bacteria. Soil moisture content declines and if there is no water input into the unsaturated system the moisture content declines until there is only a little water accessible by plants roots (Brouwer et al., 1985). Plants suffer from water deficiency condition and their growth is hindered, their leaves turn yellow. Moisture content continues to decline until a very small amount of water, see Figure 4 (c), is left in the soil and cannot be accessed by plants (Chanasyk and Verschuren, 1983). Consequently plants dry out and die. This moisture condition that results in the death of plants is known as the permanent wilting point.

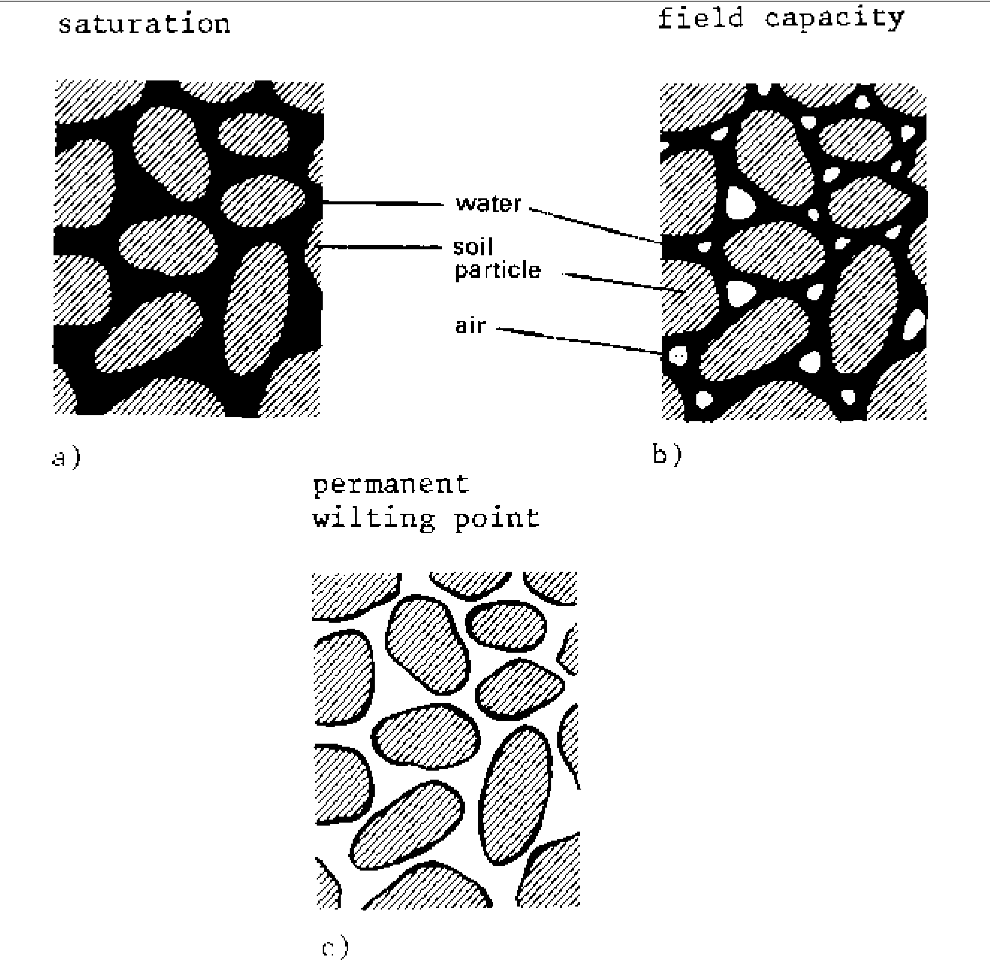

Figure 4: An illustration of soil moisture conditions: (a) soil water at saturation, (b) soil water at field capacity and (c) soil water at wilting point (Brouwer et al., 1985)

2.2.1.5 Types of water

After infiltration water is stored between pore spaces in the unsaturated zone as soil moisture which is then redistributed in the subsurface as either gravitational water, capillary water or hygroscopic water. Gravitational water is that part of soil moisture that is drained downwards into deeper parts of the unsaturated zone by the gravitational force (Boulding and Ginn, 2013). Water that resists gravitational force is held back in pore spaces by capillary forces, namely adhesion and cohesion, is called capillary water. This water is available for plants uptake, it sustains shallow subsurface life. Lastly, the water that is held back by adhesion and is not found in pore spaces but on the particle surface is the hygroscopic water. This water contributes to film flow and is dominant in very dry areas.

2.3. Unsaturated zone flow processes

The fate of water that infiltrates into the soil is broad, before joining groundwater flow precipitation or irrigation water goes through a number of processes, see Figure 5. These processes play a significant role in the quantity of recharge. The following section covers processes occurring in the unsaturated zone starting from infiltration to groundwater recharge.

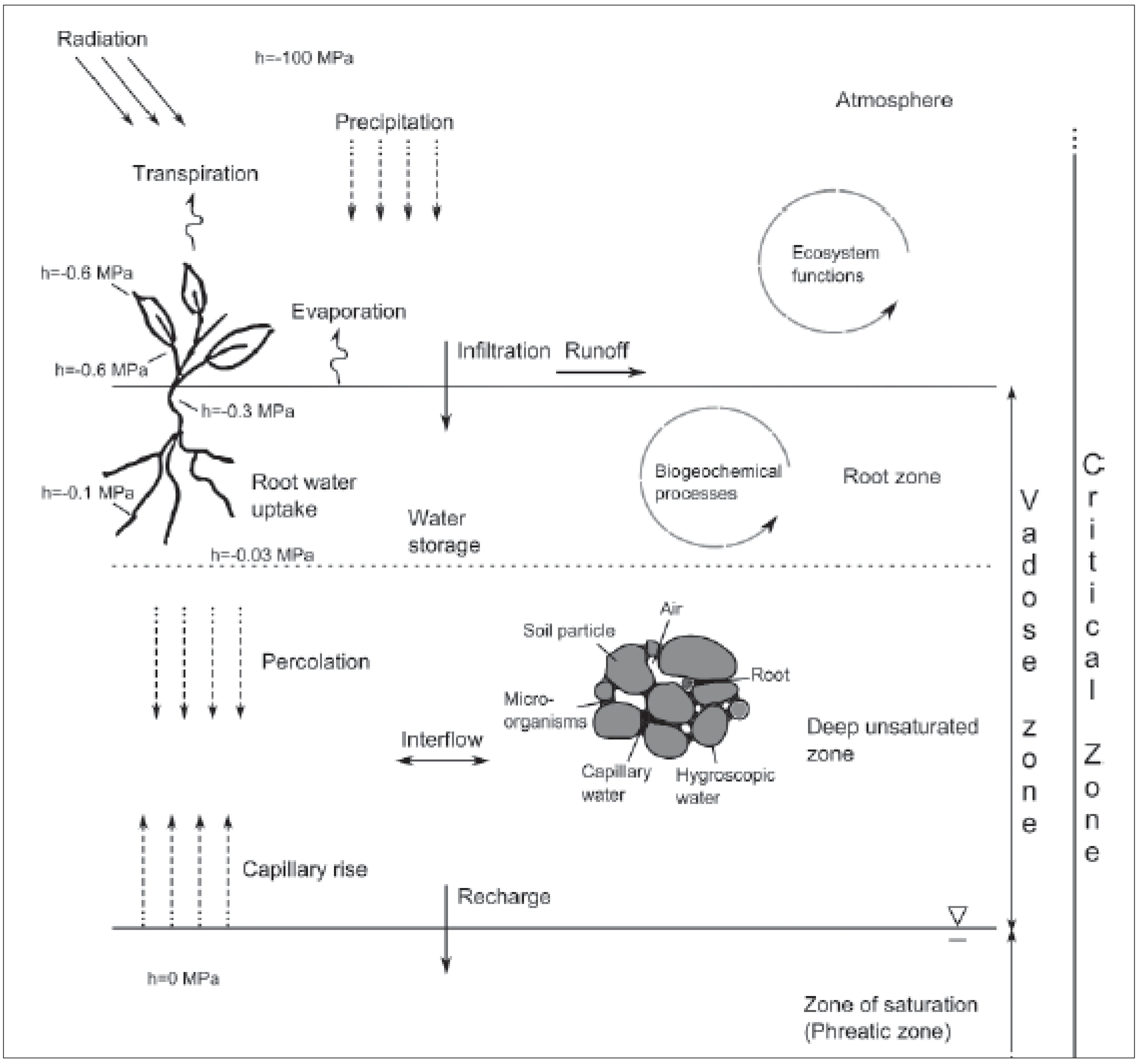

Figure 5: Paths followed by water in the unsaturated zone (Heinse and Link, 2013)

2.3.1 Input fluxes

2.3.2.1 Infiltration

This is a process whereby throughfall, part of precipitation that reaches the soil or ground surface, or irrigation water is absorbed into the soil (Nimmo, 2005). During absorption one of the two conditions occurs. The intensity of precipitation may be high in such a way that local infiltration capacity, the maximum amount of water that soil can hold or absorb, is lower than the throughfall rate. Precipitation intensity may be lower than infiltration rate and the local soil surface gets saturated, water will start flowing on the earth's surface as surface runoff in response to topographic gradients (Wetzel et al., 1996). Runoff can be defined as all liquid water that flows over the soil surface. At the beginning infiltration rate is usually high especially if the soil surface is relatively dry; this is when the soil water intake capacity is still high. As infiltration proceeds, the soil moisture content increases and the capillary pores become filled with water hindering the further intake of water into the soil. Thus, infiltration rate declines rapidly until saturation is reached and no infiltration occurs (Nimmo, 2005). Various soil types have various infiltration capacity. Even though a certain soil type characterizes a flow medium the infiltration capacity is still not fixed, it varies as a function of water content. Infiltration occurs until a state of pseudo-saturation is reached on the topsoil layer. If percolation does not distribute water from the topsoil to other dry parts of the soil to reduce the moisture content at the surface, infiltration stops until drainage occurs making a room for new incoming water in the soil. This explains the common trend of infiltration graphs. Figure 6 provides a graphical representation of a trend where infiltration if high at the beginning of the storm followed by a rapid decline in infiltration rate and an extended period of relatively low rates before infiltration ceases. Researchers believe that this trend is not only caused by local surface saturation but also by physical changes that occur on the soil as infiltration proceeds. Raindrops or water drops from irrigation practices alter soil structure (Boulding and Ginn, 2013) and affect the infiltration rate. To expand, raindrops can cause alteration of pore spaces; closing of some cracks and preferential pathways and swelling in cases where clays are present.

The measure of how fast the water can go into the soil is governed by many factors. Soil that has been exposed to dry atmospheric conditions has little moisture content and is considered to be relatively dry and has high water intake capacity (Boulding and Ginn, 2013). This is because there is more room for incoming water than in relatively wet soils. Because of that, when precipitation or irrigation occurs water is absorbed instantaneously into the soil. However, prolonged dry conditions can make the soil surface to be hard and soil can respond to precipitation the same way that pavements do. Nature of precipitation is important especially the intensity. In terms of rain heavy showers give no time for water on the soil surface to actually seep into the ground. Once water drops reach the ground they accumulate and start flowing as surface runoff. In contrast, soft showers promote infiltration and more water is absorbed into the soil. The state at the ground surface plays a significant role in the partitioning of rainwater into either infiltration or surface runoff. Pavements and other impervious structures on the soil surface act as an umbrella during storms. No water goes through impervious structures thus more water will flow on the surface. Vegetation cover adds resistance to water flow and assists in infiltration. Moreover, Plants are rooted in the soil which increases the permeability of the soil and allows water to go into the soil. Soil permeability is referred to as the ability of soil to permit water flow; is also known as the ability of soil to conduct liquid flow. Soil that allows water to flow easily has a high infiltration rate than soil that is less permeable. This is because water that has already seeped into the soil requires to be redistributed to other parts where there is less moisture content. In cases where soil permits fast redistribution of water, the topsoil will have more room for surface water to infiltrate into.

Depending on the aforementioned factors infiltration rate can be considered fast or slow. To add, Boulding and Ginn (2013) pointed out that factors such as topography; the quantity of air present in soils; thermodynamic conditions; as well as microstructures that open pores in soils also affect infiltration rate.

Since the infiltration process is one of the key processes to the occurrence of subsurface water and most importantly groundwater, it is important to understand it. Some researchers use Richards' equation to model infiltration. The effectiveness of Richards' equation seems to be highly affected by the heterogeneity in water content; pressures; and randomly changing fluxes with time. This limits it from yielding results that mimic the physical unsaturated system. Alternatively, other studies make use of models that incorporate numerous assumptions that oversimplify the physical system. One of them is an infiltration model by Green and Ampt (1911) which is based on the assumptions that a porous media has homogeneous and isotropic properties. The mathematical expression of the Green and Ampt (1911) model is given by

$$f_p = \frac{K_s(L+S)}{L} \tag{2.2}$$

Where K_s is hydraulic conductivity when the soil is saturated; L is the depth of infiltration, and S is capillary suction. Green and Ampt model is based on oversimplified assumptions that do not really exist in a real natural system but its application has produced useful results. Another popular model for expressing infiltration is the one proposed by Horton (1940). Horton described infiltration based on the theory that the infiltration rate is less than the rainfall intensity. He also assumed that water ponds form on the soil surface and that infiltration rate declines continuously with time. Horton's function is commonly used to describe infiltration; it is mathematically expressed as

$$f(t) = f_c + (f_0 - f_c)e^{-kt} \tag{2.3}$$

$$0 \leq \mathrm{t} \leq \mathrm{t_d}$$

Where

k is the decay constant

f_c is the final equilibrium infiltration capacity

f_0 is the initial capacity at $t = 0$

$f(t)$ is the infiltration capacity at any time as from the beginning of the rainfall

t_d is the rainfall duration

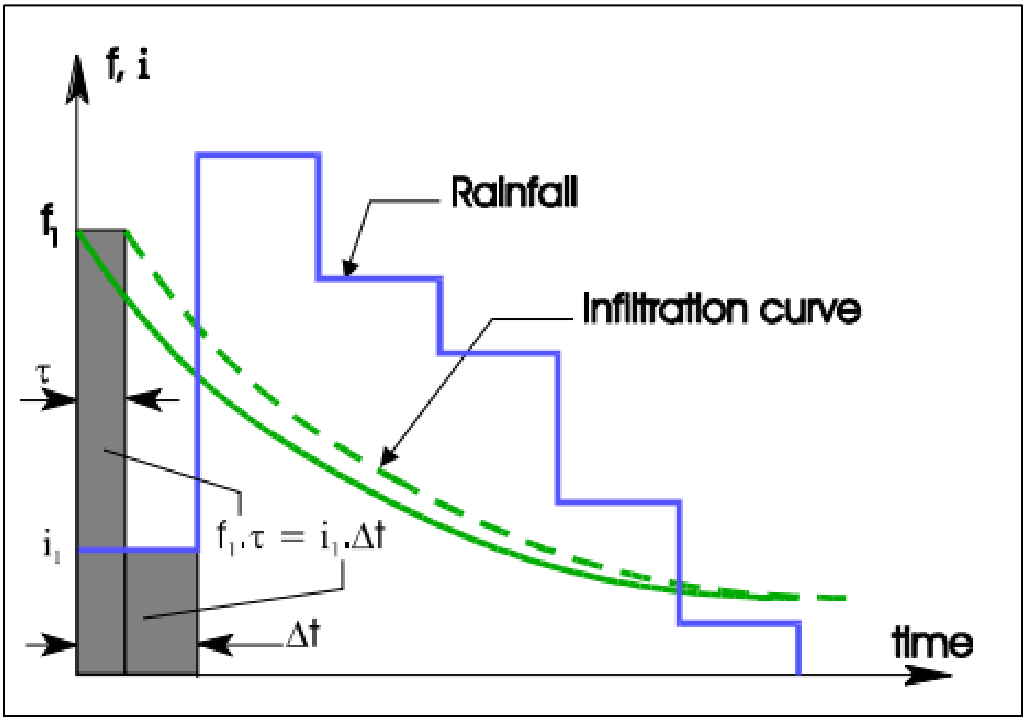

Figure 6: Horton's model for infiltration (MIDUSS version 2 Reference manual, 2004).

Figure 6 above is a typical graph for expressing the infiltration capacity of soils obtained using Horton's model. At any time interval, it is possible to obtain the depth of infiltration by calculating the area under the infiltration capacity curve. Assumptions made by Horton (1940) are not always valid. Sometimes rainfall intensity is less than infiltration rate. For this reason, many studies consider infiltration capacity to vary with cumulative infiltration volume than with time. This leaves Horton's equation to be valid only when storm intensity exceeds soil infiltration capacity, usually during heavy storms. Since there is no perfect model for infiltration, researchers make use of these models with the aid of some modifications and extensions of assumptions. The choice on which model to use depends on the nature of a problem and whether the model is based on realistic assumptions for a given natural situation.

2.3.2 Drainage and redistribution

Infiltration process introduces water to the soil to wet the soil from the surface to a certain depth, sometimes the entire soil profile gets saturated. After some time when precipitation or irrigation has stopped ponding water on the surface disappears and infiltration stops. However, the migration of water in the subsurface does not stop immediately (Wetzel et al., 1996). Water continues to move (Youngs and Poulovassilis, 1976) to regions with lower total potential energy by sucking water from the wetted top layer. In cases where the soil was fully saturated during infiltration, water movement occurs by means of internal drainage. This usually occurs in the presence of a shallow groundwater table, eventually soil water gets discharged to groundwater as groundwater recharge. In cases where the soil was partially saturated during infiltration water movement occurs by means of redistribution (Hillel, 2004). In most cases redistribution occurs where the groundwater table is deep and does not pose a significant role in soil water percolation processes. The movement of water can be in either vertical or horizontal direction or both depending on the potential gradients. Gravity plays a major role combined with the matric pressure gradients and soil hydraulic conductivity in continuously draining the water to deeper parts of the unsaturated zone until the saturated flow is reached.

2.3.2.1 Internal drainage

In a soil volume that was fully saturated when infiltration stopped gravitational potential becomes the only active energy. Under the influence of gravity, water tends to flow towards the groundwater table (Gallage et al., 2013). The vertical movement of water towards the groundwater table draws water from the top layer resuming unsaturated flow conditions. If another infiltration episode does not occur pores get emptied. Larger pores are emptied first and moisture content declines continuously leaving the flow narrowed to small pores (Tarboton, 2003). Therefore, the rate for internal drainage highly depends on pore sizes.

2.3.2.2 Soil water redistribution

As water is absorbed into the top parts of the unsaturated zone through infiltration moisture content in soil rises. Depending on the amount of water that has been absorbed the wet portion extends to a certain depth below the earth's surface. The forces that influence water movement during infiltration continue to act and water continues moving in the subsurface (Peck, 1971). For water to move from the wet upper parts of the unsaturated to other parts drainage of moisture from wet parts occurs due to the influence of gravity and matric potential. The pores are drained and water is replaced by air; as mentioned above larger pores are drained first and filled with air leaving only small pores filled with water. Water content tends to decline with depth and time (Youngs and Poulovassilis, 1976). Figure 7 clearly elaborates how moisture declines with depth after some time when a storm has passed. When water moves from a wetted soil layer at the top to dry deeper soil the rate of movement declines (Hillel, 2004). This is because the capillary forces in soil tend to hold back some moisture resulting in a decrease in residual flow. The amount of water that is held back depends on the soil texture; fine sands tend to retain more water compared to coarse sands. To add, coarse-grained soils lose water quickly and a lot of water at once and a typical graph of water content decline is expected to be much steeper compared to a typical graph for fine grained-sands.

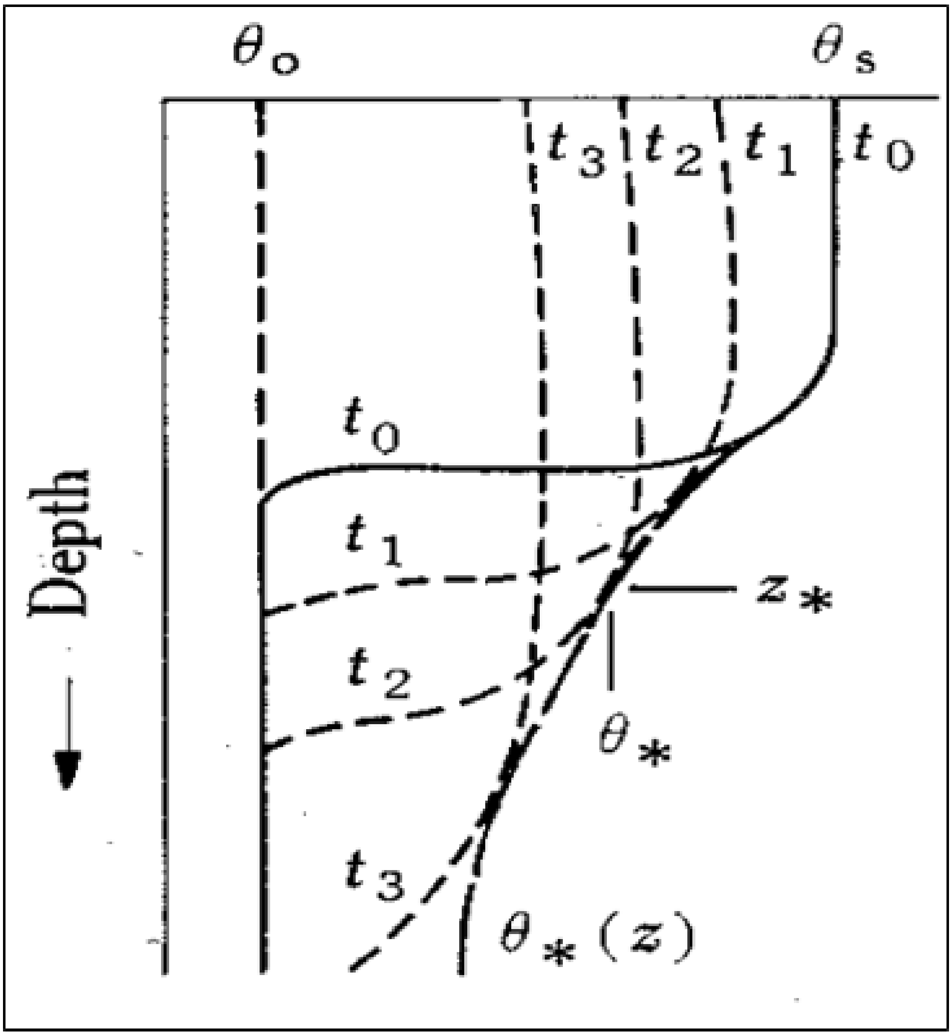

Figure 7: A schematic illustration of how soil moisture is redistributed across space and time (Peck, 1971).

The decline in moisture content leaves a small volume of pores with water and flow path becomes more tortuous and complex. Moisture content declines continuously which increases the tortuosity of the flow path (Gallage et al., 2013).

2.3.2.3 Lateral flow

Lateral flow occurs in unsaturated soils (Neitsch et al., 2011). Even though the vertical flow is most common and tends to grab most of the attention in moisture flow modelling, it is important to look at lateral flow as well. The condition for lateral flow is that the soil horizon must be at a slope so that gravity can pull water down the slope. Results from a laboratory experiment conducted by Singh and O'Callaghan (1978) proved that horizontal moisture flow in soils occurs especially in stratified soils with layers characterised by significantly different hydraulic conductivities. Moreover, in cases where the groundwater table is shallow lateral flow is common.

2.3.3 Output fluxes in the unsaturated zone

After sometime soil moisture leaves the unsaturated zone to groundwater through percolation as groundwater recharge; atmosphere through evapotranspiration, and surface water bodies through interflow. This section provides a review of those processes that flash out water from the unsaturated zone.

2.3.3.1 Evapotranspiration

Some researchers use the term exfiltration to describe the process that is the exact opposite of infiltration. This is all water fluxes that remove water from the soil surface. The main exfiltration process in tropical and hot climates is evapotranspiration which consists of two processes namely evaporation and transpiration (Rosas-Anderson et al., 2018; Tesfuhuney et al., 2015). Transpiration is a loss of water that is drawn from the soil by plants and leaves plants bodies through evaporation on the surface of plants leaves. In short, transpiration is evaporation of water through plants leaves and stems. It is common in tropical climates where intense vegetation cover is present (Neitsch et al., 2011). Evaporation of soil water directly from the soil surface is the most important one of the two evapotranspiration processes in arid climates with soil surfaces characterized by little or no vegetation cover. When there is enough moisture on the soil surface and atmospheric conditions favour evaporation water will leave the soil back to the atmosphere. Evaporation occurs in two ways, one way is where there is high moisture content at the soil surface and enough radiation energy to extract water from the soil. Another way is when the soil surface is relatively dry and atmospheric conditions are less effective but soil properties (Klocke, 2002). The amount of moisture that leaves the soil through evaporation depends on how exposed the soil is relative to the sun. A study by Gava et al (2013) showed that evaporation is high in bare soil and less where the soil surface is concealed. To add, evapotranspiration is one of the most significant fluxes in the unsaturated zone because it governs energy transfers between the subsurface and the atmosphere (Kang et al., 2009).

2.3.3.2 Interflow

This is a process where water flows laterally in the unsaturated zone and gets discharged from a soil layer before joining groundwater flow (Wetzel et al., 1996). Usually, it occurs where a soil horizon contains soil layers with various hydraulic conductivities. The basic condition is that the layers must be at a slope (Minshall and Jamison, 1965). The main driving force of interflow is the soil layer hydraulic conductivity. If a soil horizon has various types of soil their hydraulic conductivity will also vary and water flow in that specific soil horizon will be affected. If the hydraulic conductivity of the layer on top is significantly greater than that of the layer below (Singh and O'Callaghan, 1978), water will drain fast in the top layer. When it reaches the boundary where it intercepts with the layer having significantly low conductivity the flow will be slow. Water will start to accumulate along the boundary between two soil layers forming a thin layer of wet soil. Continuous accumulation of moisture will feed the thin wet layer until saturation is reached at the boundary and water holding capacity will be exceeded. Where there is a steep slope enough for horizontal flow, the horizontal flow of water will dominate at the boundary of these layers and vertical flow into the less conductive layer will be slow. Continuous horizontal flow of water will result in interflow where it intercepts the earth's surface (Chanasyk and Verschuren, 1983). Interflow is common in watersheds characterized by steep slopes and has an impact on drainage. Minshall and Jamison (1965) studied the impact of interflow on soil water drainage and found that interflow reduces soil moisture. According to Wetzel et al (1996), a sink term for interflow should be included when modelling flow in the unsaturated zone to account for moisture loss to avoid overestimation of soil moisture at certain depths.

2.3.3.3 Groundwater recharge

If there is still access free soil water that is still migrating even after evapotranspiration and interflow, groundwater recharge occurs. By definition, groundwater recharge is a geohydrological process whereby access soil moisture in continuous vertical motion reaches the groundwater table and join saturated flow as new input water to groundwater resources. Recharge occurs both naturally and artificially. In this case, attention is given to natural recharge that is influenced by unsaturated flow processes. All unsaturated flow processes affect groundwater recharge and thus the existence of groundwater resources. Infiltration introduces water to the subsurface which then escapes through evapotranspiration to the atmosphere; get redistributed to other parts of soil with lower total potential energy; discharged on the earth's surface as interflow through lateral flow on hilly slopes; and lastly get discharged to the saturated groundwater zone ("C hapter 6 Groundwater Recharge," 2014). Therefore, all input, redistribution; and output fluxes are essential in understanding the quantity of recharge. In most cases, groundwater recharge is a very slow process and occurs in very small quantities especially in areas with deep groundwater tables. To add, groundwater recharge is divided into direct and indirect recharge (Condesso de Melo, 2015). Direct recharge refers to water that joins saturated flow directly from infiltration water that percolates into groundwater resources. Indirect recharge, on the other hand, refers to recharge through connected streams and surface flow channels.

2.3.4 Other important unsaturated flow processes

2.3.4.1 Capillarity

Capillarity is the process whereby water opposes the pull of gravity and resist flow resulting in unsaturated zone storage. It is controlled by adhesion and cohesion. Water molecules tend to be attracted to the boundaries of particles and remain behind when some water is drained by gravity; this process is known as adhesion. Water molecules are also attracted to one another rising surface tension; this process is defined as cohesion. Mostly capillarity in soils is conceptualised using a bundle of capillary tubes (Childs and Collis-George, 1950; Richards, 1931). Water in capillary tubes rise to a certain level depending on the width of the tube; water rises to higher heights in thin tubes compared to thick tubes. Pores between soil particles are commonly considered as capillary tubes. Since capillary rise is high at thin tubes soils with small pores are expected to hold more water than larger pores. This is the reason why sands drain quickly (Brooks and Corey, 1964) and clays have high water holding capacities. Capillarity is the governing force for soil water retention. Moreover, capillarity also causes upward and horizontal movement of water in soils given a sublayer with high moisture content, high enough to be shared to upper parts. For example, a thin saturated layer just above the water table is saturated from groundwater under capillary pull.

2.3.4.2 Water retention

This is where some water is trapped around or between soil particles and becomes disconnected from the flow which reduces the residual flow quantity. After infiltration percolation occurs in response to gravity to distribute water into deeper parts of soil. As already mentioned water in larger pores is drained first while water in small pores is held back by capillary forces. Some of the water that is draining downward is also sucked into capillary pores and separated from the downward migrating moisture. It is through this process that moisture content in the unsaturated zone decreases through space and time. As mentioned in the previous section, this process is achieved with the aid of capillary forces, adhesive and cohesive forces.

Soil-water retention curve

Understanding water retention process is significant for parameterizing Richards' equation used in modelling flow in the unsaturated zone. Information about water retention is provided in the form of water retention curves. These are curves representing the relationship between the volumetric soil water content and matric head (Boulding and Ginn, 2013)The knowledge of water retention assist in describing pore-size distribution parameters that are used in many models that predict unsaturated hydraulic conductivity (e.g. Burdine, 1953). In a rigid homogeneous soil horizon with only water as a wetting phase and air as a drying phase the air-water system is formed. The typical changes in volumetric water content with a further decline in matric pressure is presented in Figure 8 below.

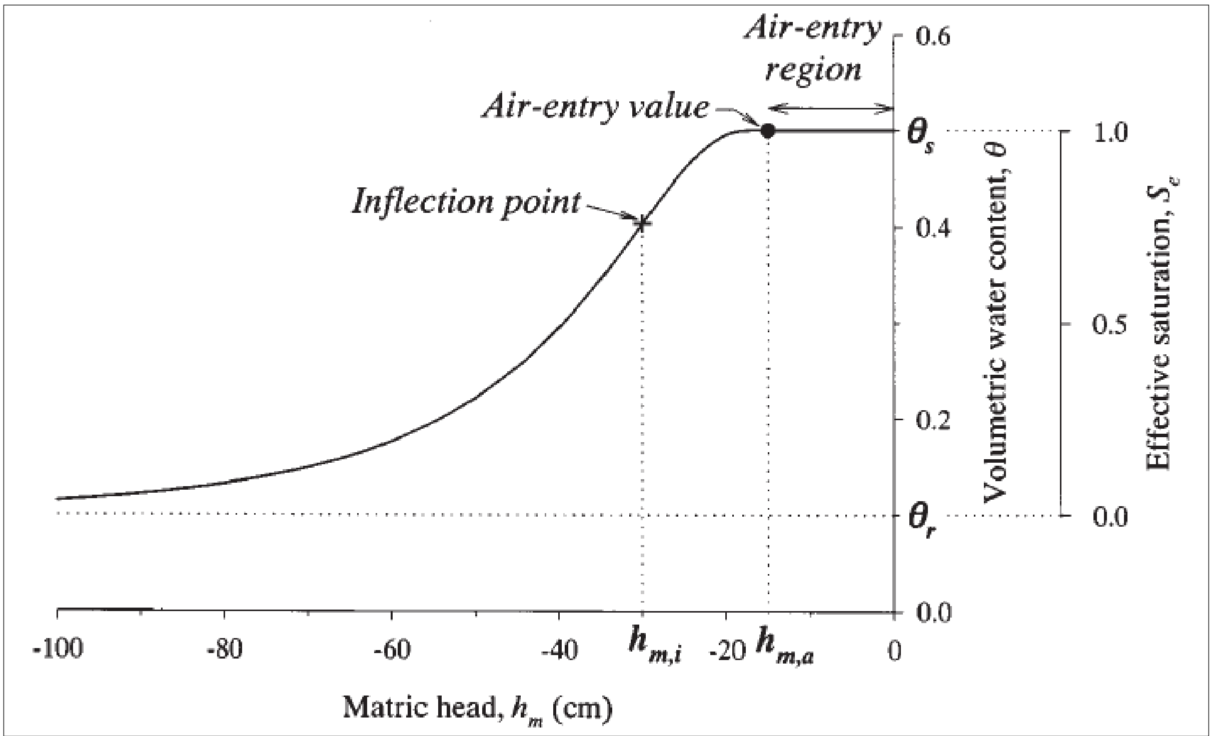

Figure 8: A schematic representation of a typical water retention curve for porous soils (Kosugi et al., 2002)

The main parameters in a water retention curve are: volumetric water content θ; water content at saturation θ_s ; and residual water content θ_r. At saturation, the matric head is zero and volumetric content equals to water content at saturation. Depending on soil hydraulic properties θ remains at θ_s for some time after a storm as long as h_m is approximately zero. At some point h_m goes below zero, with a continuous decline in h_m an air-entry point is reached where the matric head is $h_{m,a}$. At an air entry point soil moisture content starts to decline and air start to replace water in pores, therefore the system becomes unsaturated. h_m becomes more negative when there are many connected large pores forming paths for water to flow through as it drains down a soil volume. When h_m declines to values less than $h_{m,a}$, volumetric soil water content also declines. The decline in θ follows a path similar to a shape, s-shape, of WRC presented in Figure 8 above. The s-shape curve is characterised by an inflection point. Matric head at this point is h_{mi}. If there is no additional moisture that joins the flow system θ continues to decline with h_m towards the lowest water content of the system, residual water content θ_r (Mawer et al., 2015). The water retention curve becomes more flattened towards θ_r (Kosugi et al., 2002). Many models consider θ_s and θ_r as the most wet and dry water contents a system can have respectively. Thus their models fall within the $\theta_r \leq \theta \leq \theta_s$ range. Based on this range the definition of effective saturation is

$$Se = \left(\frac{\theta - \theta_r}{\theta_s - \theta_r}\right) \tag{2.4}$$

and it can only be $0 \leq Se \leq 1$. Direct prediction of WRC data is time-consuming and expensive. Alternatively, there are many reliable theoretical models for estimating the water retention function in the literature (Assouline et al., 1998; Brooks and Corey, 1964; van Genuchten, 1980).

CHAPTER 3: REVIEW OF MODELS PREDICTING UNSATURATED HYDRAULIC CONDUCTIVITY

3.1 Introduction

Unsaturated hydraulic conductivity is one of the key parameters for understanding water flow in porous unsaturated soils. Modelling flow in unsaturated soils starts with understanding this parameter and ways to estimate it. As mentioned in section 2.2.1 there are direct methods, field and laboratory experiments, and indirect methods, theoretical models, for obtaining this parameter. Direct methods are mostly more accurate. However, they are more sophisticated and too demanding (McCartney et al., 2007). Alternatively, theoretical methods are the most preferred. Although theoretical methods are the most preferred they come with a challenge due to the extreme dependence of hydraulic conductivity on water content and pressure which makes it highly non-linear. Researchers have utilized a number of soil properties that are easier to obtain (Burdine, 1953; Childs and Collis-George, 1950; Mualem, 1976; van Genuchten, 1980; Vereecken, 1995) to develop models predicting conductivity. In literature, there are several existing theories and analytical expressions that were developed to estimate unsaturated hydraulic conductivity. Most models require knowledge of water retention functions. This section provides a short review of water retention models followed by a review of some common models for estimating conductivity in unsaturated flows.

3.2 Water retention models

The soil water retention function relates the energy state of the soil water to its water content. If the soil pores are represented by an equivalent bundle of capillaries with identical retention properties as the real soil, a retention function provides the soil's pore-size distribution from which the unsaturated hydraulic conductivity can be predicted. In literature, there is quite a number of models to fit soil water retention data that can be combined with retention curves to obtain unsaturated hydraulic conductivity. The choice on which water retention model to use depend on whether assumptions made to develop a model are suitable for a given natural problem. This involves soil type; how accurate the results are supposed to be; and of cause personal preference in cases where more than one models are suitable to serve the purpose. This section presents two water retention models that are combined with relative hydraulic conductivity models to predict unsaturated hydraulic conductivity functions.

3.2.1 Brooks and Corey (1964) model

In 1964 Brooks and Corey suggested the existence of a power law relationship between effective saturation and soil water energy state. This relationship is mathematically expressed as

$$Se = \left(\frac{h_{m,a}}{h_m}\right)^{\lambda} \tag{3.1}$$

For $h_m < h_{m,a}$

and

$$Se = 1 \tag{3.2}$$

For $h_m \geq h_{m,a}$

As mention in section 2. $h_{m,a}$ is the air-entry head value, see Figure 2.7, λ is a dimensionless parameter associated with pore-size distribution, it is referred to as the pore-size distribution index. It ranges from zero to infinity, with an infinite value for a perfect uniform soil pore-size distribution and zero for highly non-uniform pore-size distribution.

3.2.2 van Genuchten (1980) model

van Genuchten (1980) suggested a continuous empirical model for describing a soil water retention curve by utilizing soil parameters.

$$Se = \left(1 + \left(\frac{h_{m,a}}{h_m}\right)^{\alpha}\right)^{-\beta} \tag{3.3}$$

Where α and β are fitting parameters. This model, as well as the aforementioned model, are popular; they are used in conjunction with relative conductivity models to parameterize Richards' equation presented in section 1.6 covered in the first chapter. Despite their success, they are also associated with some accuracy problems due to the nature of given unsaturated flow situation. For example, Brooks and Corey model does not have an inflection point which makes its accuracy dissipates in situations where the soil is wetted close to saturation and when the soil moisture content is very low. On the other hand, van Genuchten model has a point of inflection which makes it capable of handling highly wetted soils but it shows unsatisfactory performance when dealing with very low soil moisture contents. Therefore, deviations of assumed functions from the true water retention curves are critical at near saturation and at the dry end of the curve. Accuracy of the predictive unsaturated hydraulic conductivity equations is controlled by the adequacy of the soil water retention model over the water content range of interest. A common assumption made in both above models is that water content never goes below residual water content irrespective of how small the pressure head becomes. This is not always true in real soils; it is possible and common in arid climates for water content to be less than residual water content and sometimes it can be zero. For this reason, Zhang (2010) suggested a model for soil water retention by extending the lower limit of capillary-based models to zero. This was done in order to accommodate conditions where water content is less than residual water content. The proposed model covers water retention for full-range saturation and is accurate for soils with very low water contents, see Figure 9. The model accounts for both capillary flow and flow due to absorptive forces in the soil, film flow. The resultant water retention curve comprises of two parts, I and II representing capillary and film flow respectively. Part I and part II are separated by a critical point which is a point where relatively dry conditions start.

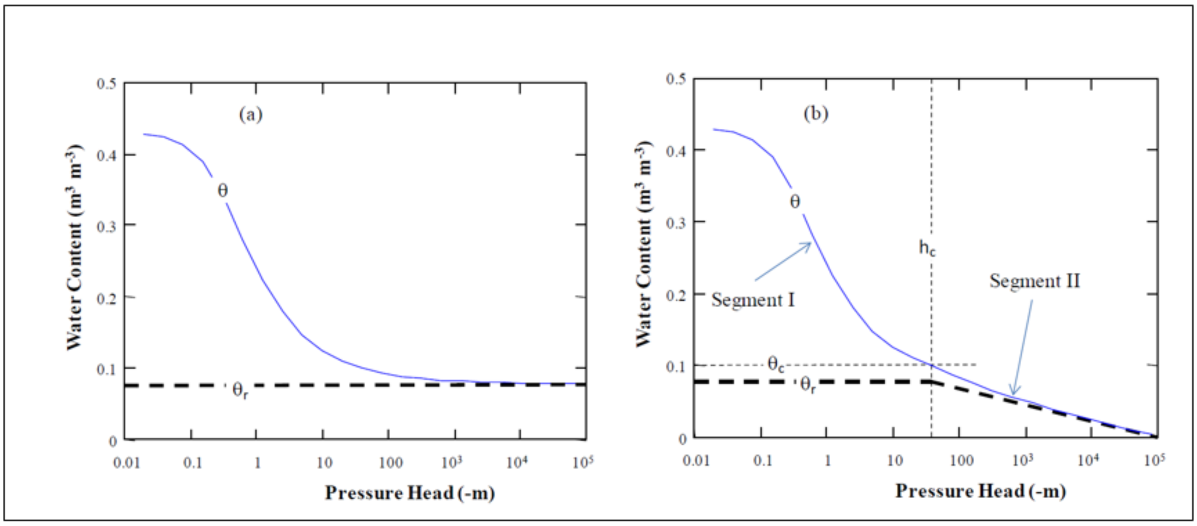

Figure 9: A schematic representation of a typical Water Retention Curve based on (a) Capillary flow and (b) both Capillary and Film flow (Zhang, 2010).

3.3 Models for predicting hydraulic conductivity in unsaturated flows

The models that will be reviewed are Child and Collis-George (1950) model; Burdine (1953) model; Brooks and Corey (1964) model; Mualem model (1976) model; and van Genuchten (1980) model. Hydraulic conductivity of unsaturated soils is a product of saturated hydraulic conductivity (K_s) and relative conductivity (K_r).

$$K(\theta) = Kr * K_s \tag{3.5}$$

To estimate hydraulic conductivity many approaches start with models for estimating relative hydraulic conductivity.

$$Kr = \frac{K_s}{K} = Se^x \tag{3.6}$$

and substitute the resultant expression into equation 3.5 to obtain an expression describing conductivity. K is absolute conductivity; Se is effective saturation, and the power on Se mostly describe parameters associated with soil properties.

3.3.1 Theoretical basis of some popular models

3.3.1.1 Child and Collis-George (1950) model

A Kozeny-type model was revised to come up with a model for estimating conductivity. Unlike Kozeny-type that use soil particle sizes to estimate hydraulic conductivity Child and Collis-George (1950) used pore-size distribution. To achieve that, they used a bundle of capillary tubes to reproduce a natural unsaturated flow system. They conducted an experiment on a fraction of a sand volume to describe the distribution of pore sizes. The fraction has a cross-sectional area described by $f(r)\delta r$; where $f(r)$ represents pore space distribution of pores with r to $r + \delta r$ radius. The sand is split into two identical planes. If one plane is considered to have an area of a_σ and a radius ranging from σ to $\sigma + \delta\sigma$ and the other one has the area of a_ρ and a radius ranging from ρ to $\rho + \delta\rho$ the following equation describes the area in both planes

$$a_\rho = f(\rho)\delta r, \quad a_\sigma = f(\sigma)\delta r \tag{3.7}$$

The pore sequence $\rho \rightarrow \sigma$ will have an area of

$$a_{\rho\rightarrow\sigma} = f(\rho)\delta r f(\sigma)\delta r \tag{3.8}$$

Child and Collis-George (1950) model is based on the assumption that as drainage occurs in unsaturated flows larger pores lose their moisture first and small pores have a tendency of resisting flow thus water is retained in small pores. Another assumption is that contribution to flow permeability is only by connected pores. If σ represents the radius of the small pores, then the number of small pores is proportional to σ^{-2}. By applying the Poisseailles' equation the rate of flow in each pore becomes proportional to σ^4 per unit potential gradient. The contribution of small pores to the total permeability is

$$\delta K = \sigma^2 M f(\rho)\delta r f(\sigma)\delta r \tag{3.9}$$

and the total permeability is

$$K = M \sum_{\rho=0}^{\rho=R} \sum_{\sigma=0}^{\sigma=R} \sigma^2 f(\rho)\, \delta r f(\sigma) \delta r \tag{3.10}$$

This equation emphasizes the effect of cross-sectional area and neglects the fact that some cells may have different sizes which result in different lengths.

<u>3.3.1.2 Burdine (1953) model</u>

Burdine (1953) conducted a study to formulate relative permeability functions of unsaturated flows. The model is an extension of models that are based on capillary columns to mimic pores in soils. Burdine (1953) incorporated the flow tortuosity term in the equation and developed equations predicting relative permeability for both wetting and non-wetting phases. It was pointed out that tortuosity is directly related to volumetric water content and the relationship is linear. The model for relative hydraulic conductivity during wetting is given by

$$K_{rw} = \left(\frac{S - S_r}{1 - S_r}\right)^2 \int_0^S \frac{ds}{{P_c}^2} \Big/ \int_0^1 \frac{ds}{{P_c}^2} \tag{3.11}$$

Burdine's theory has been adopted by many researchers to develop theoretical expressions for predicting unsaturated hydraulic conductivity (e.g. Brooks and Corey, 1964; Mualem, 1976; van Genuchten, 1980) which are essential for modelling unsaturated flow processes.

<u>3.3.1.3 Brooks and Corey (1964) model</u>

This model utilizes bubbling pressure and pore-size distribution index to predict hydraulic conductivity in a system with two non-mixing fluid phases namely the non-wetting phase and wetting phase. In most cases, it is only the wetting phase that is expressed using Darcy's law. Brooks and Corey (1964) made an assumption that as long as there are connected pores in a system to allow flow Darcy's law may be applicable in expressing both wetting and drying phases. Darcy's law is given by

$$q_x = -\frac{K_x}{\mu}\left(\frac{\Delta P}{L_x} + \frac{\gamma \Delta h}{L_x}\right) \tag{3.12}$$

Where q is the flux and x is the flow direction; K is flow conductivity; μ is the fluid viscosity; L is the flow distance; γ is the term for specific yield; ΔP and Δh are changes in pressure and elevation respectively.

The governing assumption of this model is that the two phases are immiscible and separated by curved interfaces. Another assumption is that saturation conditions are relatively high in a flow system with pores that are large enough to permit flow. Therefore, model validity is highly dependent on the presence of large pores and moisture content. It is not accurate for cases where the system is relatively dry with saturation less than field capacity and porous media with extremely small pores such as clays.

Capillary pressure P_C exists at the interface of wetting and drying phase. In most cases, capillary pressure is greater in the drying phase and less in the wetting phase

$$P_C = P_{gas} - P_{Liquid} \tag{3.13}$$

For a given saturation small pore tend to have high capillary pressure compared to larger pores. To come up with a model, Burdine theory was adopted for relative hydraulic conductivity

$$K_{rw} = \left(\frac{S - S_r}{1 - S_r}\right)^2 \int_0^S \frac{ds}{{P_c}^2} \Big/ \int_0^1 \frac{ds}{{P_c}^2} \tag{3.14}$$

which by placing an effective saturation term becomes

$$K_{rw} = (Se)^2 \int_0^{Se} \frac{dSe}{{P_c}^2} \Big/ \int_0^1 \frac{dSe}{{P_c}^2} \tag{3.15}$$

An expression defining the relationship between effective saturation and capillary pressure was proposed after close observations of experimental data in the petroleum industry

$$Se = \left(\frac{P_b}{P_c}\right)^{\lambda} \tag{3.16}$$

For $P_c \geq P_b$

Where P_b is pressure due to the largest pores forming a continuous network and λ is pore-size distribution index. The famous Brooks and Corey model was then developed by combining equations n and m to yield

$$K_{rw} = (Se)^{\frac{2+3\lambda}{\lambda}} = (Se)^{\varepsilon} \tag{3.17}$$

This model is associated with some limitations. As the bubbling pressure becomes more negative it affects results from numerical simulations. The slope of both unsaturated conductivity curve and water-retention curve becomes discontinuous; it can result in delayed convergence in numerical simulations of coupled unsaturated-saturated systems. This is not a universal model since it was developed for sands and is limited to relatively dry and moderately wet soils. In soils with very high moisture content this model is not accurate. To add, the model cannot be used for very fine soils such as clays because they are associated with extremely high capillary pressures which hinder flow. Moreover, it is assumed that the geometry of the porous media is fixed throughout the whole range of applicable saturation which is extremely rare in soils.

3.3.1.4 Mualem (1976) model

Mualem suggested a model for approximating unsaturated hydraulic conductivity from water retention curves. He made use of the moisture content-capillary head curve and the saturated hydraulic conductivity as parameters for determining unsaturated hydraulic conductivity. Mualem's theory is similar to the one of Childs and Collis-George discussed above with modification on the contribution of large pores to the total permeability. In this case, it is assumed that there is a significant contribution to permeability by large pores. Like other pre-existing expressions of relative hydraulic conductivity, Mualem used a power law relationship to express the relationship between relative conductivity and effective saturation

$$K_r = K/K_{sat} = Se^{\alpha} \tag{3.18}$$

Soil water conductivity was approximated with the aid of capillary head-water content curves. Same procedure as that performed by Childs and Collis-George was followed using a homogeneous soil profile. Considering two similar portions of soil taken out from the same profile; one with pore radius r and another one with pore radius p where the contribution of connected pores with radius r to $r + dr$ to the moisture content θ is

$$F(r)\, dr = d\theta \tag{3.19}$$

Equation (3.10b) is also

$$\int_{R_{min}}^{R} f(r)\, dr = \theta(R) \tag{3.20}$$

To be particular

$$\int_{R_{min}}^{R_{max}} f(r)\, dr = \theta_{sat} \tag{3.21}$$

$f(r)\, dr$ is also the ratio of area covered by pores with radius ranging from r to $r + dr$ to the total area. The probability of pores at different slabs to be in contact is expressed as

$$a(r, \rho) = f(r) f(\rho\,)\, dr\, d\rho \tag{3.22}$$

This means that there is no direct connection between pores in different slabs. One of Mualem's objectives was to find the effect of pores having different sizes on the conductivity of a porous media under unsaturated conditions. When slab consisting of pores with a radius ranging from ρ to $\rho + d\rho$ have the length equal to the pore radii the probability becomes

$$a(r,\rho) = G(R,r,\rho)f(r)f(\rho)\; dr\; d\rho \tag{3.23}$$

In the above equation $G(R,r,\rho)$ accounts for the partial correlation that exists between pores with radius r and ρ for a given water content. It was assumed that the bypass flow between the pores in two slabs is absent; and that the pore configuration may be replaced by a pair of capillary elements whose lengths are proportional to their radii

$$l_1/l_2 = r/\rho \tag{3.24}$$

This means that large pores really have a significant contribution to unsaturated conductivity than it is usually assumed. It was found that conductivity varies with pore size distribution and tortuosity. To account for tortuosity a correction factor $T(R,r,\rho) < 1$ was introduced. The factor also accounts for the contribution of the $r \rightarrow \rho$ element to the relative conductivity and equation below was obtained

$$dK_r(r,p) = \frac{T(R,r,\rho)G(R,r,\rho)r\rho f(r)f(\rho)\; dr\; d\rho}{\int_{R_{min}}^{R_{max}}\int_{R_{min}}^{R_{max}} T(R_{max},r,\rho)G\;(R_{max},r,\rho)r\rho f(r)f(\rho)\; dr\; d\rho} \tag{3.25}$$

For a given $\theta(R)$ the equation above is written as

$$K_r(\theta) = \frac{\int_{R_{min}}^{R}\int_{R_{min}}^{R} T(R,r,\rho)G(R,r,\rho)r\rho f(r)f(\rho)\; dr\; d\rho}{\int_{R_{min}}^{R_{max}}\int_{R_{min}}^{R_{max}} T(R,r,\rho)G(R,r,\rho)r\rho f(r)f(\rho)\; dr\; d\rho} \tag{3.26}$$

The values of correction factors seem to be highly dependent on R. Hence

$$K_r(\theta) = Se^n \frac{\int_{R_{min}}^{R} rf(r)\; dr \int_{R_{min}}^{R} \rho f(\rho)\; d\rho}{\int_{R_{min}}^{R_{max}} rf(r)\; dr \int_{R_{min}}^{R_{max}} \rho f(\rho)\; d\rho} = Se^n \left[\frac{\int_{R_{min}}^{R} rf(r)\; dr}{\int_{R_{min}}^{R_{max}} rf(r)\; dr}\right]^2 \tag{3.27}$$

A much simpler equation that is easy to apply is obtained by applying capillary law and substituting equation (3.21) on the above equation

$$K_r(\theta) = Se^n \left[\int_0^{\theta} \frac{d\theta}{\psi} \Big/ \int_0^{\theta_{sat}} \frac{d\theta}{\psi}\right]^2 \tag{3.28}$$

Where n may be positive or negative. By substituting analytical expressions for $\varphi(\theta)$ to the above equation, $K_r(\theta)$ can be easily derived. For example, the expression by Brooks and Corey (1964)

$$Se = (\varphi/\omega_{cr})^{-\lambda} \tag{3.29}$$

yields

$$K_r(Se) = Se^{n+2+\frac{2}{\lambda}} \tag{3.30}$$

This expression has been useful and produced reliable results that are close to natural unsaturated systems. n has a significant impact on how close the results physical mimic experimental data. Some literature include it (Burdine, 1953) and some exclude it (Brooks and Corey, 1964).

<u>3.3.1.5 van Genuchten (1980) model</u>

Van Genuchten (1980) used Mualem (1976) capillary theory to derive a closed-form analytical expression using a continuous soil water retention curve with a continuous slope. The derived expression for unsaturated hydraulic conductivity has three independent parameters which are obtained by matching the soil-water retention curve to empirical data. Mualem (1976) used saturated hydraulic conductivity and soil-water retention curve to formulate a model of approximating unsaturated hydraulic conductivity. Using the same theory van Genuchten (1980) came up with a reliable expression for conductivity. The definition of relative hydraulic conductivity by Mualem (1976) is given as

$$K_r = Se^{\frac{1}{2}}\left[\int_1^{Se} \frac{1}{h(x)}\,dx \Big/ \int_0^1 \frac{1}{h(x)}\,dx\right]^2 \tag{3.31}$$

Where Se is effective saturation and h is the pressure head which is given as a function of Se. The relationship between Se and h is expressed as

$$Se = \left[\frac{1}{1+(\alpha h)^n}\right]^m \tag{3.32}$$

Where α, m, n are fitting parameters that are determined empirically. To derive an expression for conductivity van Genuchten (1980) imposed certain restrictions on the values of m and n in equation (3.32) and solved it to obtain an expression that was then substituted into equation (3.31). The following was obtained

$$K_r(Se) = Se^{\frac{1}{2}}\left[\frac{f(Se)}{f(1)}\right]^m \tag{3.33}$$

Where

$$f(Se) = \int_0^{Se}\left[\frac{x^{\frac{1}{m}}}{1-x^{\frac{1}{m}}}\right]^{\frac{1}{n}} dx \tag{3.34}$$

y is considered as an auxiliary variable, substituting $x = y^m$ into equation (3.34) to obtain a general particular form of Beta-function

$$f(Se) = m\int_0^{Se^{\frac{1}{m}}} y^{m-1+\frac{1}{n}}(1-y)^{-\frac{1}{n}}\,dy \tag{3.35}$$

This is not a closed form equation; to obtain a closed form all integer values of $K = m - 1 + \frac{1}{n}$ integration becomes easy. When $K = 0$ then $m = 1 - \frac{1}{n}$ and

$$f(Se) = 1 - \left(1 - Se^{\frac{1}{m}}\right)^m \tag{3.36}$$

Since $f(1) = 1$, equation (3.33) becomes

$$K_r(Se) = \left[1 - \left(1 - Se^{\frac{1}{m}}\right)^m\right]^2 \tag{3.37}$$

van Genuchten (1980) also derived an expression based on Burdine's model (1953). He used the same procedure explained above and substituted expression that was obtained from solving equation (3.32) into equation (3.33) to obtain

$$K_r(Se) = Se^2\left(\frac{f(Se)}{f(1)}\right) \tag{3.38}$$

Where

$$f(Se) = \int_0^{Se}\left[\frac{x^{\frac{1}{m}}}{1-x^{\frac{1}{m}}}\right]^{\frac{2}{n}} dx \tag{3.39}$$

Substituting $x = y^m$ into equation (3.39) to yield

$$f(Se) = m\int_0^{Se^{\frac{1}{m}}} y^{m-1+\frac{2}{n}}(11-y)^{-\frac{2}{n}}\,dy \tag{3.40}$$

To reduce equation (3.40) it was assumed that the power of y, $m = 1 - \frac{2}{n}$, vanishes and equation (3.39) becomes

$$f(Se) = 1 - \left(1 - Se^{\frac{1}{m}}\right)^m \tag{3.41}$$

Therefore an expression for relative hydraulic conductivity is given by

$$K_r(Se) = Se^2\left[1-\left(1-Se^{\frac{1}{m}}\right)^m\right] \tag{3.42}$$

$$m = 1-\frac{2}{n};\ 0 < m < 1; n > 2$$

The above expression is equivalent to the one that was obtained using Mualem (1976) theory.

Models by Childs and Collis-George; Burdine; and Mualem are all based on the use of capillary bundles to represent the pore spaces in a homogeneous porous media. The common governing theory in these models is that water in soils flows through interconnected pores and that the size distribution of these pores is characterized by the shape of the water retention curve of a specific soil. They all utilize pore-size distribution to predict unsaturated hydraulic conductivity. They go separate ways when it comes to relating r_e to r, ρ and R_f. Childs and Collis-George considered flow effective radius to be equivalent to the radius of pores with small radius assuming that only pores with small radius contribute to the hydraulic conductivity. Burdine used $r_e = r\left(\theta\left(R_f\right)\right)^{\frac{1}{2}}$ to describe the relationship between r_e and r, ρ and R_f. Mualem, on the other hand, proposed that the effective radius is equal to the product of radius of both pores with small a radius and pores with a large radius. In this case, it is assumed that pores with a large radius also contribute to hydraulic conductivity. All three theories yield

$$\frac{K(\theta)}{K_s} = \left(\frac{\theta-\theta_r}{\theta_s-\theta_r}\right)^b\left[\int_0^{Se}\frac{dx}{\psi(x)}\Big/\int_0^1\frac{dx}{\psi^{2-r}(x)}\right]^m \tag{3.43}$$

Where constants b, r, and m are associated with pore-size distribution. The values of these constants tend to vary for each model. For example, according to Mualem (1976), the constants are: $b = 0.5$; $r = 1$; and $m = 2$; Burdine, on the other hand, suggested that $b = 2$; $r = 0$; and $m = 1$.

These theories provide a basis for estimating unsaturated hydraulic conductivity. Analytical models describing $\theta - \psi$ relationship such as those proposed by Brooks and Corey (1964) and van Genuchten (1980) may then be used to obtain a hydraulic conductivity function. Assouline et al (1998) suggested a model for soil water retention function based on the concept of particle size distribution, by assuming that fragmentation processes change the soil structure. The resultant soil water retention function is applicable to both high and low moisture conditions and consists of two fitting parameters.

$$Se(\psi) = 1 - exp\left(-\xi\left(|\psi|^{-1} - |\psi_L|^{-1}\right)\right)^{\mu} \tag{3.44}$$

$$\text{For } 0 \leq |\psi| \leq |\psi_L|$$

Where ξ and μ are fitting parameters, ψ_L represents capillary head at relatively low moisture conditions. Assouline and Tartakovsky (2001) proposed a model based on soil structure and texture

$$K_r(Se) = \left[\int_0^{Se} \frac{ds}{\psi} \Big/ \int_0^1 \frac{ds}{\psi}\right]^{\eta} \tag{3.45}$$

η is a parameter associated with soil structure and texture. Combining the above equation with the WRC model proposed by Brooks and Corey yields

$$K_r(Se) = Se^{\frac{(\eta+\eta\lambda)}{\lambda}} \tag{3.46}$$

Assouline (2005) conducted a study to relate the pore-size distribution index and η a soil structure and texture describing parameter

$$\eta = 1.4\lambda^{0.717} \tag{3.47}$$

and found that λ can be used to obtain η which can be substituted in Assouline and Tartakovsky (2001) model to obtain another model describing relative hydraulic conductivity

$$K_r(Se) = Se^{\alpha} \tag{3.48}$$

Where

$$\alpha = a\left(\lambda^b + \lambda^{(b-1)}\right) \tag{3.49}$$

a and b are empirical parameters. The use these models have produced great success in literature. With recent technologies and scientific inputs on soil hydrological sciences modifications have been made and new models have been developed based ancient theories. For example, Neto (2013) developed a model by combining Burdine (1953) and Mualem (1976) relative conductivity predicting models with the water retention curve model by van Genuchten (1980). His focus was on getting rid of restricting factors associated with these theories to produce more a flexible analytical solution that is applicable to a wide range of soil type. A less restricted model proposed by Neto (2013) based on Mualem (1976) model is given by

$$K_r(Se) = \left[\frac{Se^{\frac{\lambda}{2}+\frac{1}{m.n}+1}\left(1+\eta_1 Se^{\frac{1}{m}}+\eta_2 Se^{\frac{2}{m}}+\eta_3 Se^{\frac{3}{m}}+\eta_4 Se^{\frac{4}{m}}\right)}{1+\beta}\right]^2 \tag{3.50}$$

Where

$$\beta = \frac{(mn+1)}{n^4}\left[\frac{n^3}{(mn+n+1)}+\frac{(n+1)n^2}{2(mn+2n+1)}+\frac{(n+1)(2n+1)n}{6(mn+3n+1)} + \frac{(n+1)(2n+1)(3n+1)}{24(mn+4n+1)}\right] \tag{3.51}$$

and

$$\eta_1 = \frac{(mn+1)}{n(mn+n+1)} \tag{3.52}$$

$$\eta_2 = \frac{(mn+1)(n+1)}{2n^2(mn+2n+1)} \tag{3.54}$$

$$\eta_3 = \frac{(mn+1)(n+1)(2n+1)}{6n^3(mn+3n+1)} \tag{3.55}$$

$$\eta_4 = \frac{(mn+1)(n+1)(2n+1)(3n+1)}{24n^4(mn+4n+1)} \tag{3.56}$$

Apart from the afore-reviewed capillary models, there are other approaches that have provided great success in predicting hydraulic conductivity for unsaturated flows. There are those that are based on percolation theory (Ghanbarian-Alavijeh and Hunt, 2012). It has been proven that compared to capillary tube models these models yield best results for soils with high moisture contents. However, at very low moisture contents like capillary models, they underestimate hydraulic conductivity.

3.4 Accuracy tests

Two comparison procedures, Root of the Mean Squared Error (RMSE) and Akaike's information criterion (AIC) are used to evaluate the performance of the theoretical models for predicting unsaturated hydraulic conductivity.

The Root of the Mean Squared Error (RMSE)

RMSE is a tool for evaluating the performance of theoretical models on reproducing the natural unsaturated system. It demonstrates how predicted values deviate from observed data. Mathematically RMSE is expressed as

$$RMSE = \sqrt{\frac{\sum_{i=1}^{n}((Kmeas)_i - (Kest)_i)^2}{N}} \tag{3.57}$$

Where $Kmeas$ and $Kest$ represent measured and estimated hydraulic conductivity respectively and N is the sample size. It has been used by many researchers to test models which are best fit for observed experimental data. For example, Neto (2013) and Assouline (2005) used RMSE to evaluate the performance of models that they proposed compared to the performance of pre-existing popular models.

The Akaike's information criterion (AIC)

AIC is another way of evaluating the performance of conductivity models and is expressed mathematically as

$$AIC = N \ln\left(\frac{RSS}{N}\right) + 2q \tag{3.58}$$

Where N is the sample size; RSS is the likelihood and q is a number of parameters in a model. This is a statistical tool that is used to select models sustainable for a given problem (Akaike, 1973). It provides the relative performance of models.

CHAPTER 4: THE NON-LINEAR UNSATURATED FLOW MODELS

4.1 Introduction

Richards' equation is the tool for modelling non-steady vertical movement of moisture in the unsaturated zone. Finding solutions to this governing equation requires knowledge on soil water retention function and unsaturated hydraulic function such as those presented in the previous chapter. This chapter presents solutions to Richards' equation with unsaturated hydraulic conductivity described by Mualem (1976) and Brooks and Corey (1964) theoretical models. The models are combined with a soil water retention function suggested by Brooks and Corey (1964). Because of the non-linear nature of these models, the resultant Richards' equation is highly non-linear; therefore solving it requires numerical analysis with appropriate numerical approximation schemes. In this thesis, solutions will be obtained using the well-known Crank-Nicolson Scheme and a recently proposed Laplace Adam-Bashforth Scheme.

4.2 Theory

Understanding non-steady vertical soil moisture flow is challenging but Richards' equation has been utilized for decades and showed great success. As mentioned in section 1.6 mixed-form Richards' equation can be split into a water content based form or a head based form. In this study, unsaturated water movement will be expressed using a water content based form of Richards' equation. To recall,

$$\frac{\partial \theta}{\partial t} = D\frac{\partial^2 \theta}{\partial z^2} + \frac{\partial K(\theta)}{\partial z} \tag{4.1}$$

Where θ is volumetric water content; $K(\theta)$ is unsaturated hydraulic conductivity, D is the term for pore water diffusivity; t is the time elapsed and z is the vertical distance in a soil column. Solving equation (4.1), as already mentioned, requires the knowledge on unsaturated hydraulic function. Obtaining unsaturated hydraulic function requires knowledge on soil water retention characteristic which is a unique signature for every soil volume. Therefore, a procedure for understanding unsaturated flow starts with identifying a soil moisture retention curve that is based on assumptions that reflects water retentions of a natural system. Secondly, finding a model that will be combined with a retention function to estimate hydraulic conductivity. Then incorporating hydraulic conductivity function into Richards' equation to find solutions that represent the unsaturated flow system. Existing models for predicting retention curves and conductivity functions are highly non-linear but they based on assumptions that simplify a complex system to a more understandable system.

Consider a homogeneous soil volume with pores equivalent to cylindrical capillary tubes. Assuming that pore-size distribution is equivalent to the shape of soil water retention curve proposed by Brooks and Corey (1964) given by

$$Se(\theta) = (\varphi/\omega_{cr})^{-\lambda} \tag{4.2}$$

Then the definition of effective saturation becomes

$$Se(\theta) = \left(\frac{\theta - \theta_r}{\theta_s - \theta_r}\right) \tag{4.3}$$

Assuming a pore-size distribution index of 2 for the soil, two parametric theoretical models are used to predict unsaturated hydraulic conductivity

$$K(\theta) = K_s * Kr \tag{4.4}$$

Saturated hydraulic conductivity is easy to obtain. Using equation (4.4) above unsaturated hydraulic conductivity can be estimated as long as knowledge on relative hydraulic conductivity is available. The following two subsections present models for estimating relative hydraulic conductivity based on basic soil properties.

4.2.1 Application of Brooks and Corey (1964) model to Richards' equation

A model by Brooks and Corey relating relative hydraulic conductivity to effective saturation will be used to obtain unsaturated hydraulic conductivity. This model utilizes an empirical parameter, pore-size distribution index λ, and saturated hydraulic conductivity K_s to describe the relationship between K_r and Se. Mathematically the relationship is presented as

$$K_r(\theta) = Se^n \left[\int_0^{\theta} \frac{d\theta}{\psi} \Big/ \int_0^{\theta_{sat}} \frac{d\theta}{\psi}\right]^2 \tag{4.5}$$

Combination of equations (4.2) and (4.5) gives

$$K_r(Se) = Se^{\varepsilon} \tag{4.6}$$

Where ε is Brooks and Corey exponent. In this study pore-size distribution index is given the value of 2, therefore ε is expressed as

$$\varepsilon = 3 + \frac{2\lambda}{\lambda} = 5 \tag{4.7}$$

Substituting for ε in equation (4.6) and combining equation (4.6) with equation (4.4) gives the following unsaturated hydraulic conductivity model

$$K(\theta) = K_s * \left(\frac{\theta - \theta_r}{\theta_s - \theta_r}\right)^5 \tag{4.8}$$

Which is substituted into equation (4.1) to get rid of the term for unsaturated hydraulic conductivity resulting in the following equation

$$\frac{\partial\theta}{\partial t} = D\frac{\partial^2\theta}{\partial z^2} + \frac{\partial}{\partial z}\left[K_s\left(\frac{\theta - \theta_r}{\theta_s - \theta_r}\right)^5\right] \tag{4.9}$$

This is the unsaturated flow equation with both soil retention characteristic and hydraulic conductivity function described by Brooks and Corey Models.

4.2.2 Application of Mualem (1976) model to Richards' equation

Relative hydraulic conductivity model proposed by Mualem (1976) will be used to obtain results that will be compared with those from the Brooks and Corey model. The mathematical expression below was suggested to relate relative hydraulic conductivity to effective saturation.

$$K_r(\theta) = Se^n\left[\int_0^\theta \frac{d\theta}{\psi} \Big/ \int_0^{\theta_{sat}} \frac{d\theta}{\psi}\right]^2 \tag{4.10}$$

Substituting an analytical $\varphi(\theta)$ expression by Brooks and Corey (1964)

$$Se = (\varphi/\omega_{cr})^{-\lambda} \tag{4.11}$$

into equation (4.10) yields

$$K_r(Se) = Se^{n+2+\frac{2}{\lambda}} \tag{4.12}$$

Where n is a parameter describing flow tortuosity and λ is pore-size distribution index which is given a value of 2 in this study. Mualem defined n as 0.5, substituting these values and remembering that $Se = (\theta - \theta_r)/(\theta_s - \theta_r)$ yields

$$K_r(Se) = \left(\frac{\theta - \theta_r}{\theta_s - \theta_r}\right)^{3.5} \tag{4.13}$$

Which is substituted into equation (4.4) to obtain

$$K(\theta) = K_s * \left(\frac{\theta - \theta_r}{\theta_s - \theta_r}\right)^{3.5} \tag{4.14}$$

which is the unsaturated hydraulic conductivity model. This equation is substituted into the governing Richards' equation in equation (4.1) to obtain

$$\frac{\partial\theta}{\partial t} = D\frac{\partial^2\theta}{\partial z^2} + \frac{\partial}{\partial z}\left[K_s\left(\frac{\theta-\theta_r}{\theta_s-\theta_r}\right)^{3.5}\right] \tag{4.15}$$

Equation (4.15) is the unsaturated flow equation with soil retention characteristic and hydraulic conductivity function described by Brooks and Corey model and Mualem model respectively. Both governing equations, equations (4.9) and (4.15) are highly non-linear as due to the unsaturated hydraulic conductivity models used. Thus analytical solutions cannot be obtained. Finding solutions to these equations requires the use of computer code. For discretisation purposes equations (4.9) and (4.15) are presented by one non-linear equation

$$\frac{\partial\theta}{\partial t} = D\frac{\partial^2\theta}{\partial z^2} + \frac{\partial}{\partial z}\left[K_s\left(\frac{\theta-\theta_r}{\theta_s-\theta_r}\right)^{\omega}\right] \tag{4.16}$$

Where ω represents the exponent of effective saturation for both equations, $\omega = \varepsilon$ for equation (4.9) and $\omega = 3.5$ for equation (4.15). The next section will cover the numerical analysis of non-linear governing equations.

4.3 Numerical analysis

Obtaining computer simulations of physical systems described by time-dependent differential and partial differential equations requires numerical analysis of equations by means of numerical approximation methods. In this case, the numerical approximation methods of choice must be able to give adequate representations of soil moisture flow. The flow is described by means of a non-linear partial differential equation. There are many schemes that can be used to solve this equation thus a close consideration need to be made when choosing schemes that will give the most appropriate results. For the best choice an overview of different schemes is done, the schemes include: explicit; implicit; Crank-Nicolson; and a recently suggested scheme by Gnitchogna and Atangana (2018), the Laplace Adam-Bashforth method. An explicit method is one that is based on the computation of dependent variables by means of known quantities. It requires less computational effort and computation is easy. However, it is not stable for large size time steps thus conditionally stable. In contrast, the implicit method uses unknown quantities to evaluate the dependent variables. It is stable throughout all sizes of time step although its accuracy decreases with an increase in the size of the time step. Thus for very large size time step, the formulation has to be carefully constructed; this is the reason it requires high computational effort and complicated computation process thus time-consuming. If the computation goal is accuracy an explicit method is best, and if the goal is stability an implicit method is best. On the other hand, Crank-Nicolson scheme is a finite difference scheme that is based on approximating first order derivatives by means of central difference and second order derivatives by means of averages at $(i,j)^{th}$ and $(i,j+1)^{th}$. This scheme is stable and convergent. It is commonly used in many studies since it conquers convergence and stability issues that the explicit scheme has. It is an implicit scheme; therefore it is associated with disadvantages similar to those of the implicit scheme. At every time step, it requires the equation to be solved simultaneously thus time-consuming. The two-step Laplace Adam-Bashforth scheme is the combination of Adam-Bashforth scheme and Laplace transform (Gnitchogna and Atangana, 2018). Since the ordinary Adam-Bashforth scheme has some limitations when solving partial differential equations, the partial differential equations are transformed to ordinary differential equations using Laplace transform. The equations are analyzed in Laplace space to obtain a numerical solution in time variables; the solution is then taken back to its original space by applying the inverse Laplace Transform. This scheme is considered to be highly accurate and stable; the computational procedure is also simple and not time-consuming. In this case both stability and accuracy are of significant importance. Therefore, the Crank-Nicolson scheme and Laplace Adam-Bashforth scheme serve the purpose better than the explicit and implicit schemes because they are both unconditionally stable and convergent. The following subsections will give numerical discretization of equation (4.16) using Crank-Nicolson scheme and Laplace Adam-Bashforth scheme.

Equation (4.16) can be simplified into

$$\frac{\partial\theta}{\partial t} = D\frac{\partial^2\theta}{\partial z^2} + \frac{K_s}{(\theta_s-\theta_r)^\omega}\frac{\partial}{\partial z}(\theta-\theta_r)^\omega \tag{4.17}$$

$$\frac{\partial\theta}{\partial t} = D\frac{\partial^2\theta}{\partial z^2} + \frac{K_s}{(\theta_s-\theta_r)^\omega}\omega\frac{\partial\theta}{\partial z}(\theta-\theta_r)^{\omega-1} \tag{4.18}$$

4.4.1 Crank-Nicolson scheme

The Crank-Nicolson scheme is defined as

$$\frac{\partial\theta}{\partial t} \to \frac{\theta_i^{j+1}-\theta_i^j}{\Delta t} \tag{4.19}$$

The Crank-Nicolson scheme for a first-order derivative is defined as

$$\frac{\partial \theta}{\partial t} \to \frac{1}{2}\left(\left(\frac{\theta_{i+1}^{j+1} - \theta_{i-1}^{j+1}}{2\Delta z}\right) + \left(\frac{\theta_{i+1}^{j} - \theta_{i-1}^{j}}{2\Delta z}\right)\right) \tag{4.20}$$

The Crank-Nicolson scheme for a second order derivative is defined as

$$\frac{\partial^2 \theta}{\partial t^2} \to \frac{1}{2(\Delta z)^2}\left(\left(\theta_{1+1}^{j+1} - \theta_{i}^{j+1} + \theta_{i-1}^{j+1}\right) + \left(\theta_{i+1}^{j} - \theta_{i}^{j} + \theta_{i-1}^{j}\right)\right) \tag{4.21}$$

The Crank-Nicolson scheme is at a particular time defined as

$$\theta \to \frac{1}{2}\left(\theta_i^{j+1} - \theta_i^{j}\right) \tag{4.22}$$

The Crank-Nicolson scheme for the previous channel is defined as

$$\theta_N \to \frac{1}{2}\left(\theta_{Ni}^{j+1} - \theta_{Ni}^{j}\right) \tag{4.23}$$

The Crank-Nicolson scheme for the next channel is defined as

$$\theta_M \to \frac{1}{2}\left(\theta_{Mi}^{j+1} - \theta_{Mi}^{j}\right) \tag{4.24}$$

Just to recall the non-linear transient soil moisture flow equation

$$\frac{\partial \theta}{\partial t} = D\frac{\partial^2 \theta}{\partial z^2} + \frac{K_s}{(\theta_s - \theta_r)^{\omega}}\,\omega\,\frac{\partial \theta}{\partial z}(\theta - \theta_r)^{\omega - 1} \tag{4.25}$$

The Crank-Nicolson finite-difference approximation to the above equation is given by

$$\begin{aligned}\frac{\theta_i^{j+1} - \theta_i^{j}}{\Delta t} = {} & \left[\frac{1}{2(\Delta z)^2} D\left(\left(\theta_{i+1}^{j+1} - 2\theta_i^{j+1} + \theta_{i-1}^{j+1}\right) + \left(\theta_{i+1}^{j} - 2\theta_i^{j} + \theta_{i-1}^{j}\right)\right)\right] \\ & + \left[\frac{1}{2}.\left(\frac{K_s}{(\theta_s - \theta_r)^{\omega}}.\omega\right)\left(\left(\frac{\theta_{i+1}^{j+1} - \theta_{i-1}^{j+1}}{2\Delta z}\right.\right.\right. \\ & \left.\left.\left. + \frac{\theta_{i+1}^{j} - \theta_{i-1}^{j}}{2\Delta z}\right)\left(\frac{\theta_i^{j+1} + \theta_i^{j}}{2} - \theta_r\right)^{\omega - 1}\right)\right]\end{aligned} \tag{4.26}$$

4.4.2 Laplace Adams-Bashforth scheme

The governing partial differential equation

$$\frac{\partial \theta}{\partial t} = D\frac{\partial^2 \theta}{\partial z^2} + \frac{K_s}{(\theta_s - \theta_r)^{\omega}}\,\omega\,\frac{\partial \theta}{\partial z}(\theta - \theta_r)^{\omega - 1} \tag{4.27}$$

is solved by applying Laplace transform on both sides of the equation in order to transform the equation from a partial differential equation to a differential equation

$$\mathcal{L}\left(\frac{\partial\theta}{\partial t}\right) = \mathcal{L}\left(D\frac{\partial^2\theta}{\partial z^2} + \frac{K_s}{(\theta_s - \theta_r)^\omega}\omega\frac{\partial\theta}{\partial z}(\theta - \theta_r)^{\omega-1}\right) \tag{4.28}$$

Where $\mathcal{L}$ is the Laplace transform operator. The resultant equation is given by

$$\frac{d\theta(s,t)}{dt} = \mathcal{L}\left(D\frac{\partial^2\theta}{\partial z^2} + \frac{K_s}{(\theta_s - \theta_r)^\omega}\omega\frac{\partial\theta}{\partial z}(\theta - \theta_r)^{\omega-1}\right) \tag{4.29}$$

s can be silenced by

$$\frac{d\theta(s,t)}{dt} = F(\theta,t) \tag{4.30}$$

$$\theta(t) = \theta(s,t) \tag{4.31}$$

and equation (4.29) can be written as

$$F(\theta,t) = \mathcal{L}\left(D\frac{\partial^2\theta}{\partial z^2} + \frac{K_s}{(\theta_s - \theta_r)^\omega}\omega\frac{\partial\theta}{\partial z}(\theta - \theta_r)^{\omega-1}\right) \tag{4.32}$$

Applying the fundamental theorem of calculus on the equation above yields

$$\theta(t) = \theta(t_0) + \int_0^t F(\theta,\tau)\,d\tau \tag{4.33}$$

Which is also

$$\theta(t) = \theta_0 + \int_0^t F(\theta,\tau)\,d\tau \tag{4.34}$$

When $t = t_{n+1}$, the equation becomes

$$\theta_{n+1} = \theta(t_{n+1}) = \theta_0 \int_0^{t_{n+1}} F(\theta,\tau)d\tau \tag{4.35}$$

When $t = t_n$, the equation becomes

$$\theta_n = \theta(t_n) = \theta_0 \int_0^{t_n} F(\theta,\tau)d\tau \tag{4.36}$$

and

$$\theta_{n+1} - \theta_n = \int_0^{t_{n+1}} F(\theta,\tau)d\tau - \int_0^{t_n} F(\theta,\tau)d\tau \tag{4.37}$$

$$\theta_{n+1} - \theta_n = \int_n^{t_{n+1}} F(\theta,\tau)d\tau \tag{4.39}$$

The Langrange polynomial is used for the approximation of $F(\theta, t)$ to obtain

$$P(t)\big(\approx F(\theta,t)\big) = \frac{t - t_{n-1}}{t_n - t_{n-1}} F(\theta, t_n) + \frac{t - t_n}{t_{n-1} - t_n} F(\theta, t_{n-1}) \tag{4.40}$$

$$P(t) = \frac{t - t_{n-1}}{t_n - t_{n-1}} F_n + \frac{t - t_n}{t_{n-1} - t_n} F_{n-1} \tag{4.41}$$

Therefore,

$$\theta_{n+1} - \theta_n = \int_n^{t_{n+1}} F(\theta,\tau)d\tau \tag{4.42}$$

$$\theta_{n+1} - \theta_n = \int_{t_n}^{t_{n+1}} \left(\frac{t - t_{n-1}}{t_n - t_{n-1}} F_n + \frac{t - t_n}{t_{n-1} - t_n} F_{n-1}\right) dt \tag{4.43}$$

$$\theta_{n+1} - \theta_n = \frac{F_n}{t_n - t_{n-1}} \int_{t_n}^{t_{n+1}} (t - t_{n-1})dt + \frac{F_{n-1}}{t_{n-1} - t_n} \int_n^{t_{n+1}} (t - t_n)dt \tag{4.44}$$

$$\theta_{n+1} - \theta_n = \frac{F_n}{t_n - t_{n-1}} \left[\frac{1}{2}t^2 - tt_{n-1}\right]_{t_n}^{t_{n+1}} + \frac{F_{n-1}}{t_{n-1} - t_n} \left[\frac{1}{2}t^2 - tt_n\right]_{t_n}^{t_{n+1}} \tag{4.45}$$

If $h = t_n - t_{n-1}$, then the following is obtained

$$\begin{aligned} \theta_{n+1} - \theta_n = {} & \frac{F_n}{h}\left(\frac{1}{2}t^2{}_{n+1} - t_{n+1}t_{n-1} - \frac{1}{2}t^2{}_n + t_n t_{n-1}\right) \\ & - \frac{F_{n-1}}{h}\left(\frac{1}{2}t^2{}_{n+1} - t_{n+1}t_n - \frac{1}{2}t^2{}_n + t^2{}_n\right) \end{aligned} \tag{4.46}$$

Further simplification gives

$$\begin{aligned} \theta_{n+1} - \theta_n = {} & \frac{F_n}{h}\left(\frac{1}{2}(t_{n+1} - t_n)(t_{n+1} + t_n) - t_{n-1}(t_{n+1} - t_n)\right) \\ & - \frac{F_{n-1}}{h}\left(\frac{1}{2}(t_{n+1} - t_n)(t_{n+1} + t_n) - t_n(t_{n+1} - t_n)\right) \end{aligned} \tag{4.47}$$

$$\theta_{n+1} - \theta_n = \frac{F_n}{h}\left(\frac{1}{2}h(t_{n+1} + t_n) - ht_{n-1}\right) - \frac{F_{n-1}}{h}\left(\frac{1}{2}h(t_{n+1} + t_n) - ht_n\right) \tag{4.48}$$

$$\theta_{n+1} - \theta_n = F_n\left(\frac{1}{2}(t_{n+1} + t_n) - t_{n-1}\right) - F_{n-1}\left(\frac{1}{2}(t_{n+1} + t_n) - t_n\right) \tag{4.49}$$

$$\begin{aligned}\theta_{n+1} - \theta_n = {} & F_n\left(\frac{1}{2}\big((n+1)h + nh\big) - (n-1)h\right) \\ & - F_{n-1}\left(\frac{1}{2}\big((n+1)h + nh\big) - nh\right)\end{aligned} \tag{4.50}$$

$$\theta_{n+1} - \theta_n = F_n\left(nh + \frac{1}{2}h - nh + h\right) - F_{n-1}\left(nh + \frac{1}{2}h - nh\right) \tag{4.51}$$

$$\theta_{n+1} = \theta_n + h\left(\frac{3}{2}F_n - \frac{1}{2}F_{n-1}\right) \tag{4.52}$$

Applications of inverse Laplace transform to take back the equation to its real space is given by

$$\mathcal{L}^{-1}[\theta_{n+1}] = \mathcal{L}^{-1}\left[\theta_n + h\left(\frac{3}{2}F_n - \frac{1}{2}F_{n-1}\right)\right] \tag{4.53}$$

$$\begin{aligned}\theta(\mathrm{z}, t_{n+1}) = {} & \theta(\mathrm{z}, t_n) \\ & + h\frac{3}{2}\Bigg(D\frac{\partial^2\theta(\mathrm{z}, t_n)}{\partial z^2} \\ & + \frac{K_s}{(\theta_s - \theta_r)^\omega}\omega\frac{\partial\theta(\mathrm{z}, t_n)}{\partial z}(\theta(\mathrm{z}, t_n) - \theta_r)^{\omega-1}\Bigg) \\ & - h\frac{1}{2}\Bigg(D\frac{\partial^2\theta(\mathrm{z}, t_{n-1})}{\partial z^2} \\ & + \frac{K_s}{(\theta_s - \theta_r)^\omega}\omega\frac{\partial\theta(\mathrm{z}, t_{n-1})}{\partial z}(\theta(\mathrm{z}, t_{n-1}) - \theta_r)^{\omega-1}\Bigg)\end{aligned} \tag{4.54}$$

The equation above is discretised forward and backward in space to yields

$$
\begin{aligned}
\theta(z_i, t_{n+1}) = \theta(z_i, t_n) \\
&+ h\frac{3}{2}\left(D\frac{\partial^2\theta(z_i, t_n)}{\partial z^2}\right. \\
&\left.+ \frac{K_s}{(\theta_s - \theta_r)^{\omega}}\,\omega\,\frac{\partial\theta(z_i, t_n)}{\partial z}\left(\theta(z_i, t_{n-1}) - \theta_r\right)^{\omega-1}\right) \\
&- h\frac{1}{2}\left(D\frac{\partial^2\theta(z_i, t_{n-1})}{\partial z^2}\right. \\
&\left.+ \frac{K_s}{(\theta_s - \theta_r)^{\omega}}\,\omega\,\frac{\partial\theta(z_i, t_{n-1})}{\partial z}\left(\theta(z_i, t_{n-1}) - \theta_r\right)^{\omega-1}\right)
\end{aligned}
\tag{4.55}
$$

Let $\theta(z_i, t_n) = \theta_i^n$ and $\Delta z = l$, then the above equation becomes

$$
\begin{aligned}
\theta_i^{n+1} = \ \theta(z_i, t_n) \\
&+ h\frac{3}{2}\left[D\left(\frac{\theta_{i+1}^n - 2\theta_i^n + \theta_{i-1}^n}{(\Delta l)^2}\right)\right. \\
&\left.+ \frac{K_s}{(\theta_s - \theta_r)^{\omega}}\,\omega\left(\frac{\theta_i^n - \theta_{i-1}^n}{\Delta l}\right)(\theta_i^n - \theta_r)^{\omega-1}\right] \\
&- h\frac{1}{2}\left[D\left(\frac{\theta_{i+1}^{n-1} - \theta_i^{n-1} + \theta_{i-1}^{n-1}}{(\Delta l)^2}\right)\right. \\
&\left.+ \frac{K_s}{(\theta_s - \theta_r)^{\omega}}\,\omega\left(\frac{\theta_i^{n-1} - \theta_{i-1}^{n-1}}{\Delta l}\right)(\theta_i^{n-1} - \theta_r)^{\varepsilon-1}\right]
\end{aligned}
\tag{4.56}
$$

The above is the numerical solution to Richards' equation obtained using Laplace Adam-Bashforth numerical approximation scheme.

CHAPTER 5: THE LINEAR UNSATURATED FLOW MODEL

5.1 Introduction

The only thing that makes Richards' equation impossible to solve analytically is its highly non-linear nature associated with spatial variation of the unsaturated hydraulic conductivity. Since the analytical approach is not an option computer codes are used to find solutions. However, numerical approximation methods show convergence issues when it comes to Richards' equation. If it is linearized analytical solutions may be obtained and convergence issues associated with non-linear Richards' equation will be solved as well. There are few analytical solutions available in the literature. In this chapter conditions where the unsaturated hydraulic conductivity model by Mualem (1976) may be linear are suggested and an analytical solution to Richards' equation is obtained. Numerical analysis of the proposed analytical solution is also covered and two numerical approximation methods are used namely: the popular Crank-Nicolson method; and a recently proposed Laplace Adam-Bashfoth method. Stability analysis for both methods is provided as well.

5.2 Theoretical basis

The unsaturated flow system is complex (Ojha et al., 2017) because moisture content evolves as water moves through a soil volume. It has been proven that hydraulic conductivity strongly depends on evolving water content (van Genuchten, 1980). As water migrates in the downward direction pores are emptied in upper parts of the unsaturated zone and water is replaced with air. Water content tends to decrease with depth. This is due to water that is retained in disconnected pores as residual water content, refer to section 2.3.4 for more details in soil water retention. Eventually, a number of pores conducting water flow declines. As a result, the flow becomes more tortuous since there are only a few connected pores that are filled with water and flow has to follow those pores. The decline in water content and number of connected pores with water is the reason for the spatial variation of the unsaturated hydraulic conductivity.

Unsaturated hydraulic conductivity is a function of effective saturation and pressure, it is highly variable in space and requires spatial characterization. As mentioned in chapter 3 the function of unsaturated hydraulic conductivity is given by the product of relative hydraulic conductivity and saturated hydraulic conductivity

$$K(\theta) = K_s * k_r \tag{5.1}$$

Estimation of unsaturated hydraulic conductivity requires the substitution of a relative hydraulic conductivity estimation model into equation (5.1) such as substitutions in section 4.2 where relative hydraulic conductivity models by Brooks and Corey and Mualem were used. In this chapter, a relative conductivity model that will be used is based on the basis of theories proposed by Childs and Collis-George, Burdine, and Mualem.

$$\frac{K(\theta)}{K_s} = (Se)^b \left[\int_0^{Se} \frac{dx}{\psi(x)} \Big/ \int_0^1 \frac{dx}{\psi^{2-r}(x)}\right]^m \tag{5.2}$$

Childs and Collis-George, Burdine, and Mualem proposed different values for model parameter b, r and m. For example, Mualem suggested that $b = 0.5$; $r = 1$; and $m = 2$; Burdine, on the other hand, suggested that $b = 2$; $r = 0$; and $m = 1$

When Mualem parameter values are adopted equation (5.2) becomes

$$K_r(\theta) = Se^{0.5} \left[\int_0^{\theta} \frac{d\theta}{\psi} \Big/ \int_0^{\theta_{sat}} \frac{d\theta}{\psi}\right]^2 \tag{5.3}$$

Where

$$Se = \frac{\theta - \theta_r}{\theta_s - \theta_r} \tag{5.4}$$

0.5 in equation (5.3) is a value representing an empirical term for the pore-size interaction term. The values of this term have been carefully selected by researchers; the most common ones are 0.5 as indicated in the equation above; 2 which is associated with Burdine model. Brooks and Corey suggested that pore-size interaction term is not necessary when the pore-size distribution index is used and considered it to be 0. Pore-size interaction term adds flexibility to relative hydraulic conductivity models. Leij et al (1994) proved that the pore-size interaction term is not confined to these values only, however it can have any value including negative values. Therefore, the wide range for values of this term, referred to as n from now on, allows both linear and non-linear relationship between effective saturation and relative hydraulic conductivity. Assuming that $n = -2$ and adopting other soil physical parameters proposed by Mualem equation (5.3) becomes

$$K_r(\theta) = Se^{-2} \left[\int_0^{\theta} \frac{d\theta}{\psi} \Big/ \int_0^{\theta_{sat}} \frac{d\theta}{\psi}\right]^2 \tag{5.5}$$

Incorporating a water retention characteristic described by Brooks and Corey

$$Se = (\varphi/\omega_{cr})^{-\lambda} \tag{5.6}$$

into equation (5.5) yields

$$K_r = Se^{\omega} = Se^{-2+2+\frac{2}{\lambda}} \tag{5.7}$$

Where λ is an empirical parameter representing the pore-size distribution index. The same completely homogeneous soil volume with pore-size distribution index of 2 considered in the previous chapter will be used in this chapter as well. $\omega = 1$ when the value of λ is substituted in the equation (5.7). Therefore, the relative permeability of the soil is assumed to be equivalent to effective saturation and unsaturated hydraulic conductivity varies linearly across space. The soil profile is assumed to be completely homogeneous. Mathematically, the above assumptions can be expressed as

$$K_r = Se = \frac{\theta - \theta_r}{\theta_s - \theta_r} \tag{5.8}$$

and the resultant unsaturated hydraulic conductivity function is given by

$$K(\theta) = K_r * K_s = K_s\left(\frac{\theta - \theta_r}{\theta_s - \theta_r}\right) \tag{5.9}$$

Therefore, $K(\theta)$ can be eliminated from the equation (1.9) by combining it with equation (5.9) to obtain

$$\left(D\frac{\partial\theta}{\partial z}\right) + \frac{\partial}{\partial z}\left(K_s\left(\frac{\theta - \theta_r}{\theta_s - \theta_r}\right)\right)\frac{\partial\theta}{\partial t} = \frac{\partial}{\partial z} \tag{5.10}$$

Equation (5.10) is a linearized Richards' equation and it can be simplified to obtain

$$\frac{\partial\theta}{\partial t} = D\frac{\partial^2\theta}{\partial z^2} + \frac{\partial}{\partial z}\left(K_s\frac{\theta}{\theta_s - \theta_r}\right) \tag{5.11}$$

$$\frac{\partial\theta}{\partial t} = D\frac{\partial^2\theta}{\partial z^2} + \frac{\partial\theta}{\partial z}\left(K_s\frac{1}{\theta_s - \theta_r}\right) \tag{5.12}$$

If $K_s\frac{1}{\theta_s-\theta_r} = \beta$ then equation (5.12) can be written as

$$\frac{\partial\theta}{\partial t} = D\frac{\partial^2\theta}{\partial z^2} + \beta\frac{\partial\theta}{\partial z} \tag{5.13}$$

The above equation is a one-dimension partial differential equation for unsaturated flow in a vertical direction which will be solved in the following section to obtain an exact solution using Laplace Transform and Green's Function.

5.3 The exact solution to Richards' equation

In this section, the partial differential equation (5.13) obtained in the previous section is solved using Laplace transform to obtain the exact solution. The transform is applied to equation (5.13) with an assumption that variable t meets the following condition: $0 < t < \infty$, t is transformed from being a variable to a parameter so that equation (5.13) becomes an algebraic equation which is easy to solve compared to differential equations. The Laplace transform of a function is given by

$$\mathcal{L}\big(f(t)\big) = \tilde{f}(s) \tag{5.14}$$

Where $\mathcal{L}$ is a Laplace transform operator, $\tilde{f}(s)$ is a function in Laplace space, $f(t)$ is a function in its original space where $0 < t < \infty$, and s is a parameter representing t in Laplace space. Application of Laplace transform on both sides of equation (5.13)

$$\mathcal{L}\left(\frac{\partial\theta}{\partial t}\right) = D\mathcal{L}\left(\frac{\partial^2\theta}{\partial z^2}\right) + \beta\mathcal{L}\left(\frac{\partial\theta}{\partial z}\right) \tag{5.15}$$

yields

$$s\tilde{\theta} - \theta(0) = D\left(\frac{\partial^2\tilde{\theta}}{\partial z^2}\right) + \beta\left(\frac{\partial\tilde{\theta}}{\partial z}\right) \tag{5.16}$$

by rearranging the equation above

$$D\frac{\partial^2\tilde{\theta}}{\partial z^2} + \beta\frac{\partial\tilde{\theta}}{\partial z} - s\tilde{\theta} = \theta(0) \tag{5.17}$$

is obtained. Where $\theta(0)$ represents the initial soil water content, and $s\tilde{\theta}$ is an expression of Laplace transform of function $\frac{\partial\theta}{\partial z}$ involving parameter s and which corresponds to t in the original space. The above equation is non-homogeneous because $\theta(0)$ is not equal to zero. Just for the purpose of obtaining a particular solution of the above equation soil water content $\theta(0)$ is considered to be 0. If $\theta(0)$ is zero, equation (5.17) becomes a homogeneous equation and is written as

$$D\frac{\partial^2\tilde{\theta}}{\partial z^2} + \beta\frac{\partial\tilde{\theta}}{\partial z} - s\tilde{\theta} = 0 \tag{5.18}$$

The above equation is in the form of a quadratic equation, if $\tilde{\theta} = Ae^{rz}$, then equations

$$\frac{\partial\tilde{\theta}}{\partial z} = rAe^{rz} \tag{5.19}$$

and

$$\frac{\partial^2\tilde{\theta}}{\partial z} = r^2 A e^{rz} \tag{5.20}$$

are obtained and substituted into the Laplacian quadratic equation in equation (5.18) to obtain

$$Dr^2 A e^{rz} + \beta r A e^{rz} - s A e^{rz} = 0 \tag{5.21}$$

which is a particular equation for equation (5.13). Equation (5.21) is further simplified into

$$Dr^2 + r\beta - s = 0 \tag{5.22}$$

A quadratic formula is used to solve the above equation for r values and the following values are obtained

$$r_- = \frac{-\beta - \sqrt{\beta^2 + 4Ds}}{2D}$$

and

$$r_+ = \frac{-\beta + \sqrt{\beta^2 + 4Ds}}{2D} \tag{5.23}$$

Since soil water content cannot increase to infinity, r_- is used and $\tilde{\theta}(z,s)$ can be expressed as

$$\tilde{\theta}(z,s) = Ae^{z\left(\frac{-\beta-\sqrt{\beta^2+4Ds}}{2D}\right)} \tag{5.24}$$

The inverse Laplace Transform of equation (5.22) yields a particular solution to equation (5.13) in its original space. The inverse Laplace transform of equation (5.22) is given by

$$\mathcal{L}^{-1}\left(\tilde{\theta}(z,s)\right) = A\mathcal{L}^{-1}\left(e^{z\left(\frac{-\beta-\sqrt{\beta^2+4Ds}}{2D}\right)}\right) = \tilde{\theta}(z,t) \tag{5.25}$$

$$\theta_1(z,t) = A.\left(\frac{ze^{\left(\frac{-(-\beta t+z)-t}{4Dt}\right)}}{2\sqrt{\frac{\pi}{D}}\,t^{\frac{3}{2}}}\right) \tag{5.26}$$

Since equation (5.17) is non-homogeneous with $\theta(0) \neq 0$ finding the exact solution will require the use of Green's function. Green's function gives a solution to non-homogenous linear differential equations defined on a domain with boundary problems. In Green terms equation (5.17) can be expressed as

$$D\frac{\partial^2 G}{\partial z^2} + \beta\frac{\partial G}{\partial z} - sG = \delta(z) \tag{5.27}$$

The above Green's function is solved by applying Laplace transform both sides to obtain

$$\mathcal{L}\left(D\frac{\partial^2 G}{\partial z^2} + \beta\frac{\partial G}{\partial z} - sG\right) = \mathcal{L}\big(\delta(z!)\big) \tag{5.28}$$

$$D\big(p^2\tilde{G} - pG' - G(0)\big) + \beta\left(p\tilde{G} - G(0)\right) - s\tilde{G} = 1 \tag{5.29}$$

Where p a parameter in the second Laplace is space and $p\tilde{G}$ is a function sG in the second Laplace space. Grouping and rearranging of equation (5.29) yields

$$(Dp^2 + \beta p - s)\tilde{G} = 1 \tag{5.30}$$

$$\tilde{G} = \frac{1}{(Dp^2 + \beta p - s)} \tag{5.31}$$

Using the quadratic formula equation (5.31) can be written as

$$\tilde{G} = \frac{1}{\left(\frac{-\beta - \sqrt{\beta^2 + 4Ds}}{2D}\right)}$$

or

$$\tilde{G} = \frac{1}{\left(\frac{-\beta + \sqrt{\beta^2 + 4Ds}}{2D}\right)} \tag{5.32}$$

From the above equation the values of Δ; $p_+; and\ p_-$ are obtained and given as follows

$$\Delta = \beta^2 + 4sD \tag{5.33}$$

$$p_- = \frac{-\beta - \sqrt{\Delta}}{2D} = a_1 \tag{5.34}$$

$$p_+ = \frac{-\beta + \sqrt{\Delta}}{2D} = a_2 \tag{5.35}$$

Using the above values equation (5.31) can be written as

$$\tilde{G} = \frac{1}{(p - a_1)(p - a_2)} \tag{5.36}$$

$\tilde{G}$ is a convolution of two functions and it can be expressed in the form of

$$\mathcal{L}\big(f(z) * h(z)\big) = \mathcal{L}\big(f(z)\big)\mathcal{L}\big(h(z)\big) = \tilde{G} \tag{5.37}$$

where $\tilde{f}(p)$ and $\tilde{h}(p)$ are chosen as

$$\frac{1}{(p-a_1)} = \tilde{f}$$

and

$$\frac{1}{(p-a_2)} = \tilde{h}$$

Equation (5.36) can be written in the form of equation (5.37) as

$$\tilde{G} = \frac{1}{p-a_1} . \frac{1}{p-a_2}, \tag{5.38}$$

The inverse Laplace transform of a convolution is given by the product of the inverse of the individual functions. In this case the inverse of $\tilde{G}$ will be a product inverse of $\tilde{f}(p)$ and $\tilde{h}(p)$ and is given by

$$\mathcal{L}^{-1}(\tilde{f}).\mathcal{L}^{-1}(\tilde{h}) = e^{a_1 z}.e^{a_2 z} \tag{5.39}$$

The inverse Laplace transform of equation (5.38) can be obtained using the convolution theorem given by the following integrals

$$\mathcal{L}^{-1}(\tilde{G}) = \int_0^z f(\tau)\, h(z-\tau) d\tau \tag{5.40}$$

Using the above equation and equation (5.39) G becomes

$$G = \int_0^z e^{a_1 \tau} e^{a_2 (z-\tau)} . d\tau \tag{5.41}$$

$$G = e^{a_2 z} \int_0^z e^{(a_1 \tau - a_2 \tau)} . d\tau \tag{5.42}$$

$$G = e^{a_2 z} \int_0^z e^{\tau(a_1 - a_2)} . d\tau \tag{5.43}$$

After the integration

$$G = e^{a_2 z} \frac{1}{a_1 - a_2} e^{\tau(a_1 - a_2)} |_0^z \tag{5.44}$$

$$G = e^{a_2 z} \left(\frac{1}{a_1 - a_2} e^{z(a_1 - a_2)} - \frac{1}{a_1 - a_2} \right) = G(z, s) \tag{5.45}$$

Substituting equations (5.34) and (5.35) into the above equation yields

$$G(z,s) = \left[e^{z\left(\frac{-\beta-\sqrt{s}}{2D}\right)}\right] . \left[\frac{1}{\left(\frac{-\beta+\sqrt{s}}{2D}\right) - \left(\frac{-\beta+\sqrt{s}}{2D}\right)} e^{z\left(\frac{-\beta+\sqrt{s}}{2D} - \frac{-\beta-\sqrt{s}}{2D}\right)} - \frac{1}{\left(\frac{-\beta+\sqrt{s}}{2D}\right) - \left(\frac{-\beta+\sqrt{s}}{2D}\right)}\right] \tag{5.46}$$

The above equation is simplified into

$$G(z,s) = \left[e^{z\left(\frac{-\beta-\sqrt{s}}{2D}\right)}\right]\left[\frac{1}{\left(\frac{-\beta+\sqrt{s}}{2D}\right) - \left(\frac{-\beta+\sqrt{s}}{2D}\right)}\right]\left[e^{z\left(\frac{-\beta+\sqrt{s}}{2D} - \frac{-\beta-\sqrt{s}}{2D}\right)} - 1\right] \tag{5.47}$$

Substituting equation (5.33) into the above equation yields

$$G(z,s) = \left[e^{z\left(\frac{-\beta-\sqrt{\beta^2+4Ds}}{2D}\right)}\right]\left[\frac{1}{\left(\frac{-\beta+\sqrt{\beta^2+4Ds}}{2D}\right) - \left(\frac{-\beta+\sqrt{\beta^2+4Ds}}{2D}\right)}\right]\left[e^{z\left(\frac{-\beta+\sqrt{\beta^o+4Ds}}{2D} - \frac{-\beta-\sqrt{\beta^2+4Ds}}{2D}\right)} - 1\right] \tag{5.48}$$

The exact solution in Laplace space is given by

$$\theta(z,s) = \theta_1(z,s) + \int_0^z \theta(0,s)\, G(z-\tau,s)\, d\tau \tag{5.49}$$

Where $\theta(z,s)$ is the term for the exact solution; $\theta_1(z,s)$ is the particular solution given by equation (5.25); $\theta(0,s)$ is the term for initial soil pore-water content; and $\int_0^z G(z-\tau,s)\, d\tau$ is the integral of equation (5.48) in τ direction.

To obtain the exact solution each term must be substituted into the above equation; and substitution of the particular solution, equation (5.25) yields

$$\theta(z,s) = A.e^{z\left(\frac{-\beta-\sqrt{\beta^2+4Ds}}{2D}\right)} + \theta(0,s) \int_0^z G(z-\tau,s)\, d\tau \tag{5.50}$$

To find $\int_0^z G(z-\tau,s)\, d\tau$ equation (5.48) is again expressed as equation (5.45) and by simplifying it can be expressed as

$$G(z,s) = e^{a_2 z}\left(\frac{1}{a_1 - a_2}\right)\left(e^{z(a_1-a_2)} - 1\right) \tag{5.51}$$

and its integral is expressed as

$$\int_0^z G(z-\tau,s)\,d\tau = \frac{1}{a_1-a_2}\int_0^z e^{a_2 z}.\left(e^{z(a_1-a_2)}-1\right).d\,\tau \tag{5.52}$$

$$\int_0^z G(z-\tau,s)\,d\tau = \frac{1}{a_1-a_2}\int_0^z e^{a_2(z-\tau)}.e^{(z-\tau)(a_1-a_2)} - e^{a_2(z-\tau)}.d\tau$$

$$= \frac{1}{a_1-a_2}\int_0^z \left(e^{a_1(z-\tau)} - e^{a_2(z-\tau)}\right).d\tau \tag{5.53}$$

Let $(z-\tau)$ be y; when $\tau = 0$, $y = z$ and when $z = 0$, $y = 0$; thus $dy = -d\tau$

Thus

$$\int_0^z G(z-\tau,s)\,d\tau = \frac{1}{a_1-a_2}\int_z^0 (e^{a_2 y} - e^{a_2 y})\,(-dy)$$

$$= \frac{1}{a_1-a_2}\int_z^0 (e^{a_1 y} - e^{a_2 y}).dy \tag{5.54}$$

and after integration, the following is obtained

$$\int_0^z G(z-\tau,s)\,d\tau = \frac{1}{a_1-a_2}\left(\frac{1}{a_1}e^{a_1 y} - \frac{1}{a_2}e^{a_2 y}\right)|_0^z \tag{5.55}$$

By substituting equations (5.33), (5.34) and (5.35) into the above equation, the following equation is obtained

$$\int_0^z G(z-\tau,s)\,d\tau = \left(\frac{1}{\left(\frac{-\beta-\sqrt{\beta^2+4Ds}}{2D}\right)-\left(\frac{-\beta+\sqrt{\beta^2+4Ds}}{2D}\right)}\right)\left(\frac{1}{\left(\frac{-\beta-\sqrt{\beta^2+4Ds}}{2D}\right)}e^{z\left(\frac{-\beta-\sqrt{\beta^2+4Ds}}{2D}\right)} - \frac{1}{\left(\frac{-\beta+\sqrt{\beta^2+4Ds}}{2D}\right)}e^{z\left(\frac{-\beta+\sqrt{\beta^2+4Ds}}{2D}\right)} - \frac{1}{\left(\frac{-\beta-\sqrt{\beta^2+4Ds}}{2D}\right)} + \frac{1}{\left(\frac{-\beta+\sqrt{\beta^2+4Ds}}{2D}\right)}\right) \tag{5.56}$$

Now $\int_0^z G(z-\tau,s)\,d\tau$ in equation (5.50) can be replaced by equation (5.56) to give

$$\theta(z,s) = A.e^{z\left(\frac{-\beta-\sqrt{\beta^2+4Ds}}{2D}\right)} + [\theta(0,s)]\left[\left(-\frac{D}{\sqrt{\beta^2+4Ds}}\right)\left(\frac{1}{\left(\frac{-\beta-\sqrt{\beta^2+4Ds}}{2D}\right)}e^{z\left(\frac{-\beta-\sqrt{\beta^2+4Ds}}{2D}\right)} - \frac{1}{\left(\frac{-\beta+\sqrt{\beta^2+4Ds}}{2D}\right)}e^{z\left(\frac{-\beta+\sqrt{\beta^2+4Ds}}{2D}\right)} - \frac{1}{\sqrt{\beta^2+4Ds}}\right)\right] \quad (5.57)$$

The equation above is an expression of the exact solution of linearized Richards' equation. The equation above is still in Laplace space; to remove the solution from Laplace space to its original space inverse Laplace transform is applied as follows

$$\begin{aligned}\theta(z,t) &= \mathcal{L}^{-1}\big(\theta(z,s)\big)\\ &= A\left(\frac{ze^{\left(\frac{-(-\beta t+z)-t}{4Dt}\right)}}{2\sqrt{\frac{\pi}{D}}t^{\frac{3}{2}}}\right)\\ &+ \mathcal{L}^{-1}\left\{+[\theta(0,s)]\left[\left(-\frac{D}{\sqrt{\beta^2+4Ds}}\right)\left(\frac{1}{\left(\frac{-\beta-\sqrt{\beta^2+4Ds}}{2D}\right)}e^{z\left(\frac{-\beta-\sqrt{\beta^2+4Ds}}{2D}\right)}\right.\right.\right.\\ &\left.\left.\left.- \frac{1}{\left(\frac{-\beta+\sqrt{\beta^2+4Ds}}{2D}\right)}e^{z\left(\frac{-\beta+\sqrt{\beta^2+4Ds}}{2D}\right)} - \frac{1}{\sqrt{\beta^2+4Ds}}\right)\right]\right\}\end{aligned} \quad (5.58)$$

$$\theta(z,t) = \theta_0\sum_{j=0}^{\infty} e^{-\lambda_n t}\left(Ae^{-z\left(\sqrt{\beta^2-4D\lambda^2}\right)} + Be^{z\left(\sqrt{\beta^2-4D\lambda^2}\right)}\right) \quad (5.59)$$

$$\theta(z,0) = \theta_L \quad (5.60)$$

$$\theta(z,0) = \theta_0\sum_{j=0}^{\infty} e^{-\lambda_n t}(Ae^{-rz}) \quad (5.61)$$

Where

$$r = -\sqrt{\beta^2 - 4D\lambda^2} \tag{5.62}$$

and

$$\beta = K_s \frac{1}{\theta_s - \theta_r} \tag{5.63}$$

The term

$$Be^{z\left(\sqrt{\beta^2 - 4D\lambda^2}\right)}$$

in equation (5.59) was dropped off because water cannot increase up to infinity.

5.4 Numerical analysis

5.4.1 Crank-Nicolson finite-difference approximation scheme

This sub section will provide a numerical approximation of the linearized Richards' equation using Crank-Nicolson finite-difference approximation method. Numerical approximation of equation (5.13) is given by

$$\begin{aligned} \frac{\theta_i^{j+1} - \theta_i^j}{\Delta t} &= 0.5\left(D\frac{\theta_{i+1}^{j+1} - 2\theta_i^{j+1} + \theta_{i-1}^{j+1}}{(\Delta z)^2} + \beta\frac{\theta_{i+1}^{j+1} - \theta_{i-1}^{j+1}}{2\Delta z}\right) \\ &+ 0.5\left(D\frac{\theta_{i+1}^{j} - 2\theta_i^{j} + \theta_{i-1}^{j}}{(\Delta z)^2} + \beta\frac{\theta_{i+1}^{j} - \theta_{i-1}^{j}}{2\Delta z}\right) \end{aligned} \tag{5.64}$$

Expanding and rearranging give

$$\begin{aligned} 2\left(\frac{D}{(\Delta z)^2} + \frac{1}{\Delta t}\right)\theta_i^{j+1} \\ &= 2\left(\frac{1}{\Delta t} - \frac{D}{(\Delta z)^2}\right)\theta_i^j + \left(\frac{D}{(\Delta z)^2} + \frac{\beta}{2\Delta y}\right)\theta_{i+1}^{j+1} \\ &+ \left(\frac{D}{(\Delta z)^2} - \frac{\beta}{2\Delta y}\right)\theta_{i-1}^{j+1} + \left(\frac{D}{(\Delta z)^2} + \frac{\beta}{2\Delta y}\right)\theta_{i+1}^{j} \\ &+ \left(\frac{D}{(\Delta z)^2} - \frac{\beta}{2\Delta y}\right)\theta_{i-1}^{j} \end{aligned} \tag{5.65}$$

If the following constants are used

$$a = 2\left(\frac{D}{(\Delta z)^2} + \frac{1}{\Delta t}\right)$$

$$b = 2\left(\frac{1}{\Delta t} - \frac{D}{(\Delta z)^2}\right)$$

$$c = \left(\frac{D}{(\Delta z)^2} + \frac{\beta}{2\Delta y}\right)$$

$$d = \left(\frac{D}{(\Delta z)^2} - \frac{\beta}{2\Delta y}\right)$$

Then equation (5.4.2) becomes

$$a\theta_i^{j+1} = b\theta_i^j + c\theta_{i+1}^{j+1} + d\theta_{i-1}^{j+1} + c\theta_{i+1}^j + d\theta_{i-1}^j \tag{5.66}$$

5.4.2 Laplace Adam-Bashforth Scheme

This subsection provides a numerical approximation method of the linearized Richards' equation using Laplace Adam-Bashforth method. Application of Laplace transform on both sides of equation (5.13) transforms the equation from a partial differential equation to a differential equation

$$\mathcal{L}\left(\frac{\partial\theta}{\partial t}\right) = \mathcal{L}\left(D\frac{\partial^2\theta}{\partial z^2} + \beta\frac{\partial\theta}{\partial z}\right) \tag{5.67}$$

The resultant equation is given by

$$\frac{d\theta}{dt} = \mathcal{L}\left(D\frac{\partial^2\theta}{\partial z^2} + \beta\frac{\partial\theta}{\partial z}\right) \tag{5.68}$$

s can be silenced by

$$\frac{d\theta(s,t)}{dt} = F(\theta,t)$$

$$\theta(t) = \theta(s,t)$$

$$F(\theta,t) = \mathcal{L}\left(D\frac{\partial^2\theta}{\partial z^2} + \beta\frac{\partial\theta}{\partial z}\right)$$

The same procedure that was followed in section 4.4.2 is followed here to obtain

$$\theta_{n+1} = \theta_n + h\left(\frac{3}{2}F_n - \frac{1}{2}F_{n-1}\right) \tag{5.69}$$

Applications of inverse Laplace transform to take back the equation to its real space is given by

$$\mathcal{L}^{-1}[\theta_{n+1}] = \mathcal{L}^{-1}\left[\theta_n + h\left(\frac{3}{2}F_n - \frac{1}{2}F_{n-1}\right)\right] \tag{5.70}$$

which result in

$$\begin{aligned}\theta(\mathrm{z}, t_{n+1}) = \theta(\mathrm{z}, t_n) + h\frac{3}{2}\left(D\frac{\partial^2\theta(\mathrm{z}, t_n)}{\partial z^2} + \beta\frac{\partial\theta(\mathrm{z}, t_n)}{\partial z}\right) \\ - h\frac{1}{2}\left(D\frac{\partial^2\theta(\mathrm{z}, t_{n-1})}{\partial z^2} + \beta\frac{\partial\theta(\mathrm{z}, t_{n-1})}{\partial z}\right)\end{aligned} \tag{5.71}$$

Forward and backward discretization in space variable yields

$$\begin{aligned}\theta_i^{n+1} = \theta_i^n + h\frac{3}{2}\left[D\left(\frac{\theta_{i+1}^n - 2\theta_i^n + \theta_{i-1}^n}{(\Delta z)^2}\right) + \beta\left(\frac{\theta_{i+1}^n - \theta_i^n}{\Delta z}\right)\right] \\ - h\frac{1}{2}\left[D\left(\frac{\theta_{i+1}^{n-1} - 2\theta_i^{n-1} + \theta_{i-1}^{n-1}}{(\Delta z)^2}\right) + \beta\left(\frac{\theta_{i+1}^{n-1} - \theta_i^{n-1}}{\Delta z}\right)\right]\end{aligned} \tag{5.72}$$

Where $\theta(z_i, t_n) = \theta_i^n$. If $\Delta z = l$ then equation above becomes

$$\begin{aligned}\theta_i^{n+1} = \theta_i^n + h\frac{3}{2}\left[D\left(\frac{\theta_{i+1}^n - 2\theta_i^n + \theta_{i-1}^n}{(l)^2}\right) + \beta\left(\frac{\theta_{i+1}^n - \theta_i^n}{l}\right)\right] \\ - h\frac{1}{2}\left[D\left(\frac{\theta_{i+1}^{n-1} - 2\theta_i^{n-1} + \theta_{i-1}^{n-1}}{(l)^2}\right) + \beta\left(\frac{\theta_{i+1}^{n-1} - \theta_i^{n-1}}{l}\right)\right]\end{aligned} \tag{5.73}$$

Expanding

$$\begin{aligned}\theta_i^{n+1} = \theta_i^n + \frac{3hD}{2(l)^2}(\theta_{i+1}^n - 2\theta_i^n + \theta_{i-1}^n) + \frac{3h\beta}{2l}(\theta_{i+1}^n - \theta_i^n) \\ - \frac{hD}{2(l)^2}(\theta_{i+1}^{n-1} - 2\theta_i^{n-1} + \theta_{i-1}^{n-1}) - \frac{h\beta}{2l}(\theta_{i+1}^{n-1} - \theta_i^{n-1})\end{aligned} \tag{5.74}$$

If the following constants are substituted into equation (5.74) above

$$a = \frac{3hD}{2(l)^2}$$

$$b = \frac{3h\beta}{2l}$$

$$c = \frac{hD}{2(l)^2}$$

$$d = \frac{h\beta}{2l}$$

then the following equation is obtained

$$\theta_i^{n+1} = \theta_i^n + a(\theta_{i+1}^n - 2\theta_i^n + \theta_{i-1}^n) + b(\theta_{i+1}^n - \theta_i^n) - c(\theta_{i+1}^{n-1} - 2\theta_i^{n-1} + \theta_{i-1}^{n-1}) - d(\theta_{i+1}^{n-1} - \theta_i^{n-1}) \tag{5.75}$$

which is simplified into

$$\theta_i^{n+1} = (1 - 2a - b)\theta_i^n + (a + b)\theta_{i+1}^n + a\theta_{i-1}^n + (2c + d)\theta_i^{n-1} - (c + d)\theta_{i+1}^{n-1} - c\theta_{i-1}^{n-1} \tag{5.76}$$

5.5 Numerical Stability Analysis

Stability analysis is conducted to evaluate the performance of numerical approximation methods. It is essential for ensuring that discrete errors do not spread to the entire simulation (Allwright and Atangana, 2018). In this study, the Fourier expansion in space variables will be used.

$$\theta(z,t) = \sum_f \hat{\theta}(t)\, exp(jfl) \tag{5.77}$$

5.5.1 Crank-Nicolson Finite-difference Approximation scheme

The stability analysis of the solution obtained using the Crank-Nicolson method is provided in this subsection. Using the Fourier expansion equation (5.66) becomes

$$a\hat{\theta}_{n+1}e^{jifl} = b\hat{\theta}_n e^{jifl} + c\hat{\theta}_n e^{j(i+1)fl} + d\hat{\theta}_n e^{j(i-1)fl} + c\hat{\theta}_{n+1}e^{j(i+1)fl} + d\hat{\theta}_{n+1}e^{j(i-1)fl} \tag{5.78}$$

Where

$$\theta_i^{j+1} = \hat{\theta}_{n+1}e^{jifl} \tag{5.79}$$

$$\theta_i^{j} = \hat{\theta}_{n}e^{jifl} \tag{5.80}$$

$$\theta_{i+1}^{j+1} = \hat{\theta}_{n+1}e^{j(i+1)fl} \tag{5.81}$$

$$\theta_{i-1}^{j+1} = \hat{\theta}_{n+1}e^{j(i-1)fl} \tag{5.82}$$

Dividing equation (5.78) by e^{jifl} yields

$$a\hat{\theta}_{n+1} = b\hat{\theta}_n + c\hat{\theta}_n e^{jfl} + d\hat{\theta}_n e^{-jfl} + c\hat{\theta}_{n+1}e^{jfl} + d\hat{\theta}_{n+1}e^{-jfl} \tag{5.83}$$

At $n = 0$

Equation becomes

$$a\hat{\theta}_1 = b\hat{\theta}_0 + c\hat{\theta}_0 e^{jfl} + d\hat{\theta}_0 e^{-jfl} + c\hat{\theta}_1 e^{jfl} + d\hat{\theta}_1 e^{-jfl} \tag{5.84}$$

Rearranging

$$a\hat{\theta}_1 - c\hat{\theta}_1 e^{jfl} - d\hat{\theta}_1 e^{-jfl} = b\hat{\theta}_0 + c\hat{\theta}_0 e^{jfl} + d\hat{\theta}_0 e^{-jfl} \tag{5.85}$$

Simplifying

$$\hat{\theta}_1\left(a - ce^{jfl} - de^{-jfl}\right) = \hat{\theta}_0\left(b + ce^{jfl} + de^{-jfl}\right) \tag{5.86}$$

Rearranging

$$\frac{\hat{\theta}_1}{\hat{\theta}_0} = \frac{b + ce^{jfl} + de^{-jfl}}{a - ce^{jfl} - de^{-jfl}} \tag{5.87}$$

If

$$e^{jfl} = \cos(fl) + j\sin(fl)$$

$$e^{-jfl} = \cos(fl) - j\sin(fl)$$

Then equation (5.87)

$$\frac{\hat{\theta}_1}{\hat{\theta}_0} = \frac{b + c(\cos(fl) + j\sin(fl)) + d(\cos(fl) - j\sin(fl))}{a - c(\cos(fl) + j\sin(fl)) - d(\cos(fl) - j\sin(fl))} \tag{5.88}$$

Expanding and rearranging

$$\frac{\hat{\theta}_1}{\hat{\theta}_0} = \frac{b + c\cos(fl) + d\cos(fl) + j\,c\sin(fl) - j\,d\sin(fl)}{a - c\cos(fl) - d\cos(fl) + j\,\mathrm{d}\sin(fl) - j\,c\sin(fl)\,(d)} \tag{5.89}$$

Simplifying

$$\frac{\hat{\theta}_1}{\hat{\theta}_0} = \frac{b + \cos(fl)\,(c + d) + j\,\mathrm{d}\sin(fl)\,(c - d)}{a - \cos(fl)\,(c + d) + j\,\mathrm{d}\sin(fl)\,(c - d)} \tag{5.90}$$

The solution will be obtained when

$$\frac{(b + (c + d)\cos(fl))^2 + (c - d)^2\sin^2(fl)}{(a - (c + d)\cos(fl))^2 + (c - d)^2\sin^2(fl)} < 1 \tag{5.91}$$

$$(b + (c + d)\cos(fl))^2 < (a - (c + d)\cos(fl))^2 \tag{5.92}$$

$$b^2 + 2\cos(fl)\,(c+d) + \cos^2(fl)\,(c+d)^2 < a^2 - 2\cos(fl)\,(c+d) + \cos^2(fl)\,(c+d)^2 \tag{5.92}$$

The assumed condition for stability is true when

$$b^2 - a^2 < -4\cos(fl)(c+d) \tag{5.94}$$

Substituting for the constants $a = 2\left(\frac{D}{(\Delta z)^2} + \frac{1}{\Delta t}\right)$; $b = 2\left(\frac{1}{\Delta t} - \frac{D}{(\Delta z)^2}\right)$; $c = \left(\frac{D}{(\Delta z)^2} + \frac{\beta}{2\Delta y}\right)$; and $d = \left(\frac{D}{(\Delta z)^2} - \frac{\beta}{2\Delta y}\right)$ into equation (5.94) yields

$$\left(\frac{2}{\Delta t} - \frac{2D}{(\Delta z)^2}\right)^2 - \left(\frac{2}{\Delta t} + \frac{2D}{(\Delta z)^2}\right)^2 < -4\cos(fl)\left(\frac{D}{(\Delta z)^2} + \frac{\beta}{2\Delta y} + \frac{D}{(\Delta z)^2} - \frac{\beta}{2\Delta y}\right) \tag{5.95}$$

By simplifying the following is obtained

$$\left(\frac{2}{\Delta t} - \frac{2D}{(\Delta z)^2}\right)^2 - \left(\frac{2}{\Delta t} + \frac{2D}{(\Delta z)^2}\right)^2 < -8\cos(fl)\frac{D}{(\Delta z)^2} \tag{5.96}$$

It is concluded that the present solution is stable for $\forall n \leq 0$ when this condition is met and can be used to obtain reliable numerical simulations.

5.5.2 The Laplace Adam-Bashforth scheme

For stability analysis of equation (121) the term θ_i^n will be replaced by θ_i^j.

The stability analysis of the solution obtained using Laplace Adam-Bashforth method is provided in this subsection. Using the Fourier expansion equation (5.76) becomes

$$\hat{\theta}_{n+1}e^{jifl} = (1-2a-b)\hat{\theta}_n e^{jifl} + (a+b)\hat{\theta}_n e^{j(i+1)fl} + a\hat{\theta}_n e^{j(i-1)fl} + (2c+d)\hat{\theta}_{n-1}e^{jifl} - (c+d)\hat{\theta}_{n-1}e^{j(i+1)fl} - c\hat{\theta}_{n-1}e^{j(i-1)fl} \tag{5.97}$$

By dividing equation (5.97) above by e^{jifl} the following is obtained

$$\hat{\theta}_{n+1} = (1-2a-b)\hat{\theta}_n + (a+b)\hat{\theta}_n e^{jfl} + a\hat{\theta}_n e^{-jfl} + (2c+d)\hat{\theta}_{n-1} - (c+d)\hat{\theta}_{n-1}e^{jfl} - c\hat{\theta}_{n-1}e^{-jfl} \tag{5.98}$$

And by grouping $\hat{\theta}_n$ and $\hat{\theta}_{n-1}$ terms together equation (5.98) becomes

$$\hat{\theta}_{n+1} = \left(1-2a-b+(a+b)e^{jfl} + ae^{-jfl}\right)\hat{\theta}_n + \left(2c+d-(c+d)e^{jfl} - ce^{-jfl}\right)\hat{\theta}_{n-1} \tag{5.99}$$

And by expanding and rearranging it becomes

$$\hat{\theta}_{n+1} = (1 - 2a - b)\hat{\theta}_n + (a + b)\hat{\theta}_n e^{jfl} + a\hat{\theta}_n e^{-jfl} + 2c\hat{\theta}_{n-1} + d\hat{\theta}_{n-1} - (c + d)e^{jfl}\hat{\theta}_{n-1} - ce^{-jfl}\hat{\theta}_{n-1} \tag{5.100}$$

If

$$e^{jfl} = \cos(fl) + j\sin(fl)$$

$$e^{-jfl} = \cos(fl) - j\sin(fl)$$

Then equation (5.100) becomes

$$\begin{aligned}\hat{\theta}_{n+1} = {} & (1 - 2a - b)\hat{\theta}_n + (a + b)(\cos(fl) + j\sin(fl))\hat{\theta}_n \\ & + a(\cos(fl) - j\sin(fl))\hat{\theta}_n + 2c\hat{\theta}_{n-1} + d\hat{\theta}_{n-1} \\ & - (c + d)(\cos(fl) + j\sin(fl))\hat{\theta}_{n-1} \\ & - c(\cos(fl) - j\sin(fl))\hat{\theta}_{n-1}\end{aligned} \tag{5.101}$$

Expanding equation (5.101) gives

$$\begin{aligned}\hat{\theta}_{n+1} = {} & (1 - 2a - b)\hat{\theta}_n + (a + b)\cos(fl)\hat{\theta}_n + (a + b)j\sin(fl)\,\hat{\theta}_n \\ & + a\cos(fl)\,\hat{\theta}_n - aj\sin(fl)\,\hat{\theta}_n + 2c\hat{\theta}_{n-1} + d\hat{\theta}_{n-1} \\ & - (c + d)\cos(fl)\,\hat{\theta}_{n-1} - (c + d)j\sin(fl)\hat{\theta}_{n-1} - c\cos(fl)\,\hat{\theta}_{n-1} \\ & + cj\sin(fl)\hat{\theta}_{n-1}\end{aligned} \tag{5.102}$$

By Grouping and simplifying the following is obtained

$$\hat{\theta}_{n+1} = (1 - 2a - b + (2a + b)\cos(fl))\hat{\theta}_n + (2c + d)(1 - \cos(fl))\hat{\theta}_{n-1} + j\sin(fl)\left(b\hat{\theta}_n - d\hat{\theta}_{n-1}\right) \tag{5.103}$$

$$\begin{aligned}\hat{\theta}_{n+1} = {} & (1 - 2a - b + (2a + b)\cos(fl) + j\sin(fl)\,b)\hat{\theta}_n \\ & + \left((2c + d)(1 - \cos(fl)) - j\sin(fl)\,d\right)\hat{\theta}_{n-1}\end{aligned} \tag{5.104}$$

Equation (5.104) above can be written as

$$\hat{\theta}_{n+1} = \hat{\theta}_n A + \hat{\theta}_{n-1} B \tag{5.105}$$

Where

$$A = 1 - 2a - b + (2a + b)\cos(fl) + j\sin(fl)\,b$$

$$B = (2c + d)(1 - \cos(fl)) - j\sin(fl)\,d$$

At $n = 0$, equation (5.105) becomes

$$\hat{\theta}_1 = \hat{\theta}_0 A + \hat{\theta}_{-1} B \tag{5.106}$$

The condition required for the solution to be stable is $\left|\frac{\theta_1}{\theta_0}\right| < 1$

If equation (5.106) is considered to be

$$\hat{\theta}_1 = A\hat{\theta}_0 \tag{5.107}$$

Then

$$\left|\frac{\hat{\theta}_1}{\hat{\theta}_0}\right| = A \tag{5.108}$$

The condition above is assumed to be true if

$$|A| = \sqrt{x^2 + y^2} < 1 \tag{5.109}$$

Where x and y obtained by splitting

$$A = 1 - 2a - b + (2a + b)\cos(fl) + j\sin(fl)\, b \tag{5.110}$$

into

$$x = 1 - 2a - b + (2a + b)\cos(fl) \tag{5.111}$$

and

$$y = j\sin(fl)\, b \tag{5.112}$$

Substituting the x and y into equation (5.109) yields

$$|A| = \sqrt{(1 - 2a - b + (2a + b)\cos(fl))^2 + (j\sin(fl)\, b)^2} \tag{5.113}$$

$$\left|\left(1 - \frac{3hD}{(l)^2} - \frac{3h\beta}{2l} + \left(\frac{3hD}{(l)^2} + \frac{3h\beta}{2l}\right)\cos(fl)\right)^2 + \left(j\sin(fl)\frac{3h\beta}{2l}\right)^2\right| = \sqrt{\left(1 - \frac{3hD}{(l)^2} - \frac{3h\beta}{2l} + \left(\frac{3hD}{(l)^2} + \frac{3h\beta}{2l}\right)\cos(fl)\right)^2 + \left(j\sin(fl)\frac{3h\beta}{2l}\right)^2} \tag{5.114}$$

$$\sqrt{\left(1 - \frac{3hD}{(l)^2} - \frac{3h\beta}{2l} + \left(\frac{3hD}{(l)^2} + \frac{3h\beta}{2l}\right)\cos(fl)\right)^2 + \left(j\sin(fl)\frac{3h\beta}{2l}\right)^2} < 1 \tag{5.115}$$

It is concluded that the solution is stable for $\forall n = 0$. To prove that the solution is stable for $\forall n \leq 0$ the following condition is assumed $\left|\frac{\hat{\theta}_{n+1}}{\hat{\theta}_0}\right| < 1$, then

$$\hat{\theta}_{n+1} = \hat{\theta}_n A + \hat{\theta}_{n-1} B \tag{5.116}$$

$$\left|\hat{\theta}_{n+1}\right| = \left|\hat{\theta}_n A + \hat{\theta}_{n-1} B\right| \tag{5.117}$$

$$\left|\hat{\theta}_{n+1}\right| = \left|\hat{\theta}_n A + \hat{\theta}_{n-1} B\right| \leq \left|\hat{\theta}_n\right||A| + \left|\hat{\theta}_{n-1}\right||B| \tag{5.118}$$

According to the induction theory the solution is stable when

$$\left|\hat{\theta}_n\right||A| + \left|\hat{\theta}_{n-1}\right||B| < \left|\hat{\theta}_0\right||A| + \left|\hat{\theta}_0\right||B| \tag{5.119}$$

$$\frac{\left|\hat{\theta}_{n+1}\right|}{\left|\hat{\theta}_n\right|} < |A| + |B| < 1 \tag{5.120}$$

Expanding by substituting for A and B

$$\begin{aligned}\frac{\left|\hat{\theta}_{n+1}\right|}{\left|\hat{\theta}_n\right|} &< |1 - 2a - b + (2a + b)\cos(fl) + j\sin(fl)\, b| \\ &\quad + |(2c + d)(1 - \cos(fl)) - j\sin(fl)\, d| < 1\end{aligned} \tag{5.121}$$

Which is also

$$\begin{aligned}\frac{\left|\hat{\theta}_{n+1}\right|}{\left|\hat{\theta}_n\right|} &< \left|1 - \frac{3hD}{(l)^2} - \frac{3h\beta}{2l} + \left(\frac{3hD}{(l)^2} + \frac{3h\beta}{2l}\right)\cos(fl) + j\sin(fl)\frac{3h\beta}{2l}\right| \\ &\quad + \left|\left(\frac{hD}{(l)^2} + \frac{h\beta}{2l}\right)(1 - \cos(fl)) - j\sin(fl)\frac{h\beta}{2l}\right| < 1\end{aligned} \tag{5.122}$$

It can be concluded that solution obtained using Laplace Adam-Bashforth numerical method is stable.

CHAPTER 6: NUMERICAL SIMULATIONS

A computer program called MATHEMATICA was used to produce numerical simulations of water movement in the unsaturated zone. The program was used to solve both highly non-linear Richards' equation for vertical flow, equation (4.16) and the linearized Richards' equation based on system oversimplifying assumptions, equation (5.13). The following initial and boundary conditions were considered:

$\theta(z, 0) > \theta_r$

$\theta(z, l) = \theta_L$

$\theta(0, t) > \theta_r$

Flow in a homogeneous volume of soil was simulated for three different models; Brooks and Corey (1964) model; Mualem (1976) model; and the proposed linear model. The following soil hydraulic parameters are considered in this study for numerical simulations: $D = 0.05$, $\theta_r = 0.043$, $\theta_s = 0.44$, $\theta_L = 0.3$, $K_s = 6.935$, and $\theta_I = 0.43$

6.1 Results and discussion

To reproduce the unsaturated flow system three unsaturated hydraulic conductivity models were combined with Richards' equation. The first one is Brooks and Corey (1964) model; the second one is Mualem (1976) model; and the last one is the linear proposed in this study. Simulation results obtained when Richards' equation was combined with Brooks and Corey model showed that soil water content evolves across space and time. However, the evolution presented by this model is non-realistic, because for the simulated time water is less than initial water content during early and mid-simulation time. Moreover, water content seems to be constant at shallow depth and there is a sudden increase in water content. The numerical solution presented in Figure 10 shows a rapid increase in water content near the lower flow boundary; this is questionable because water content rises above initial values.

Figure 11 presents a ContourPlot of water content. Similarly, there is one characteristic contour from the surface extending towards the lower boundary. Then, a sudden change in contours' slope is present; there are steep contours close to the boundary. To add, this model is implying that for this particular soil volume almost all soil moisture is located near the lower boundary.

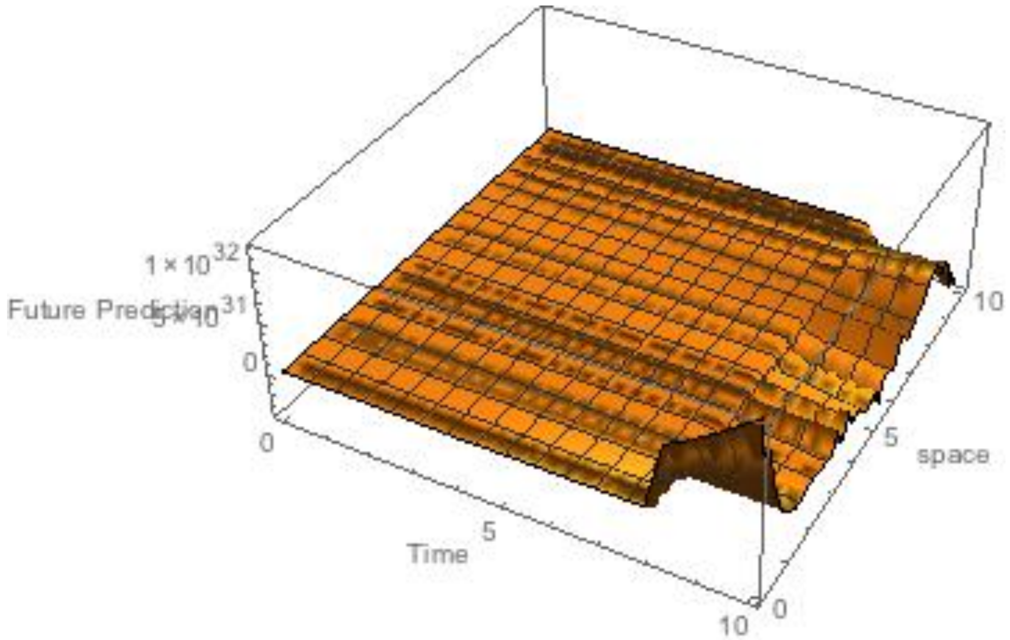

Figure 10: Numerical solution of Brooks and Corey (1964) model combined with Richards' equation

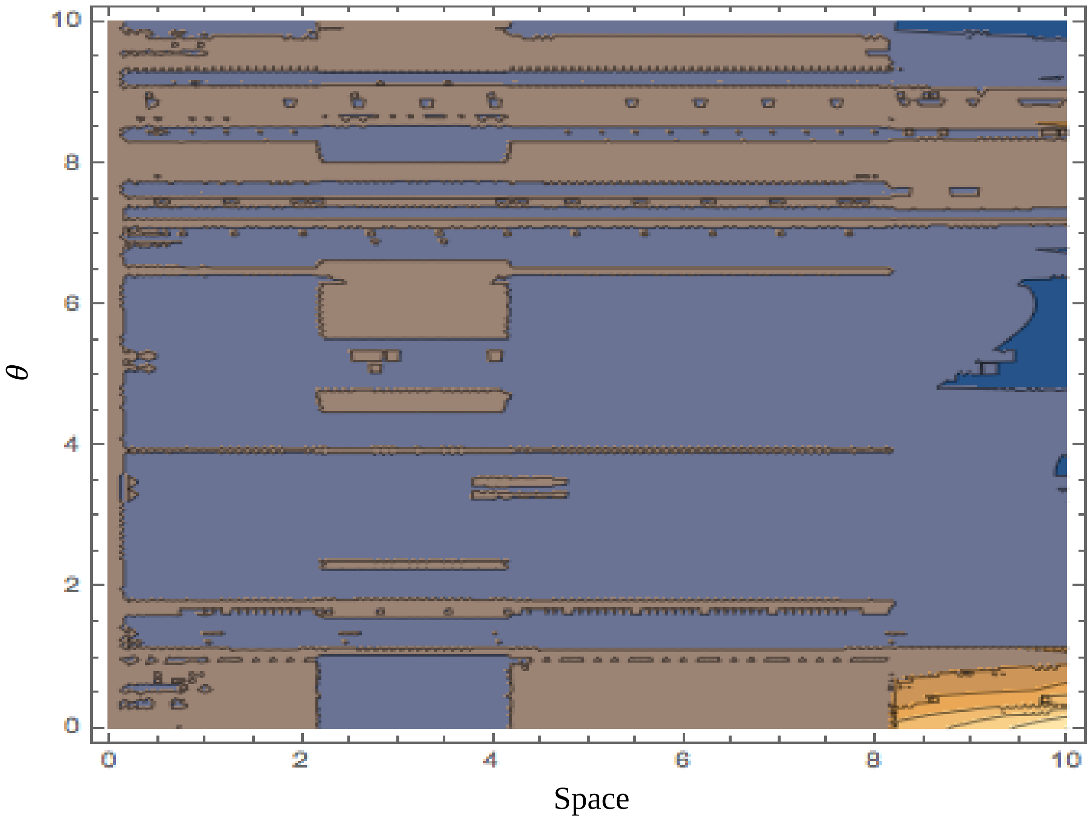

Figure 11: ContourPlot of Brooks and Corey (1964) model combined with Richards' equation

Mualem model also yielded results with water content evolution trend that is similar to the one explained above. This is expected provided that the models theories are not entirely different.

It was found necessary to revise these models to see if it will be possible to obtain realistic results. In order to revise Muleam and Brooks & Corey models, equation (4.13) and equation (4.8) respectively, close attention has to be paid on how the model parameters are related. The relationship between relative hydraulic conductivity and effective saturation suggested by these models is highly non-linear. Therefore, realistic results can be obtained if the relationship is made to be less non-linear. In this case, it is suggested that the exponent in equation (4.8) and equation (4.13) is given to $\theta - \theta_r$ only. The exclusion of $\theta_s - \theta_r$ from the base of exponent makes the resultant model to be less non-linear. The proposed non-linear model for estimating unsaturated hydraulic conductivity is given by

$$K_r = K_s \frac{(\theta - \theta_r)^{\omega}}{\theta_s - \theta_r} \tag{6.1}$$

Combining the above unsaturated hydraulic conductivity model with Richards' equation yields

$$\frac{\partial \theta}{\partial t} = D \frac{\partial^2 \theta}{\partial z^2} + \frac{\partial}{\partial z}\left[K_s \frac{(\theta - \theta_r)^{\omega}}{\theta_s - \theta_r}\right] \tag{6.2}$$

Where ω is 5 for the revised Books and Corey model and 3.5 for the revised Mualem model.

Simulation runs using these revised models yielded results that are totally different from those obtained using original models. The water content evolution trend is the opposite of the one explained above. Here, water is distributed across the soil volume; there is high water content at the beginning. As time passes, water content declines with depth towards the lower boundary. This trend is seen in both revised models. However, revised Brooks and Corey model show some oscillations of high and lower water contents towards the lower boundary. In general, the revised models seem to be more realistic compared to original models for the considered soil volume. To expand, it is expected for water content to decline with time and depth because some water becomes disconnected from flow resulting in a decline in the residual flow. The results for revised models are presented in Figure 4, Figure 5, Figure 7, Figure 8, Figure 10, and Figure 11 below.

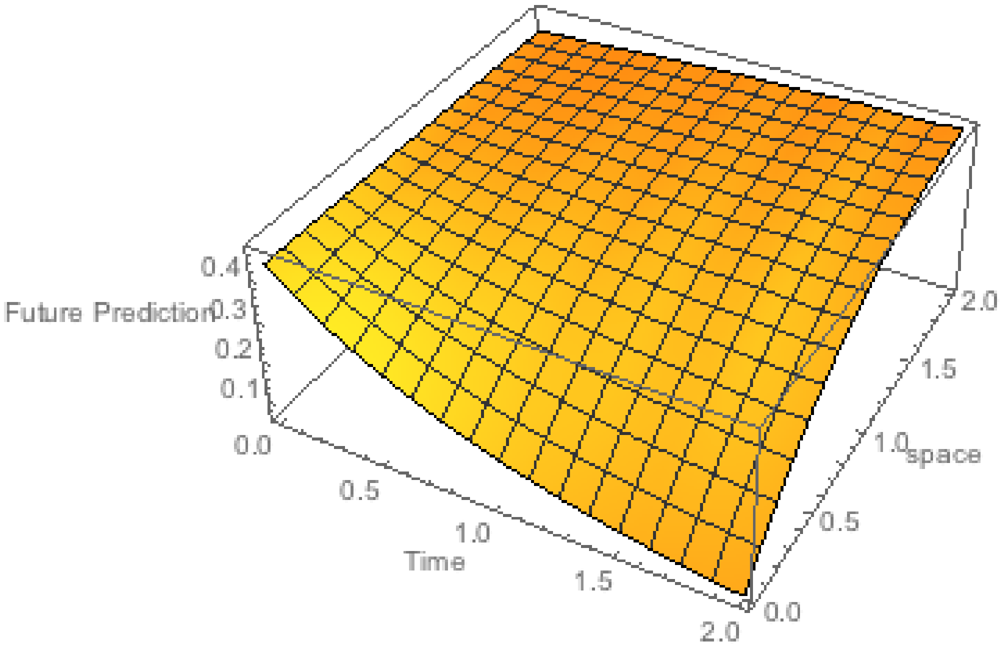

Figure 12: Numerical solution of the proposed linear model

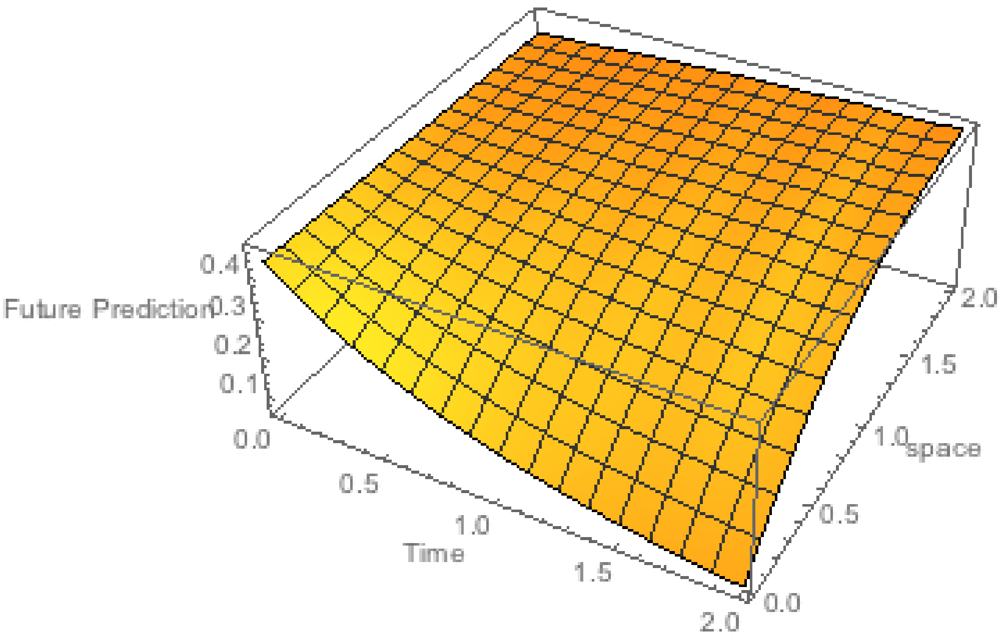

Figure 13: Numerical solution of the proposed non-linear model obtained from revising Mualem model

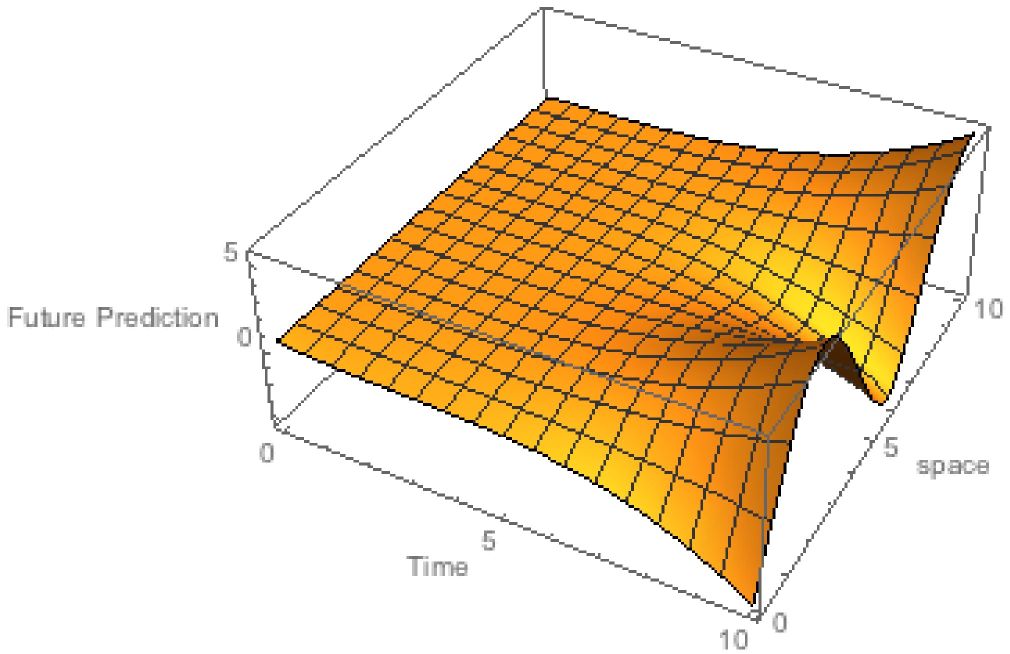

Figure 14: Numerical solution of the proposed non-linear model obtained from revising Brooks and Corey model

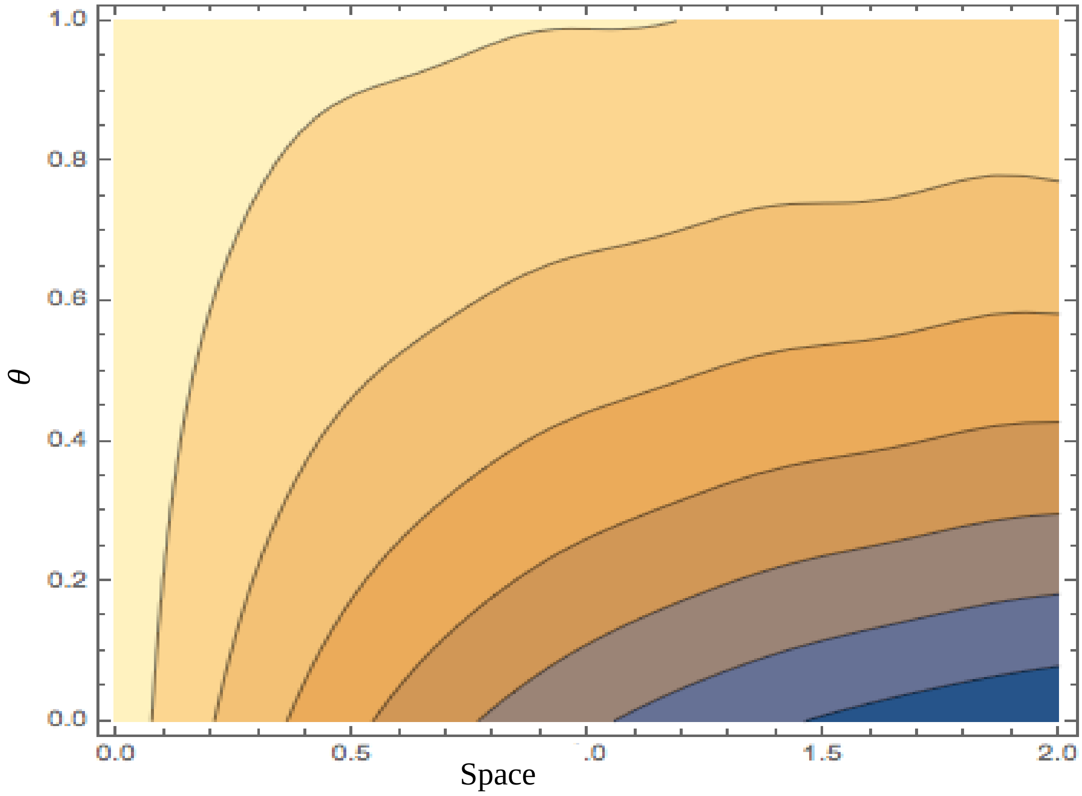

Figure 15: ContourPlot of the proposed linear model

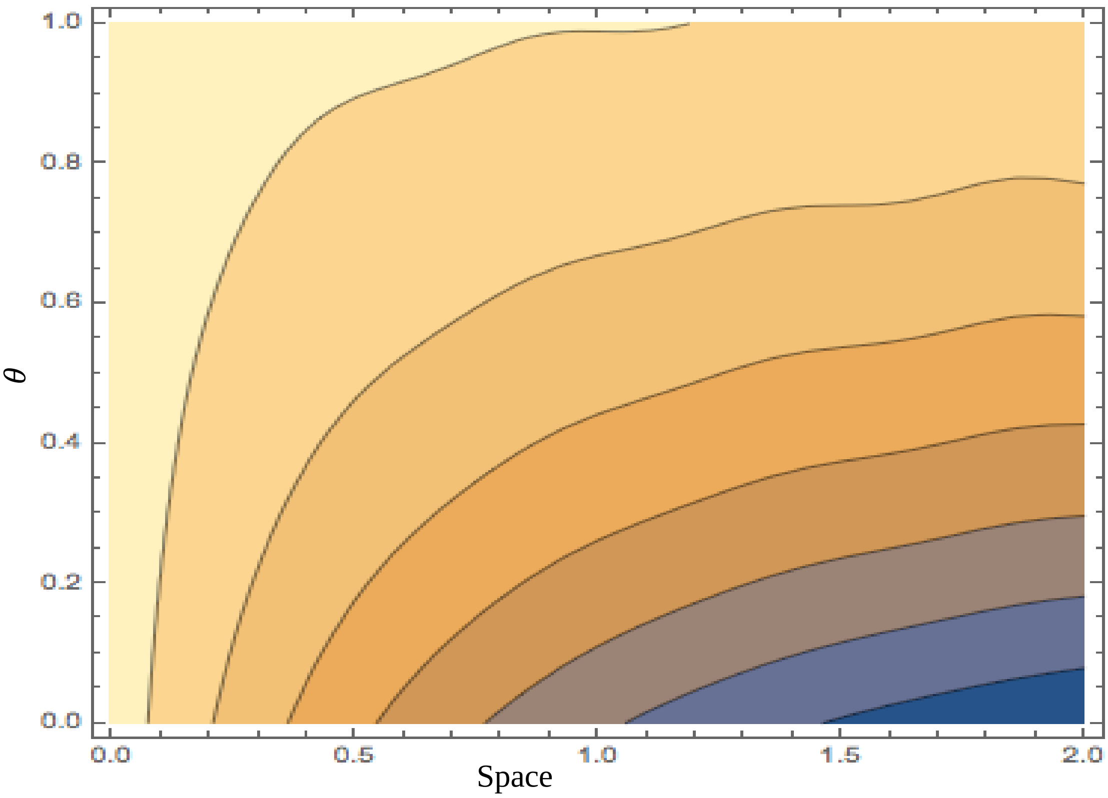

Figure 16: ContourPlot of the proposed non-linear model obtained from revising Mualem model

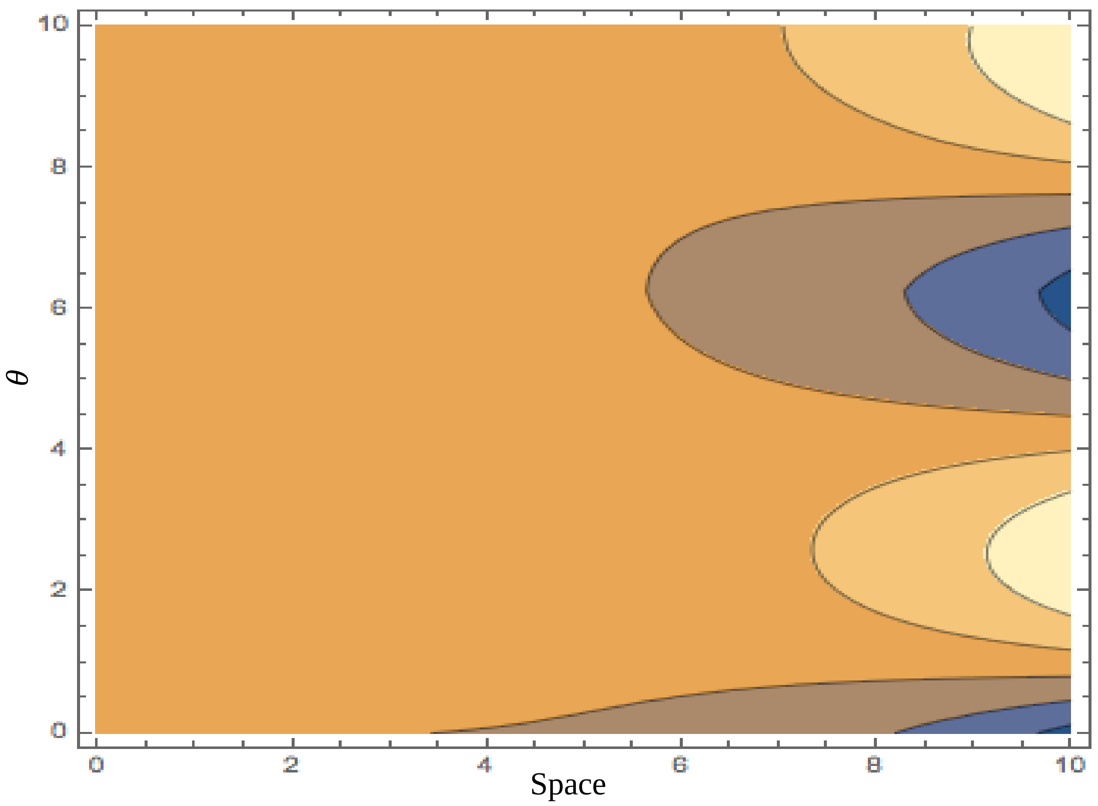

Figure 17: ContourPlot of the proposed non-linear model obtained from revising Brooks and Corey model

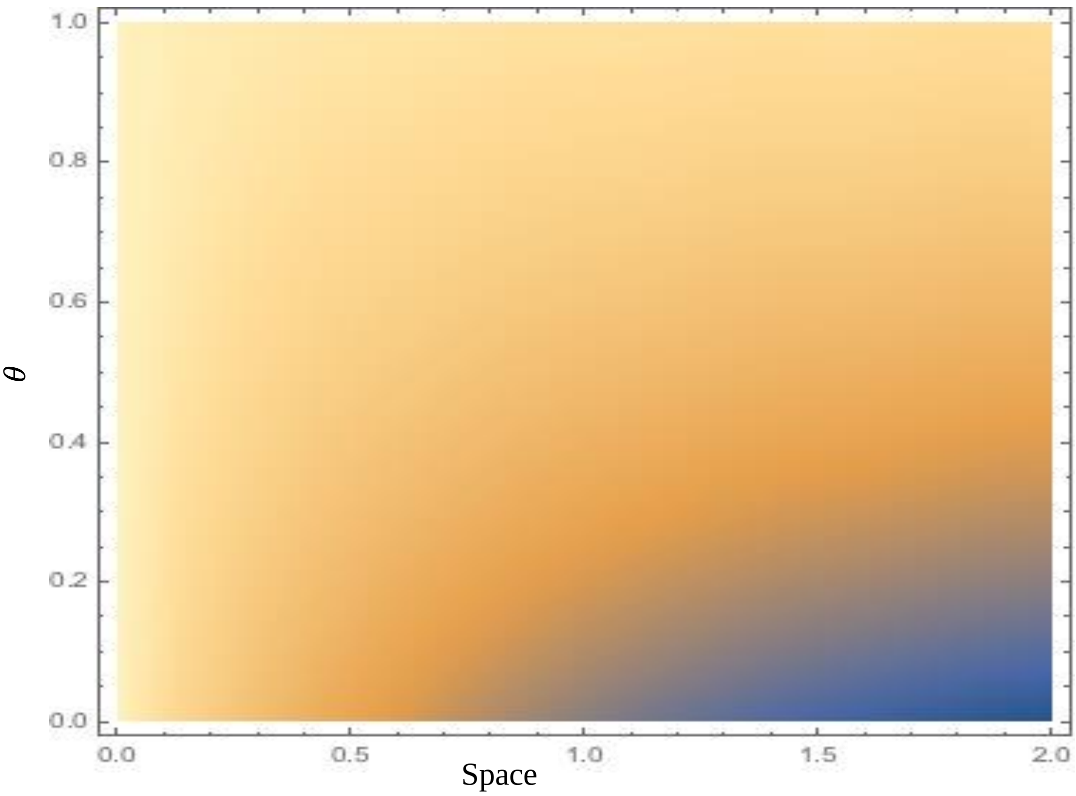

Figure 18: Density Plot of the proposed linear model

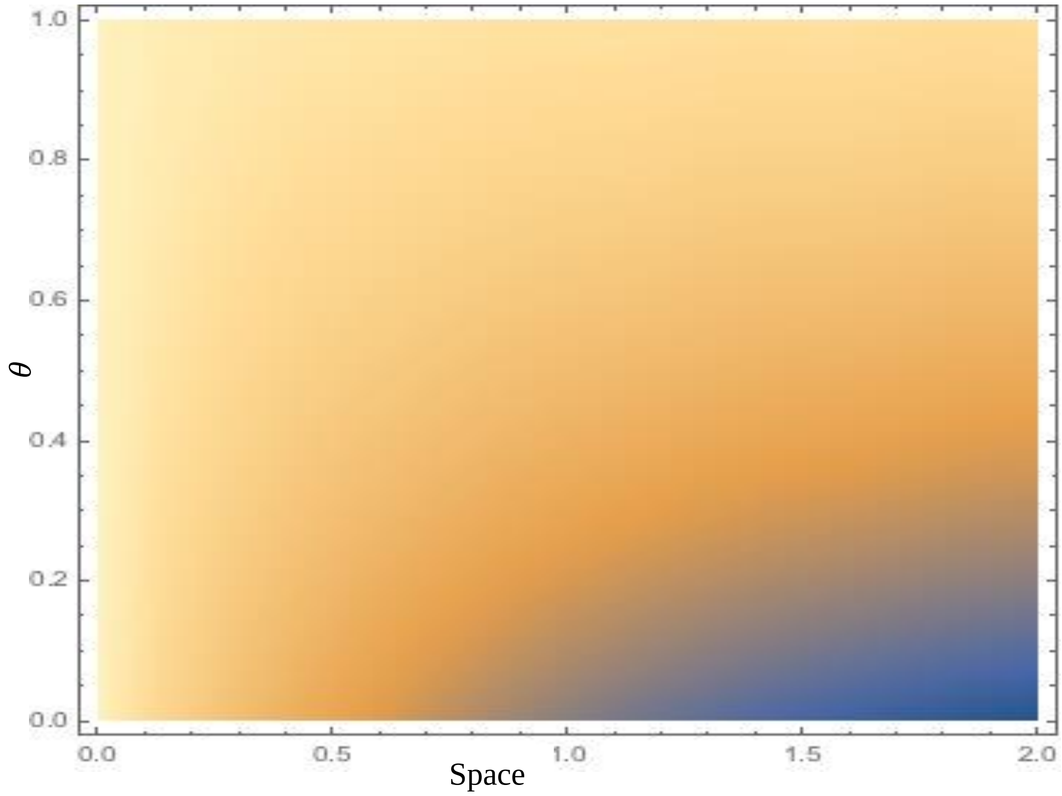

Figure 19: Density Plot of the proposed non-linear model obtained from revising Mualem model

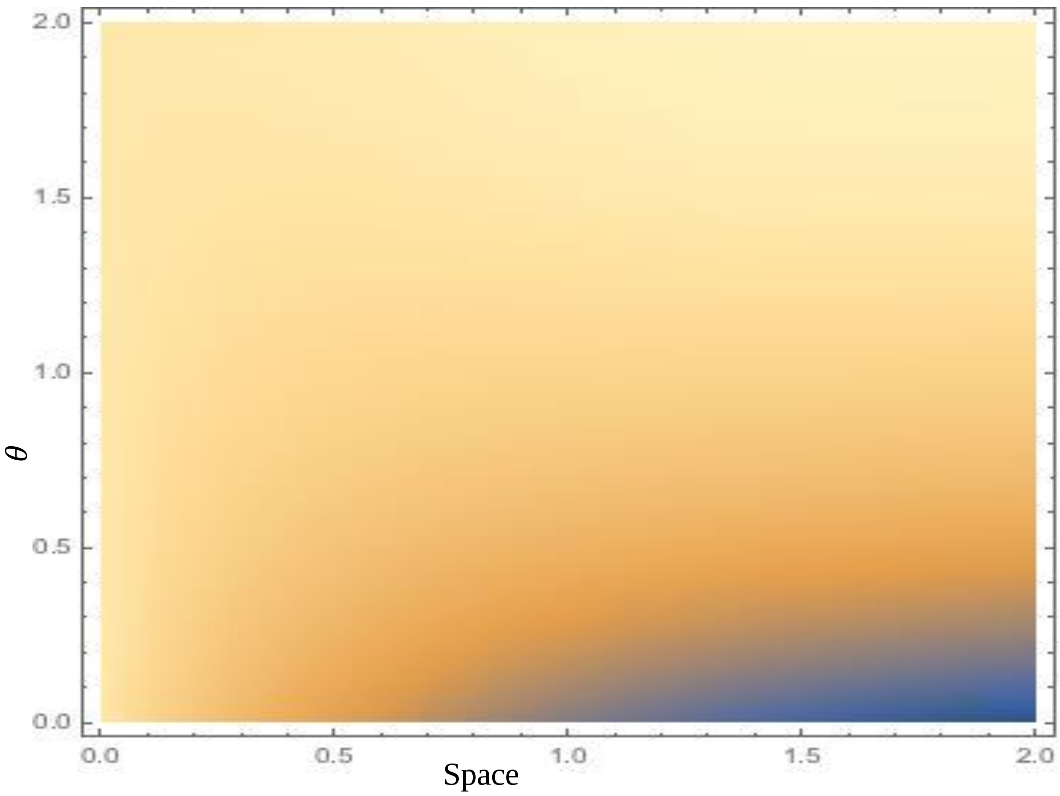

Figure 20: Density Plot of the proposed non-linear model obtained from revising Brooks and Corey model

Simulation runs using the proposed unsaturated hydraulic conductivity model combined with Richards' equation yielded results that are presented in Figure 12, Figure 15, and Figure 18 above. The numerical solution shows an evolution of water content with depth into the soil volume. Water content is decreasing as expected, the ContourPlot and Density plot show how the water content decreases in time and space. Water content is high close to the surface and low towards the lower boundary. Therefore the results are realistic for the considered soil volume.

The proposed linear and non-linear models performed similarly. Although there is a slight difference in solutions, models were able to produce valid results. The performance of the revised Mualem model and the proposed models is very close. Revised Brooks and Corey model also show same performance at early to mid-simulation time, however at late simulation time water is distributed in a wave-like form.

CONCLUSION

The purpose of this thesis was to model subsurface water flow in the unsaturated zone using selected pre-existing non-linear models and a proposed linear model. A volume of unsaturated soil with characteristic soil hydraulic properties was considered to address the afore-mentioned purpose. Incorporation of pre-existing unsaturated hydraulic conductivity models in Richards' equation yielded highly non-linear models that required numerical analysis. Application of the proposed linear unsaturated hydraulic conductivity model to Richards' equation resulted in a linearized Richards' equation which is easy to solve both numerically and analytically. The exact solution of linearized Richards' equation obtained using Laplace transform and Green's function is valid. Therefore, if parametric soil hydraulic properties are available a system can be solved without a computer program.

Numerical analysis was performed for all models using two numerical approximation methods for more reliable results. The stability of resultant solutions of linearized Richards' equation tested using the Fourier expansion stability analysis method, the equation is stable for both approximation methods provided the required conditions are met.

Numerical simulations were obtained for all models and the results showed that for a vertical water flow soil water content evolves with depth. Non-linear showed poor performance and the resultant numerical solutions were not realistic. To expand, simulations showed that there is an increase in water content with depth which is not realistic. Water content is expected to decline with depth due to the concept of water retention. Revision of these models yielded results that were found to be more realistic. The results corresponded with the results obtained using a linear model. It can be concluded that the linear model is valid provided the assumptions are met. Therefore, this model can be used for modelling flow in local soils as long as the required conditions are met. Moreover, this is not a universal model and applying it in soils with hydraulic parameters that do not correspond with the ones assumed may yield unreliable results.

REFERENCES

Akaike, H., 1973. Information theory and an extension of the maximum likelihood principle. In B. N. Petrov, & F. Csaki (Eds.), Second international symposium on information theory. pp. 265–281.

Allwright, A., Atangana, A., 2018. Augmented upwind numerical schemes for the groundwater transport advection-dispersion equation with local operators. Int J Numer Meth Fluids 1–26.

Assouline, S., 2005. On the relationships between the pore size distribution index and characteristics of the soil hydraulic functions. Water Resour. Res. 41.

Assouline, S., Tartakovsky, D.M., 2001. Unsaturated hydraulic conductivity function based on a soil fragmentation process. Water Resour. Res. 37.

Assouline, S., Tessier, D., Bruand, A., 1998. A conceptual model of the soil water retention curve. Water Resour. Res. 34, 223-231.

Barari, A., Omidvar, M., Ghotbi, A.R., Ganji, D.D., 2009. Numerical analysis of Richards' problem for water penetration in unsaturated soils. Hydrol. Earth Syst. Sci. Discuss. 6, 6359–6385.

Boulding, J.R., Ginn, J.S., 2013. Chapter 2: Groundwater and vadose zone hydrology, in: Practical handbook of soil, vadose zone, and ground-water contamination. Lewis Publishers, Boca Raton London New York Washington, D.C., pp. 41–67.

Brooks, R.H., Corey, A.T., 1964. Hydraulic properties of porous media. Hydrol. Pap. 3, 27.

Brouwer, C., Goffeau, A., Heibloem, M., 1985. Irrigation water management: Training manual No. 1-Introduction to irrigation. FAO, Rome.

Buckingham, E., 1907. Studies on the movement of soil moisture. US department of agriculture, Bureau of soils No. 38

Burdine, N.T., 1953. Relative permeability calculation from pore-size distribution data. Trans. AIME 198, 71–78.

Chanasyk, D.S., Verschuren, J.P., 1983. An interflow model: I. Model development. Can. Water Resour. J. 8, 106–109.

Chapter 4 - Water flow in unsaturated soils, 2000. , in: SSC.

Chapter 6 : Groundwater Recharge, 2014. , in: New Jersey Stormwater best management practices manual. New Jersey.

Childs, E.C., Collis-George, N., 1950. The permeability of porous materials. Proc R Soc Lond 201, 392–405.

Condesso de Melo, M.T., 2015. Groundwater recharge [WWW Document]. Tec. Lisb. URL https://fenix.tecnico.ulisboa.pt/downloadFile/1970943312278793/GROUNDWATER%20RECHARGE.pdf (accessed 5.25.18).

Eddebbarh, A.A., Zyvoloski, G.A., Robinson, B.A., Kwicklis, E.M., Reimus, P.W., Arnold, B.., Corbet, T., Kuzio, S.P., Faant, C., 2003. The saturated zone at Yucca Mountain: an overview of the characterization and assessment of the saturated zone as a barrier to potential radionuclide migration.

Gallage, C., Kodikara, J., Uchimara, T., 2013. Laboratory measurement of hydraulic conductivity functions of two unsaturated sandy soils during drying and wetting processes. Soils Found. 53, 417–430.

Gava, R., de Freitas, P.S.L., de Faria, 2013. Soil water evaporation under densities of coverage with vegetable residue. Soil Water Eng. 33.

Ghanbarian-Alavijeh, B., Hunt, A.G., 2012. Unsaturated hydraulic conductivity in porous media: Percolation theory. Geoderma 187–188, 77–84.

Gnitchogna, R., Atangana, A., 2018. New two step Laplace Adam-Bashforth method for integera noninteger order partial differential equations. Number Methods Partial Differ. Eq 34, 1739–1738.
Gordon, D., 1989. Chapter B2: Introduction to ground-water hydraulics a programed text for self-instruction, in: Techniques of water-resources investigations of the United States Geological Survey. USGS, pp. 1–29.
Green, W.H., Ampt, G., 1911. Studies of soil physics, part I – the flow of air and water through soils. J Ag Sci 4, 1–24.
Heinse, R., Link, T.E., 2013. Vadose zone processes: a compendium for teaching interdisciplinary modeling. J. Contemp. Water Res. Educ. 22–31.
Hillel, D., 2004. Chapter 16: Redistribution and retention of soil moisture, in: Introduction to Environmental Soil Physics. Elsevier Science, USA, pp. 297–314.
Horton, R.E., 1940. The infiltration-theory of surface-runoff. Am. Geophys. Union 21.
Kang, Y., Lu, G., Wu, Z., He, H., 2009. Comparison and analysis of bare soil evaporation models combined with ASTER data in Heihe River Basin. Water Sci. Eng. 2, 16–27.
Klocke, N.L., 2004. Crop residue and soil water evaporation.
Kosugi, K., Hopmans, J.W., Dane, J.H., 2002. 3.3.4 Parametric models, in: Methods of Soil Analysis. Part 4. Physical Methods, SSSA Book Series. Soil Science Society of America, USA.
Leij, F.J., van Genuchten, M.T., Yates, S.R., Russel, W.B., Kaveh, F., 1994. RETC: A computer program for analyzing soil water retention and hydraulic conductivity data.
Mawer, C., Knight, R., Kitanidis, P.K., 2015. Relating relative hydraulic and electrical conductivity in the unsaturated zone. Water Resour. Res. 51, 599–618.
McCartney, J.S., Villar, L.F.S., Zornberg, J.G., 2007. Estimation of the hydraulic conductivity function of unsaturated clays using infiltration column tests. Salvador 1, 321–328.
MIDUSS version 2 Reference manual, 2004. . Alan A. Smith Inc., Canada.
Minshall, N.E., Jamison, V.C., 1965. Interflow in claypan soils. Water Resour. Res. 1, 381–390.
Mualem, Y., 1976. A new model for predicting the hydraulic conductivity of unsaturated porous media. Water Resour. Res. 12, 513–522.
Neitsch, S.L., Arnold, J.G., Kiniry, J.R., Williams, J.., 2011. Soil and water assessment tool theoretical documentation (Technical report No. 405). Texas Water Resources Institute, Texas.
Neto, D.D., 2013. An unrestricted solution to predict the hydraulic conductivity of unsaturated soils (No. 2444–22). International Centre for Theoretical Physics, Brazil.
Nimmo, J.R., 2005. Unsaturated zone flow processes. Encyclopedia of Hydrological Sciences: Part 13-Groundwater.
Nimmo, J.R., 2004. Porosity and pore size distribution. Encycl. Soils Environ.
Ojha, R., Corradini, C., Morbidelli, R., Govindaraju, R.S., 2017. Effective saturated hydraulic conductivity for representing field-scale infiltration and surface soil moisture in heterogeneous unsaturated soils subjected to rainfall events. Water 9.
Peck, A.J., 1971. Redistribution of soil water after infiltration. Aust J Soil Res 9.
Richards, L.A., 1931. Capillary conduction of liquids through porous mediums. Physics 1.
Rosas-Anderson, P., Taggart, M.J., Heitman, J.L., 2018. Partitioning between evaporation and transpiration from Agrostis stolonifera L. during light and dark periods. Agric. For. Meteorol. 73–79.
Singh, B., O'Callaghan, J.R., 1978. Effect of interflow on soil drainage. J. Agric. Eng. Res. 23, 397–415.

Soulaine, C., 2015. Chapter 1: On the origin of Darcy's law. Stanford.
Swartzendruber, D., 1954. Capillary fringe and water flow in soil. Iowa State College.
Tarboton, D.G., 2003. Chapter 4: Soil properties, in: Rainfall-Runoff Processes. Utah State University.
Tesfuhuney, W.A., Van Rensburg, L.D., Walker, S., Allemann, J., 2015. Quantifying and predicting soil water evaporation as influenced byrunoff strip lengths and mulch cover. Agric. Water Manag. 152, 7–16.
Twarakavi, N.K.C., Simunek, J., Seo, S., 2008. Evaluating interactions between groundwater and vadose zone using the HYDRUS-based flow package for MODFLOW. Vadose Zone J. 7, 757–768.
van Genuchten, M.T., 1980. A closed-form equation for predicting the hydraulic conductivity of unsaturated soils. Soil Sci. Soc. Am. J. 44, 892–898.
Vereecken, H., 1995. Estimating the unsaturated hydraulic conductivity from theoretical models using simple soil properties. Geoderma 65, 81–92.
Vereecken, H., Huisman, J.A., Bogena, H., Vanderborght, J., Vrugt, J.A., Hopmans, J.W., 2008. On the value of soil moisture measurements in vadose zone hydrology: A review. Water Resour. Res.
Wetzel, P.J., Liang, X., Irannejad, P., Boone, A., Noilhan, J., Shao, Y., Skelly, C., Xue, Y., Yang, Z.L., 1996. Modeling vadose zone liquid water fluxes: Infiltration, runoff, drainage, interflow. Glob. Planet. Change 13, 57–71.
Whitaker, S., 1986. Flow in Porous Media I: A theoretical derivation of Darcy's law. Reidel Publ. Co. 3–25.
Wong, W., Zhang, Z., Yeh, T.J., Qiqo, G., Wong, W., Duan L, Huang S, Wen J, 2017. Flow dynamics in vadose zones with and without vegetation in an arid region. Elsevier 106, 68–79.
Youngs, E.A., Poulovassilis, A., 1976. The distribution of moisture profile developed during the distribution of soil water infiltration. Water Resour. Res. 12.
Zhang, F., 2010. Soil Water Retention and Relative Permeability for Full Range of Saturation (No. PNNL-19800). U.S. Department of Energy.
Zhang, T., 1991. A statistical approach for water movement in the unsaturated zone (Thesis No. 1010). Lund Institute of Technology, Lund University, Lund, Sweden.
Zhu, J., Ogden, F.L., Lai, W., Chen, X., Talbot, C.A., 2016. An explicit approach to capture diffusive effects in finite water-content method for solving vadose zone flow. Elsevier 270–281.